Reduction of Oscillations in Hydraulically Actuated Knuckle Boom Cranes

Jesper Kirk Sørensen

Reduction of Oscillations in Hydraulically Actuated Knuckle Boom Cranes

Doctoral Dissertation for the Degree *Philosophiae Doctor* (PhD) at
the Faculty of Engineering and Science,
Specialisation in Mechatronics

University of Agder

Faculty of Engineering and Science
2016

Doctoral Dissertation at the University of Agder 146
ISBN: 978-82-7117-840-6
ISSN: 1504-9272

Printed at: Wittusen & Jensen
Oslo

Preface

This dissertation presents results of the research I have carried out in my Ph.D. project at the Department of Engineering Sciences, Faculty of Engineering and Science, University of Agder, Norway. The research was carried out in close cooperation with National Oilwell Varco in Kristiansand in the period between September 2012 and August 2016. The project was funded by the Norwegian Ministry of Education and Research and co-funded by National Oilwell Varco. The work has been conducted under the supervision of Associate Professor Morten Kjeld Ebbesen and Professor Michael Rygaard Hansen. During the project I spent 4 months of the first half of 2015 at Purdue University, Indiana, USA, as a visiting researcher under the supervision of Associate Professor Andrea Vacca.

Acknowledgements

It has been many long evenings, nights and weekends where analyses were performed, experiments carried out or writing done - probably more than I would care to admit. However, in hindsight putting aside all the hard work, the last four years has been an amazing journey. It has been a privilege being able to work with something I like, travel the world and meet many interesting people - and still call it my job. I learned a lot during these years academically, professionally and especially personally.

I would like to extend a special thanks to my supervisors Associate Professor Morten Kjeld Ebbesen and Professor Michael Rygaard Hansen. I have enjoyed playing ball with you both; the passing of ideas, our small talks, the work towards achieving the goals and your dedication in the process. Even though the project ended in overtime, eyes were still kept on the ball and victory achieved. Thank you.

Without mentioning any names, since I am afraid that I will forget someone, I would like to thank all the colleagues and fellow Ph.D candidates at the University of Agder here in Grimstad. Everyone have always been ready with a helping hand when needed, ready for a talk when needed, both the serious ones and the not so much - it has been a pleasure getting to know you all.

Also I would like to send my gratitude to the former colleagues at department 670 at NOV, who with their inputs and sharing of knowledge helped forming this project. I learned a lot and really enjoyed my time there.

A special thanks goes to Jannik and Martin - this dissertation would not have been done if it was not for you.

Finally I would like to thank my family back home for the support. When the frustrations were high, you got me back on track, thank you.

Thank you all for making my stay in Grimstad a time I will look back on with fond memories.

I made it!

Jesper Kirk Sørensen
Grimstad, Norway
August 2016

Abstract

A knuckle boom crane is characterised by being a versatile machine that during operation experiences large load variations caused by the changes in position and payload. Common uses are as a mobile loader crane mounted on trucks and in offshore applications. Since their introduction the use of counterbalance valves (CBV) have been the de facto standard on load-carrying hydraulically actuated applications like the knuckle boom crane. It offers a simple and practical solution to one of the issues of mobile cranes: Controlling the load safely when lowering. By law (e.g. European Standard) the hydraulic circuit of load-carrying applications is required to contain a load holding protection device. The classical way of actuating such a crane is to use a circuit containing a pressure compensator valve and a directional control valve (DCV) in series with a CBV. This circuit is referred to as the base circuit. It is well known that this combination of valve components tends to introduce instability in the base circuit. This is mainly a problem when the controlled actuator is subjected to a negative load, because this will require the CBV to throttle the return flow. The instability presents itself as pressure oscillations in the hydraulic circuit which cause the mechanical structure to oscillate. The consequence of the oscillations is a decreased accuracy of the boom motion which create a safety risk, reduces productivity and introduces an undesirable extra fatigue load.

The objective of this project was to investigate the oscillations created in the hydraulic circuit of knuckle boom cranes and reduce their severity. The

effort has mainly been split in two:

First, was looked into existing solutions with the focus on the ones not requiring control systems to function. This was done with reliability and robustness in mind. The investigation identified the pressure control valve (PCV) as the best commercially available solution. The use of a PCV to control the inlet flow in crane applications was rather uncharted territory. The valve, a DCV with a pressure control spool manufactured by Danfoss, has been investigated both theoretically and experimentally. A linear stability analysis has been performed with the Routh-Hurwitz stability criterion. This analysis of the valve used together with a hydraulically actuated experimental setup indicates that the combination is stable in all situations. The use of the pressure control spool in the DCV is a simple and robust solution to the stability problem of the base circuit. Not related to the PCV's ability to reduce the oscillations the use of it in knuckle boom cranes, however, comes with certain drawbacks. The drawbacks includes a load dependent dead band and a load dependent inlet flow. In order to achieve similar behaviour as the normal pressure compensated DCV a closed loop control system is required. These issues are addressed in this project, where control schemes are proposed to handle them.

In the second part the perspective of the search was broadened to include solutions using control systems. This has lead to the development of a novel, patent pending, concept that significantly reduces the oscillations of the base circuit. It introduces a secondary circuit where a low-pass filtered value of the load pressure is generated and fed back to the compensator of the flow supply valve. The work has demonstrated a significant improvement of stability obtained for a system with the novel concept implemented both theoretically and experimentally. The stability has been investigated both using a linear and a nonlinear model of a hydraulically actuated experimental setup. The presented novel concept circuit has the same steady state characteristics as the base circuit but without the corresponding oscillatory nature. Because the main spool of the DCV is not used for stabilising the system, the novel concept can be combined with any feedback control strategy. In this project, the

novel concept is presented with linear actuators only. However, its use covers circuits with rotational actuators and CBV's as well.

The base circuit is used as a reference for comparison. Therefore, the stability of the base circuit is also investigated with a linear model.

Contents

Abbreviations

A list of the used abbreviations:

BC	Base circuit.
CBV	Counterbalance valve.
CV	Pressure compensator valve.
DCV	Directional control valve.
NCC	Novel concept circuit. Corresponds to the BC with the novel concept implemented.
PCC	Pressure control circuit. Corresponds to the BC where the DCV is replaced by a PCV.
PCV	DCV with a pressure control spool.
PV	Proportional pressure relief valve.
SC	Secondary circuit.
SMISMO	Separate meter-in separate meter-out.

Nomenclature

A list of the used nomenclature:

A_0	Opening area of the fixed orifice in the PCV.
A_A	Cross sectional area of the cylinder's piston side.
A_B	Cross sectional area of the cylinder's rod side.
$A_{b0}(x)$	Opening area of the variable orifice in the PCV. Is a function of x.
$A_d(x)$	Opening area of DCV.
C_A	Capacitance of volume A.
C_B	Capacitance of volume B.
D_p	Cylinder piston diameter.
D_r	Cylinder rod diameter.
$F_{cyl,static}$	Static external force on cylinder.
F_L	External force on cylinder.
$G(s)$	Transfer function.
H_C	Cylinder stroke.
k_{PC1}	Valve constant of PCV.
k_{PC2}	Valve constant of PCV.
$k_{qo,CBV}$	Indirect flow gain of the CBV i.e., flow pr. pressure induced opening.
$k_{qp,CBV}$	Flow-pressure gain of the CBV, i.e., flow pr. pressure difference.
$k_{qu,CBV}$	Flow gain of the CBV i.e., flow pr. normalised spool position.
$k_{qp,DCV}$	Flow-pressure gain of the DCV, i.e., flow pr. pressure difference.
$k_{qu,DCV}$	Flow gain of DCV i.e., flow pr. normalised spool position.
$k_{v,CBV}$	Valve constant of CBV.
$k_{v,DCV}$	Valve constant of DCV.

L	The distance from the bearing to the mass centre of the boom of experimental setup #2.
$L_{AB,min}$	Minimum cylinder length.
$L_{AB,max}$	Maximum cylinder length.
m	Combined mass of boom and payload of experimental setup #2.
m_{eff}	Effective mass the cylinder experiences from the mechanical system when accelerating.
p_A	Pressure at port A.
$\dot{p}_A$	Time derivative of pressure A.
p_B	Pressure at port B.
$\dot{p}_B$	Time derivative of pressure B.
p_C	Pressure at C.
$\dot{p}_C$	Time derivative of pressure C.
p_{CL}	Set pressure of the compensator spring that relates to the fully closed position.
p_{cr}	Crack pressure of the CBV.
$p_{C@0L/min}$	PV crack open pressure with a flow through it of $0L/min$.
p_D	Pressure at D.
$p_{DCVPC,max}$	Maximum pressure of the PCV.
p_{PV}^r	Rated pressure of PV. Corresponds to $p_{C@0.8L/min}$ with a flow through it of $0.8L/min$.
p_S	Supply pressure.
p_T	Tank pressure. Assumed to be $0bar$.
p_Δ	Pressure drop across the metering-in orifice.
Q_{CBV}	CBV flow.
Q_{CBV}^r	Rated flow of CBV.
Q_{DCV}	DCV flow.
Q_{DCV}^{max}	Maximum rated flow of spool.
Q_{P-B}	Flow from port P to port B of the DCV.

$S_{PC,DB}$	Spool position at dead band.
$S_{PC,max}$	Maximum spool travel.
$S_{PC,range}$	Spool range where the pressure varies.
u_{CBV}	Dimensionless valve opening the CBV.
u_{DCV}	Dimensionless valve opening the DCV.
u_{DCV}^{ref}	Input signal to the DCV, corresponds to the dimensionless valve opening before dead band compensation (removes the physical dead band).
V_A	Volume of A (piston side cylinder chamber).
V_B	Volume of B (rod side cylinder chamber).
v_C	Piston velocity.
$\dot{v}_C$	Piston acceleration.
x	DCV main spool opening.
x_C	Piston position.
$\tilde{}$	The tilde denotes any parameter variation relative to the steady state value.
α_P	Pilot area ratio of the CBV.
β	Bulk modulus.
$\Delta p\|_{@2L/min}$	Orifice pressure drop with a flow through it of $2L/min$.
$\Delta p_{op,CBV}$	Extra pressure required to fully open the CBV.
$\mu(x)$	Area ratio of the orifices of the PCV.
μ_C	Cylinder area ratio.
ρ	Fluid density.
τ	Time constant of low-pass filter.
φ	Cylinder area ratio.

Chapter 1

Introduction

Hydraulics, or fluid power, is the common term for the use of pressurised fluids to transmit power to cylinders or motors for actuation purposes. Hydraulics is a well-proven, reliable, and robust actuation solution. It is characterised by a high power density compared to the component size. The use of oil as the power medium allows for good lubrication and heat transfer properties, which permit the components to be smaller and lighter than a comparable electric actuator. Furthermore, hydraulic components are relatively cheap. Hydraulics is a widely used technology with a broad range of application areas. They span from production machinery in industry, windturbines and off-highway vehicles to the aerospace and automotive industries and many other fields. The use of hydraulics is regarded as a mature technology, however challenges still lie ahead.

This dissertation focuses on one case of an open challenge: The hydraulic knuckle boom crane. A knuckle boom crane is characterised by being versatile and by experiencing large load variations caused by the changes in position and payload. Some examples of knuckle boom cranes are shown in figure 1.1. Common uses are as mobile loader cranes mounted on trucks and in offshore applications. In the offshore applications the knuckle boom crane is used for both on-deck operations and for handling subsea equipment.

The use of hydraulics in mobile cranes started in the late 40's, when the first truck mounted hydraulically actuated crane was introduced. In the early

Figure 1.1: Examples of knuckle boom cranes. To the left is shown a mobile loader crane (Direct industry, 2016) and to the right an offshore knuckle boom crane (NOV, 2014).

70's the counterbalance valve (CBV) was introduced. It offered a simple and practical solution to one of the issues of the mobile cranes; controlling the load safely when lowering. Since their introduction the use of CBV's have been the de facto standard on load-carrying hydraulically actuated applications including cranes. The CBV serves multiple purposes in a hydraulic circuit on a crane:

- Leak tight load holding
- Load holding in case of line failure
- Overload protection
- Shock absorption
- Cavitation prevention at load lowering
- No drop before lift

By law, European Standard (2013), the hydraulic circuit of load-carrying applications is required to contain a load holding protection device. In most systems this is handled by the CBV. The steady state characteristics of the CBV are well suited for a crane application with its ability to handle large variations in loads effectively. The classical way of actuating such a crane is to use a pressure compensator valve (CV) and a directional control valve

(DCV) in series with a CBV. Often the CV and DCV are integrated in one component. A CV has two important functions. It ensures that the inlet flow is independent of the load and it also ensures the possible use of several actuators simultaneously independent of pressure levels. This is very convenient for crane applications because of the manual operation, substantial load variations, and the tendency to actuate two or more degrees of freedom simultaneously. The system with a CV, a DCV and a CBV will be referred to as the base circuit (BC). An illustration of the circuit is shown in figure 1.2.

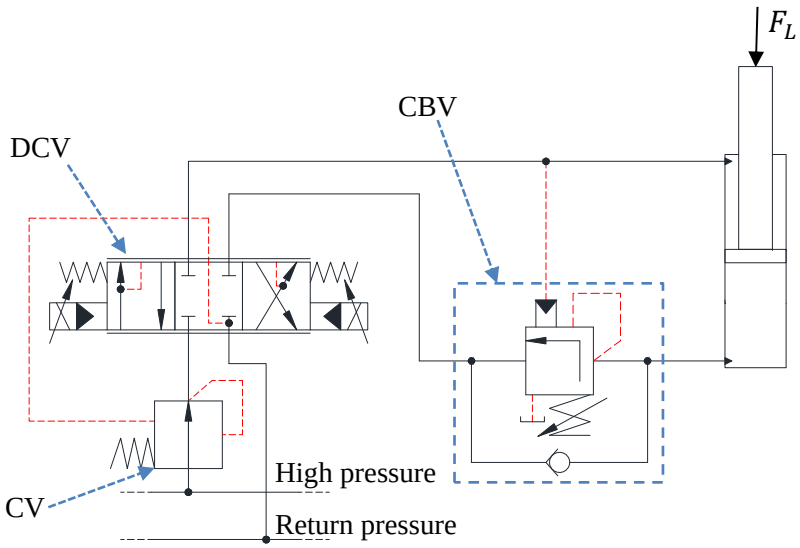

Figure 1.2: The base circuit (BC) consisting of a pressure compensator (CV), a directional control valve (DCV), and a counterbalance valve (CBV).

The term negative load is introduced at this point. A negative load is when the external force, F_L, points in the same direction as the velocity of the cylinder piston i.e. a load that tends to drive the actuator as a pump. Typically, the CBV is active (throttling) when the cylinder is subjected to a negative load.

It is well known that the combination of valve components found in the BC tends to introduce instability. The problem has previously been investigated by e.g. Miyakawa (1978), Persson et al. (1989), Persson et al. (1990), Handroos et al. (1993), Zähe (1995), Hansen and Andersen (2010) and Zähe et al. (2016). It is mainly a problem when the controlled actuator is subjected

to a negative load.

The instability leads to in pressure oscillations in the hydraulic circuit which cause the mechanical structure to oscillate. The consequences of the oscillations are a decreased accuracy of the boom motion which creates a safety risk and a reduced productivity. In addition, the oscillations introduce undesirable extra fatigue load on both the mechanical structure and hydraulic system. Also, the oscillations may easily transfer to the surroundings as vibrations harming other equipment. The severity of the oscillations is affected by a wide variety of parameters, some of which are hard to predict or change: external load on the actuator, the properties of the mechanical structure, the damping and hysteresis of the CBV, the operator input as well as the volumes and restrictions in the hydraulic lines.

When designing a hydraulic system like the BC combining negative loads together with pressure compensated metering-in flow it is a major challenge to ensure stability during operation. Over the years a number of solutions have been presented for dealing with the problem of unwanted oscillations for certain applications and in specific work points. However, a general solution that can be transferred to the knuckle-boom cranes has not been presented yet. The proposed solutions struggle with a number of drawbacks, for example slowing down the response of the system, increasing energy consumption, requiring a complex system tuning or that the solution only ensures stability in a narrow window of operation.

Even though the present problem is presented in relation to knuckle boom cranes, it is certainly not exclusive to such machinery. All load-carrying applications, e.g. telehandlers, winches, personal lifts etc. struggle with the same issues if hydraulically driven.

1.1 Research motivation

The motivation behind this dissertation is that still after many years one of the classical problems within hydraulics does not have an obvious solution. The goal has been to search for a solution to reduce the oscillations in hy-

draulically actuated knuckle boom cranes.

A solution should be able to address the instabilities without unnecessarily compromising system efficiency and response. At the same time robustness and reliability are the key performance criteria. Cranes operate in rough conditions, so it is important to use as few components as possible in order to reduce the probability of failure, while attempting to avoid the use of electronic components like sensors. Furthermore, it is desired that neither the load pressure independent metering-in flow created by CV nor the CBV multifunctionality are compromised.

Price is of course always an aspect in any development process, but is has not been in focus in this work. The apparent oscillatory behaviour of the crane's mechanical structure is determined by the actuation of it and the dynamics of the structure and payload. This project has solely focused on the investigation of the hydraulic actuation system. Reduction of the oscillations created by the structure and payload using for example input shaping techniques on the control signals, see Huey (2006) and Kjelland and Hansen (2015), is not investigated.

1.2 State of the art

This section presents the state of the art of dealing with the unwanted oscillations in the hydraulic system. The efforts can be divided into three groups:

- Parameter variations (pilot area ratio of CBV, pilot line orifices, etc.) on the circuit using the same main components.
- Feedback control of DCV.
- Replacement of either the CBV or the pressure compensated DCV with alternatives.

Parameter variations: The parameters of the BC have been subjected to extensive investigations over the years by, among others, Handroos et al. (1993), Zähe (1995) and Hansen and Andersen (2001a). It has been found

that the most influential parameters on the stability are the damping of the system and the pilot ratio of the CBV. A reduction of the pilot ratio of the CBV ensures a more stable operation, however, this will come at the expense of a higher pressure level and thereby cause a higher energy consumption, see Ritelli and Vacca (2013). This is especially pronounced for small external loads. Adding damping when designing the hydraulic circuit is another proven approach. By adding volumes, adding orifices, adding logic valves, etc. more damping in the system is introduced. Especially, interest has been focused on the pilot line to the CBV. By manipulating the pressure in the line to the CBV pilot port in different ways (adding delays, creating a difference in the path back and forth) positive effects can be achieved. Different commercial solutions are available, as for example those shown in figure 1.3, from Bosch Rexroth (Bosch Rexroth, 2016) and NEM Hydraulic (NEM Hydraulics, 2016).

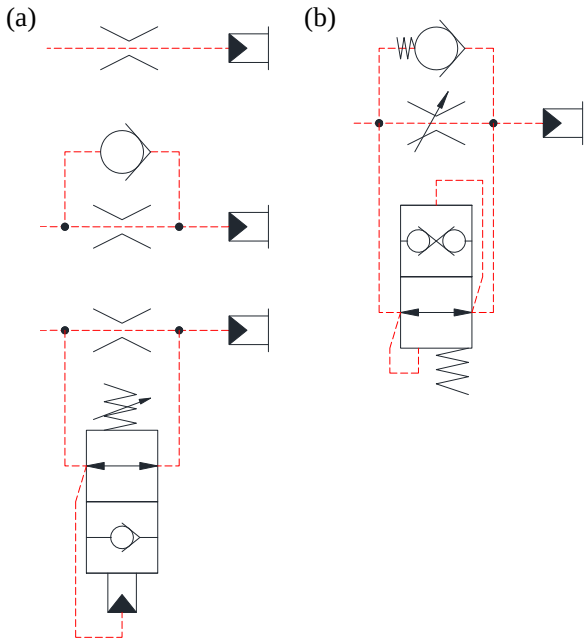

Figure 1.3: Examples of current solutions for damping the pilot line of the CBV. a) is from Bosch Rexroth (Bosch Rexroth, 2016) and b) is from NEM Hydraulic (NEM Hydraulics, 2016). The figure is also used in paper C.

However, common to the improvements presented in this category is that they are application and condition sensitive, especially towards load varia-

tions and variations in viscosity caused by temperature changes.

Feedback control of DCV: A different approach is to apply closed-loop control strategies to actively compensate for the oscillations. These strategies utilise the input signal to the DCV as the control element together with some kind of pressure feedback. One of the early examples of the use of active control was made by Krus and Palmberg (1989). Later Hansen and Andersen (2001b) proposed a feedback strategy where the idea is to keep the gradient of the high-pass filtered load pressure equal to zero. The strategy is implemented on the hydraulic circuit of a mobile loader crane with fine results. It was later investigated further in Hansen and Andersen (2010). The method has since been improved to address the narrow window of operation where the controller worked effectively by introduction an optimising routine to adjust the controller gains on-the-fly, see Cristofori et al. (2012) and Ritelli and Vacca (2014). This improved routine has shown promising results in reducing oscillations of cranes in general. However, it is yet to be seen how it handles negative loads. For all feedback control strategies relying solely on the DCV as the active control element the most important limitation is the bandwidth of typical DCVs. The valve needs a significantly higher bandwidth than the mechanical-hydraulic system.

Alternative hydraulic circuit design: The use of more than one CBV in parallel can improve stability as suggested by Zähe et al. (2016). A CBV with a low nominal flow rate is more stable than one with a high (Zähe et al., 2016). This is used by letting a CBV with a low nominal flow rate crack open first to handle low speeds and one with a high flow rate take over at high speed when the circuit is more stable.

Instead of trying to compensate on the inherently unstable BC, an alternative is to focus on the choice of valves. Given that the use of the CBV is regulated by legislation it is kept unchanged.

An option is to remove the CV, which will stabilise the system (Kjelland and Hansen, 2013). However, this also results in the loss of the direct con-

trol of the inlet flow and the flow sharing capabilities between neighbouring circuits. Both features are high on the list of demands in crane applications. They can be addressed by implementing velocity feedback control and electronic flow sharing, which increases both cost and system complexity. The performance demand of the DCV increases by implementing such features, often requiring the DCV to be replaced with a servo valve further increasing the cost.

Separate meter-in separate meter-out (SMISMO) techniques are also a possibility. They utilise two or more actively and individually controlled valves that open up for the combination of flow and pressure control in the inlet and outlet ports. However these systems are, inherently, less reliable and their performance is sensitive to parameter variations (Pedersen et al., 2010).

The use of DCV's, where the actuator inlet pressure is controlled instead of flow, is known to have a stabilising effect as suggested by Persson et al. (1990). However, it is rather undiscovered territory research-wise.

Another example is described in Nordhammer et al. (2012), where the main throttling ability is moved from the CBV to the return orifice of the DCV, thereby eliminating the oscillations. However, this is not a viable solution if the minimum load is about 60% or less of the maximum load, which strongly minimizes the applicability.

The focus in this project has been to look into alternative hydraulic circuit designs, since it was assessed that here could be found the biggest potential for improvement.

1.3 Outline of dissertation

This dissertation is based on a collection of papers while these introductory chapters are meant for tying together the work. In total the dissertation is based on four papers; two conference papers (papers A and B) and two journal papers (papers C and D).

This chapter has so far presented the motivation for the project, the re-

search question as well as the state of the art. It continues by presenting the published papers and finally the contribution of the dissertation to science is discussed.

In chapter 2 the laboratory equipment on which the experimental work has been conducted is presented.

Chapter 3-5 are each dedicated to a specific type of system, respectively the base circuit, the pressure control valve and the novel concept. Where the latter two are solutions able to minimise the oscillations from which the BC suffers. The chapters present some of the work already published in the attached papers, but they also elaborate the findings by including some so far unpublished results.

Finally chapter 6 concludes on the work and discusses the way forward.

1.4 Publications

The following papers are appended and will be referred to by the letters A-D. The papers are printed in their originally published state except for changes in format and minor errata. The referencing style to equations, figures and tables in the papers are kept local as well.

Paper A Sørensen, J.K., Hansen, M.R. and Ebbesen, M.K., "Boom Motion Control Using Pressure Control Valve", 8^{th} *FPNI Ph.D Symposium on Fluid Power.* Lappeenranta, Finland, June 10-13, 2014.

Paper B Sørensen, J.K., Hansen, M.R. and Ebbesen, M.K., "Load Independent Velocity Control On Boom Motion Using Pressure Control Valve", 14^{th} *Scandinavian International Conference on Fluid Power.* Tampere, Finland, May 20-22, 2015.

Paper C Sørensen, J.K., Hansen, M.R. and Ebbesen, M.K., "Novel concept for stabilising a hydraulic circuit containing counterbalance valve and pressure compensated flow supply", *International Journal of Fluid Power.* Publisher: Taylor & Francis, 2016. 17(3):152-162., doi: 10.1080/14399776.2016.1172446

Paper D (Submitted) Sørensen, J.K., Hansen, M.R. and Ebbesen, M.K., "Numerical and Experimental Study of a Novel Concept for Hydraulically Controlled Negative Loads", *Modeling, Identification and Control.* Publisher: Norwegian Society of Automatic Control, expected 2016.

1.5 Contributions

The main contributions to science of this project are summarised below:

- A novel concept for stabilising a hydraulic system containing a counterbalance valve and a pressure compensated flow supply is presented in paper C and is further investigated in paper D and chapter 5. Theory and experiments show a significant reduction of pressure oscillations with the concept implemented compared to the base circuit. The solution is patent pending.

- The eigen frequency of the mechanical structure has been identified as a central parameter in the pursuit of achieving stability of the system, see paper D. Lowering the eigen frequency of the mechanical structure minimise the stability problems.

- The use of a pressure control valve as a stabilising measure has been investigated theoretically and experimentally in paper A and B as well as in chapter 4. The valve shows good stabilising effects in comparison with the base circuit, however some drawbacks of the use were noticed as well.

- A control strategy has been developed to compensate for the main disadvantages of the pressure control valve: The load dependent dead band and the load dependent inlet flow. Using the proposed controller, the handling experience from an operators point-of-view is similar to the one of the flow control valve, see paper B.

- This thesis is providing an in depth comparison of stability of three

different hydraulic circuits implemented on a typical load-carrying application, see chapter 3-5 and paper C.

Chapter 2

Experimental setups

The experimental work of this project has been carried out on two different setups: One is a commercial mobile loader crane and one is a specially designed hydraulically actuated boom. Both setups are located at the mechatronics laboratory at University of Agder.

2.1 Experimental setup #1

Experimental setup #1 is a mobile loader crane manufactured by Højbjerg MaskinFabrik A/S, model 2020-K4. This setup was used as the basis for the experimental work for paper A and B.

In figure 2.1 the crane is shown together with an illustration presenting its components including sensors.

The crane is a four-degree of freedom machine consisting of a base, a slewing boom, a main boom, a jib boom, and a telescopic arm system. The experiments conducted for this dissertation only involve the cylinder controlled rotation of the jib boom relative to the main boom. The maximum reach of the crane is $4.5m$ when the telescopic arm is retracted and it has a load carrying capacity of $3910kg$ at that reach, see figure 2.2. Fully extended the reach increases to $12m$ with a load carrying capacity of $1240kg$.

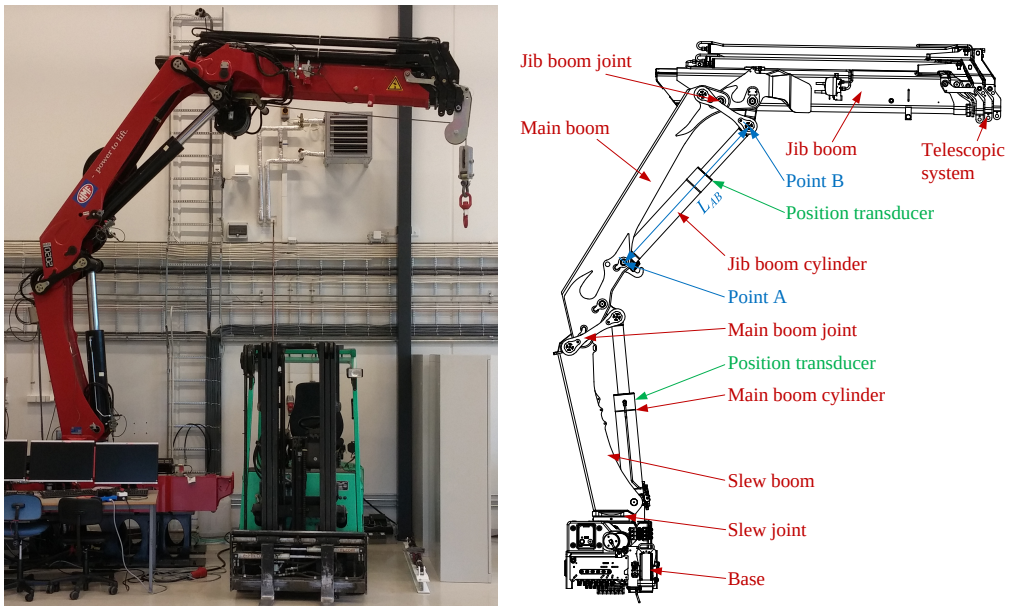

Figure 2.1: Experimental setup #1. Sensors are marked in green.

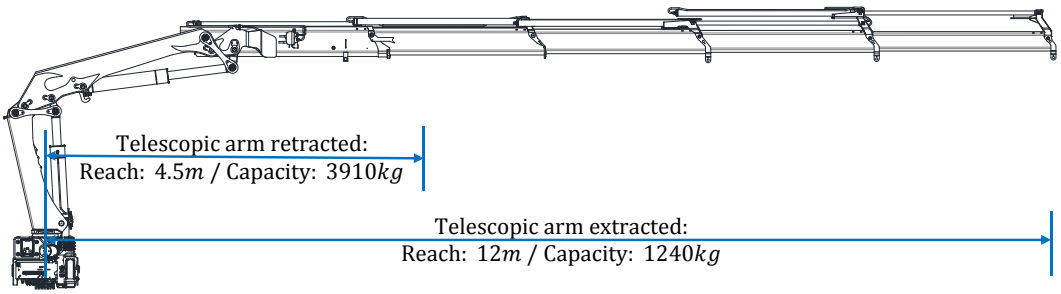

Figure 2.2: Reach and capacity of experimental setup #1.

The hydraulic diagram of the jib boom circuit is shown in figure 2.3 including the available sensors.

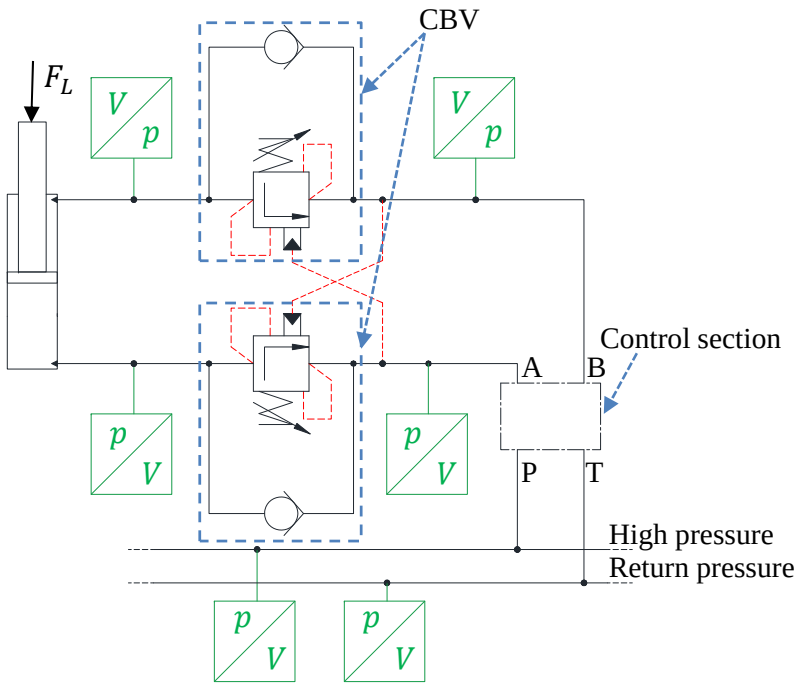

Figure 2.3: The jib boom circuit of setup #1, consisting of a pair of CBV's, a control section shown in more detail in figure 2.4 and a cylinder subjected to force in both directions. However, for these experiments only compressing force occurs. Sensors are marked in green.

Notice that the force on the cylinder, F_L, can change direction, hence the need for two CBV's. The CBV's are both 3-port versions manufactured by Oil Control with a 4.25:1 pilot area ratio, α_P, and a rated flow of $Q^r_{CBV} = 40L/min$. Some important data on the jib cylinder are listed in table 2.1.

Table 2.1: Jib cylinder data.

Parameter	Value
Minimum cylinder length	$L_{AB,min} = 1160mm$
Maximum cylinder length	$L_{AB,max} = 1980mm$
Cylinder stroke	$H_C = L_{AB,max} - L_{AB,min} = 820mm$
Cylinder piston diameter	$D_p = 150mm$
Cylinder rod diameter	$D_r = 100mm$
Cylinder area ratio	$\varphi = \frac{D_p^2}{D_p^2 - D_r^2} = 1.8$

The content of the control section shown in figure 2.3 is presented in figure 2.4.

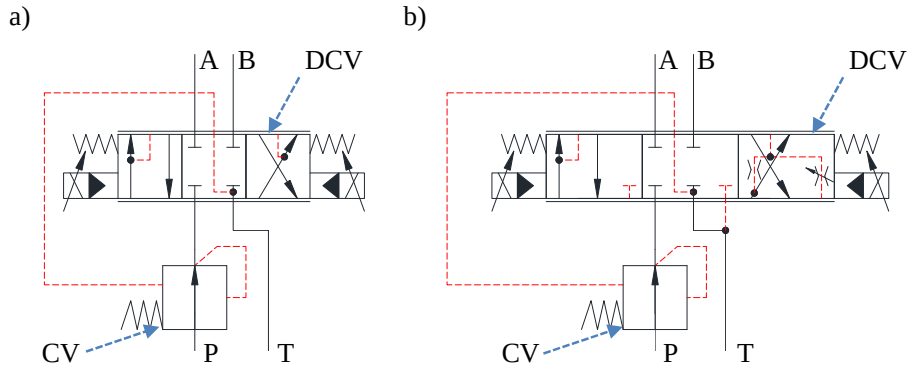

Figure 2.4: Control sections: a) DCV with a flow control spool as in the BC, b) DCV with a pressure control spool.

The hydraulic circuit is used in two different configurations. One has pressure compensation as in the BC and one has pressure control of the P-B metering-in. The variations in behavior are embedded in the main spool of the valve, i.e., the choice of main spool determines the combination of flow and/or pressure control. This ensures that flow control can be maintained during cylinder extraction and, simultaneously, be abandoned during cylinder retraction. In both cases it is a 4/3-way directional pressure compensated control valve group model PVG32 from Danfoss where the DCV and CV are embedded. It has an electro-hydraulic actuation with linear flow vs. input signal characteristics. The spools have a maximum rated flow of $Q_{DCV}^{max} = 40L/min$. The experiments are conducted with a supply pressure

$p_S = 200bar$.

A real-time I/O system (CompactRio system from National Instruments) is used to control the hydraulic valves on the boom with a loop time of $10ms$. The control system can record sensor information from all the position and pressure sensors mounted on the experimental setup.

2.2 Experimental setup #2

This setup is a hydraulically actuated boom that is designed and built specifically for this project. It was designed with a simpler and more rigid mechanical structure that in combination with the BC ensured instability.

The setup was used in paper C and D, as well as being the reference system for the linear stability analysis in sections 3.1, 4.1 and 5.1.

In figure 2.5 is the setup shown. The illustration to the right presents its components including sensors.

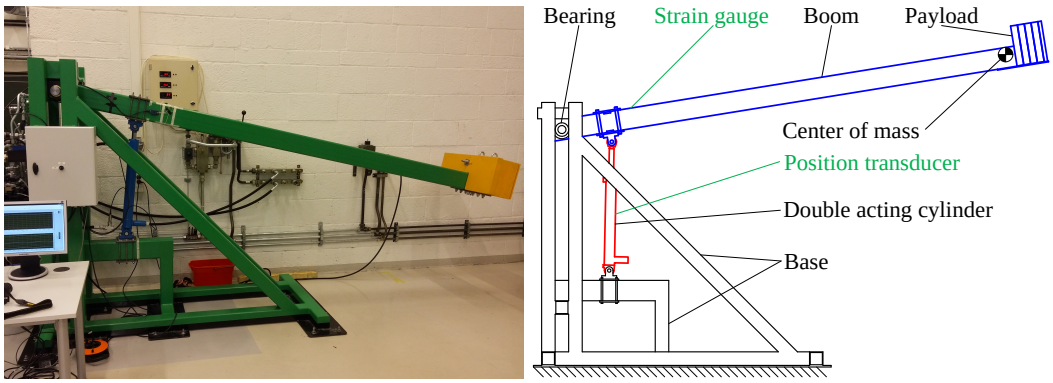

Figure 2.5: Experimental setup #2. Sensors are marked in green.

The setup is a simple one-degree of freedom structure. The distance from the bearing to the mass centre of the boom and payload is $L = 3570mm$ and the combined mass is $m = 410kg$.

The hydraulic diagram is shown in figure 2.6 including the sensors. The hydraulic system consists of two parts: a primary circuit and a secondary one required for the novel concept. The primary circuit includes the well known components: a CBV, a control section, and a cylinder subjected to

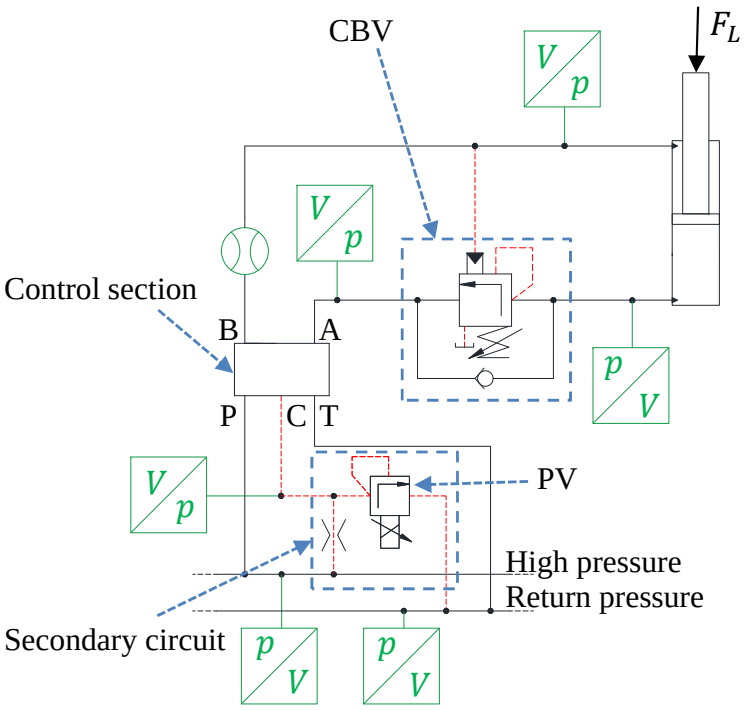

Figure 2.6: The hydraulic circuit of setup #2. It consists of a control section (see more in figure 2.7), a CBV, and a cylinder subjected to a compressing force, F_L. Besides that there is installed a secondary circuit which is utilised by the novel concept. The secondary circuit consists of a proportional pressure relief valve (PV) and an orifice. Sensors are marked in green.

a compressing force, F_L. The 4-port CBV is from Sun Hydraulics model CWCA with a 3:1 pilot area ratio, α_P, and a rated flow of $Q^r_{CBV} = 60L/min$.

The pressure controlling capabilities desired in the secondary circuit are realised by an inlet orifice and a proportional pressure relief valve (PV). The orifice has a pressure drop $\Delta p|_{@2L/min} = 220bar$ and the PV model DBETE from Bosch Rexort has a crack pressure that increases linearly with the voltage input. The valve cracks open at $p_{C@0L/min} = 185bar$ and has a rated pressure $p^r_{PV} = p_{C@0.8L/min} = 200bar$. The control strategy of the secondary circuit is described in more details in paper C and D. Information about the hydraulic cylinder is listed in table 2.2.

Table 2.2: Experimental setup #2 cylinder data.

Parameter	Value
Cylinder stroke	$H_c = 500mm$
Cylinder piston diameter	$D_p = 65mm$
Cylinder rod diameter	$D_r = 35mm$
Cylinder area ratio	$\mu_C = \frac{D_p^2}{D_p^2 - D_r^2} = 1.41$

The content of the control section shown in figure 2.6 is presented in figure 2.7.

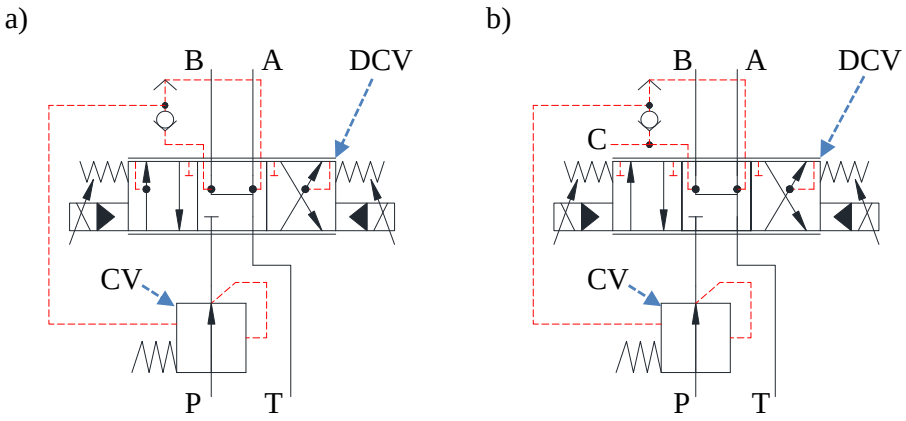

Figure 2.7: Control sections: a) DCV with a flow control spool as in the BC, b) DCV with a flow control spool used for the novel concept.

Experimental setup #2 uses the same type of DCV group as the one used

in experimental setup #1, i.e. a 4/3-way pressure compensated directional control valve group from Danfoss model PVG32 where the DCV and CV are embedded. It has electro-hydraulic actuation with linear flow vs. input signal characteristics. There are three options of configuration:

O1 The BC with flow control of the P-B metering-in i.e. the secondary circuit is not connected to port C. This is option a) in figure 2.7.

O2 This is the implementation of the novel concept. The circuit is basically the BC, where a minor modification (blocking an orifice) has been made on the main spool. This allows for the pressure of the secondary circuit (C) to control the opening of the CV instead of the load pressure from the B-port as usual. O2 is shown in figure 2.7 option b).

O3 A third option is using the pressure control of the the P-B metering-in, like experimental setup #1's option b), see figure 2.7. However, this option is only treated theoretically in this project, see section 4.1.

The maximum rated flow of $Q_{DCV}^{max} = 25L/min$ is the same for all three spool options. The experiments are conducted with a supply pressure at $p_S = 180bar$.

A real-time I/O system (CompactRio system from National Instruments) is used to control the hydraulic valves on the boom. The I/O system has a loop time of $10ms$. The control system can record sensor information from all the position and pressure sensors mounted on the experimental setup. The primary circuit is controlled by supplying an input signal to the DCV.

Chapter 3

Base circuit

This chapter presents the base circuit (BC) in more detail. The BC consists, as already introduced, of a CV, a DCV and a CBV, as shown in the hydraulic circuit in figure 1.2. The part with the CV and DCV is enlarged and shown in figure 3.1. Only the part relevant for downward motion is shown.

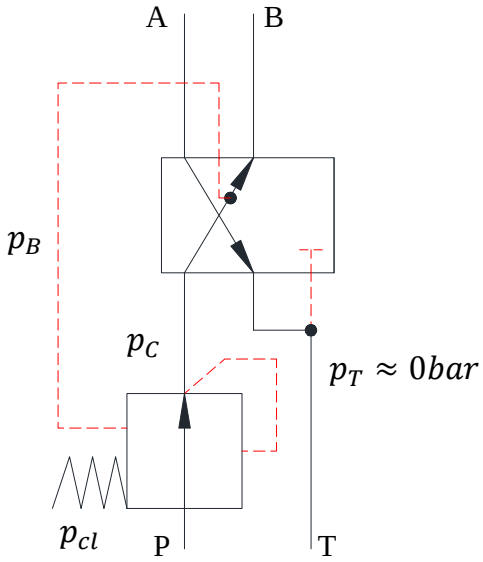

Figure 3.1: Schematic of the DCV valve (only shown for the part of moving downward) with flow controlled metering-in.

The pressure drop across the metering-in orifice is determined by the pressure compensator and is given by the following equation when assuming a

fast CV:

$$p_\Delta = p_B + p_{CL} - p_B = p_{CL} \tag{3.1}$$

where p_{CL} is the set pressure of the compensator spring that relates to the fully closed position. The orifice equation for the valve becomes:

$$Q_{P-B} = C_d \cdot A_d(x) \cdot \sqrt{\frac{2}{\rho} \cdot p_{cl}} \tag{3.2}$$

This nice relation between the opening area $A_d(x)$ and the inlet flow Q_{P-B} is one of the main advantages of adding the CV. Another advantage is that it allows for flow sharing capabilities with neighbouring valve modules. Both advantages are often asked for in crane applications.

3.1 Linear stability analysis

A linearised stability analysis is used to investigate the characteristic of the BC implemented on experimental setup #2. In figure 3.2 is shown a simplified circuit of the considered system including the core components and variables. The circuit is shown in a situation where the actuator is subjected to a negative load in a lowering motion.

The governing equations for the system are:

$$m_{eff} \cdot \dot{v}_C = p_B \cdot A_B - p_A \cdot \mu_C \cdot A_B + F_{cyl,static} \tag{3.3}$$

$$C_A \cdot \dot{p}_A = \mu_C \cdot A_B \cdot v_C - Q_{CBV} \tag{3.4}$$

$$C_B \cdot \dot{p}_B = Q_{DCV} - A_B \cdot v_C \tag{3.5}$$

$$Q_{DCV} = k_{v,DCV} \cdot u_{DCV} \cdot \sqrt{p_\Delta} = k_{v,DCV} \cdot u_{DCV} \cdot \sqrt{p_{CL}} \tag{3.6}$$

$$Q_{CBV} = k_{v,CBV} \cdot u_{CBV} \cdot \sqrt{p_A} \tag{3.7}$$

$$u_{CBV} = \frac{p_B \cdot \alpha_P + p_A - p_{cr}}{\Delta p_{op,CBV}} \tag{3.8}$$

where m_{eff} is the effective mass which the cylinder experiences from the me-

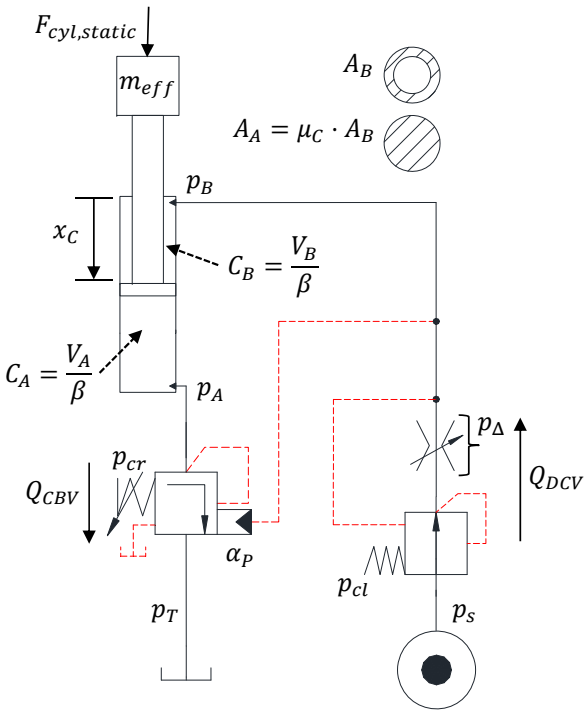

Figure 3.2: Simplified circuit of BC.

chanical system when it accelerates and $F_{cyl,static}$ is the static external force the cylinder. μ_C is the cylinder's area ratio. The variables u_{DCV} and u_{CBV} are the dimensionless opening of respectively the DCV and CBV. $k_{v,DCV}$ and $k_{v,CBV}$ are valve constants. Finally, the value $\Delta p_{op,CBV}$ is the extra pressure required to fully open the CBV, α_P is the pilot area ratio of the CBV and p_{cr} is the crack pressure of the CBV. In the equations above a number of assumptions have been made including: no back pressure, no friction or damping in the cylinder or in the valves, no valve dynamics, no flow forces, and a linear discharge characteristic of the counterbalance valve.

Linearising the above equations yields the following expressions in the Laplace domain. The tilde denotes any parameter variation relative to the steady state value.

$$m_{eff} \cdot s \cdot \tilde{v}_C = A_B \cdot \tilde{p}_B - \mu_C \cdot A_B \cdot \tilde{p}_A \tag{3.9}$$

$$C_A \cdot s \cdot \tilde{p}_A = \mu_C \cdot A_B \cdot \tilde{v}_C - \tilde{Q}_{CBV} \tag{3.10}$$

$$C_B \cdot s \cdot \tilde{p}_B = \tilde{Q}_{DCV} - A_B \cdot \tilde{v}_C \tag{3.11}$$

$$\tilde{Q}_{DCV} = k_{qu,DCV} \cdot \tilde{u}_{DCV} \tag{3.12}$$

$$\tilde{Q}_{CBV} = k_{qu,CBV} \cdot \tilde{u}_{CBV} + k_{qp,CBV} \cdot \tilde{p}_A \tag{3.13}$$

$$\tilde{u}_{CBV} = \frac{\tilde{p}_B \cdot \alpha_P + \tilde{p}_A}{\Delta p_{op,CBV}} \tag{3.14}$$

where the valve gains in equation (3.12) and (3.13) are defined by:

$$k_{qu,DCV} = k_{v,DCV} \cdot \sqrt{p_{CL}} \tag{3.15}$$

$$k_{qu,CBV} = k_{v,CBV} \cdot \sqrt{p_A^{ss}} \tag{3.16}$$

$$k_{qp,CBV} = \frac{k_{v,CBV} \cdot u_{CBV}^{ss}}{2 \cdot \sqrt{p_A^{ss}}} \tag{3.17}$$

To simplify equation (3.13) an additional valve gain is introduced:

$$k_{qo,CBV} = \frac{k_{qu,CBV}}{\Delta p_{op,CBV}} = \frac{k_{v,CBV} \cdot \sqrt{p_A^{ss}}}{\Delta p_{op,CBV}} \tag{3.18}$$

By inserting $k_{qo,CBV}$ together with equation (3.14) into equation (3.13) it simplifies to:

$$\tilde{Q}_{CBV} = (k_{qo,CBV} + k_{qp,CBV}) \cdot \tilde{p}_A + k_{qo,CBV} \cdot \alpha_P \cdot \tilde{p}_B \tag{3.19}$$

The closed loop transfer function of the system $G(s)$ with valve opening u_{DCV} as input and the cylinder displacement flow $A_B \cdot \tilde{v}_C$ as output can be derived from equations (3.9)-(3.12) and (3.19). The transfer function is of third order and is expressed by:

$$G(s) = \frac{A_B \cdot \tilde{v}_C}{u_{DCV}} = \frac{N_1 \cdot s + N_0}{D_3 \cdot s^3 + D_2 \cdot s^2 + D_1 \cdot s + D_0} \tag{3.20}$$

where

$$N_1 = k_{qu,DCV} \cdot C_A \cdot A_B^2 \tag{3.21}$$

$$N_0 = (k_{qp,CBV} + (1 + \alpha_P \cdot \mu_C) \cdot k_{qo,CBV}) \cdot k_{qu,DCV} \cdot A_B^2 \tag{3.22}$$

$$D_3 = C_A \cdot C_B \cdot m_{eff} \tag{3.23}$$

$$D_2 = (k_{qo,CBV} + k_{qp,CBV}) \cdot C_B \cdot m_{eff} \tag{3.24}$$

$$D_1 = (C_A + C_B \cdot \mu_C^2) \cdot A_B^2 \tag{3.25}$$

$$D_0 = (k_{qp,CBV} + (1 + \alpha_P \cdot \mu_C) \cdot k_{qo,CBV}) \cdot A_B^2 \tag{3.26}$$

To evaluate the stability of the linear model the Routh-Hurwitz stability criterion is used. From the Routh-Hurwitz array it is derived that the system is stable if the following two inequalities are fulfilled:

$$D_i > 0 \text{ , for } i = 0 \ldots 3 \tag{3.27}$$

$$D_2 \cdot D_1 - D_3 \cdot D_0 > 0 \tag{3.28}$$

The first requirement will always be satisfied, since no parameters exist with negative or zero value. Equation (3.28) is investigated numerically. In figure 3.3 is shown the minimum dimensionless opening of the DCV, u_{DCV}^{ref}, that yields a stable system plotted as a function of the piston position, x_C. Notice that dead band compensation has been implemented on the DCV, hence $u_{DCV}^{ref} = 0$ at the start of the actual valve opening.

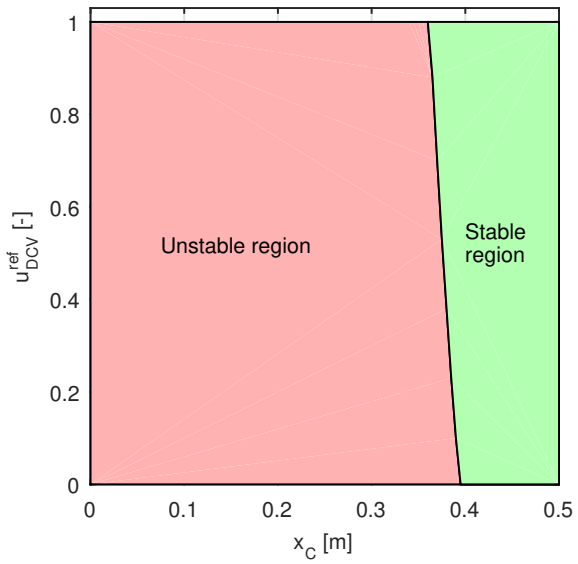

Figure 3.3: Stability of BC. The minimum dimensionless opening of the DCV, u_{DCV}^{ref}, that yields a stable system is plotted as a function of the piston position, x_C.

The red region in figure 3.3 indicates where the system is unstable according to the linear analysis. It is clear that experimental setup #2 when combined with the BC is unstable over most of the operation range. Stability is only achieved with the piston at the lowest approximately $0.1m$ of the cylinder's operation range.

In the introduction it was stated that different parameters can influence the stability of the BC. The established linear model is used to perform a parameter study.

In figure 3.4 is shown the effect which a change in the volume of the cylinder rod side chamber, V_B has on the stability of the system and how a change in payload alters the results. Again the minimum dimensionless opening of the DCV, u_{DCV}^{ref}, that yields a stable system is plotted as a function of the piston position, x_C.

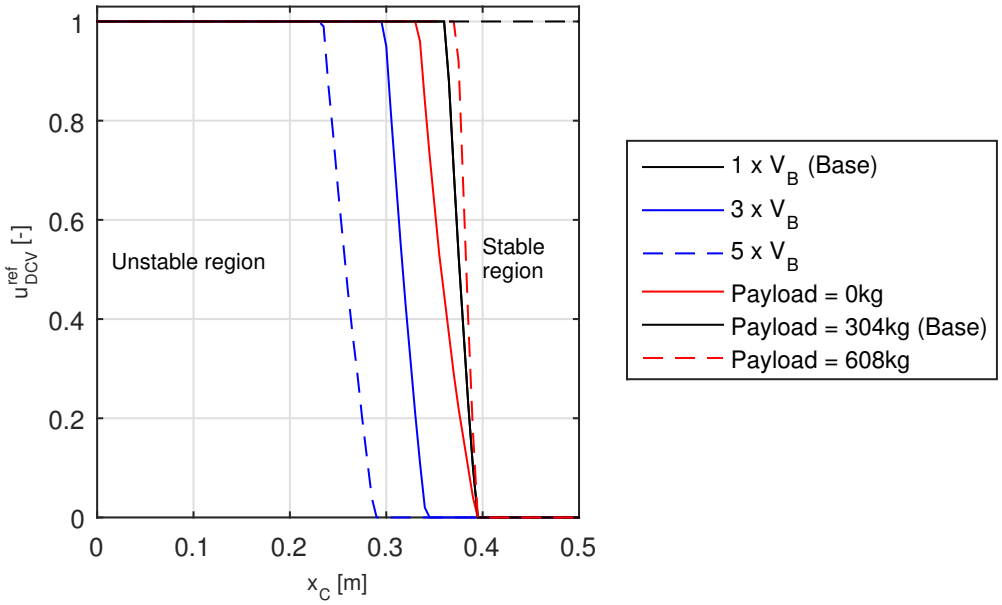

Figure 3.4: Stability of the BC when the volume of the cylinder rod side chamber, V_B, and the payload are varied. The minimum dimensionless opening of the DCV, u_{DCV}^{ref}, that yields a stable system, is plotted as a function of the piston position, x_C.

It is clear that an increased inlet volume, V_B, has a stabilising effect on the system. However, an increase of the size of the inlet volume is also known to

influence the system's response time negatively; it simply takes longer time to raise the pressure level. The influence on stability due to change in payload is less pronounced, though the actual payload is of course a quantity that the designer has little influence on.

The stability obtainable when varying the pilot area ratio of the CBV, α_P, is plotted in figure 3.5 together with curves for different sized CBV's. As expected, the pilot area ratio of the CBV has a significant effect on the stability. The downside of lowering the pilot area ratio is the increase of pressure level in the system, which results in an increase in energy consumption. Some effect of changing between CBV's with different rated flows can be observed in figure 3.5. Lowering $k_{v,CBV}$ does have a stabilising effect, however, it is not significant. Also notice that this evaluation does not take into account other changes to the system caused by the change of CBV.

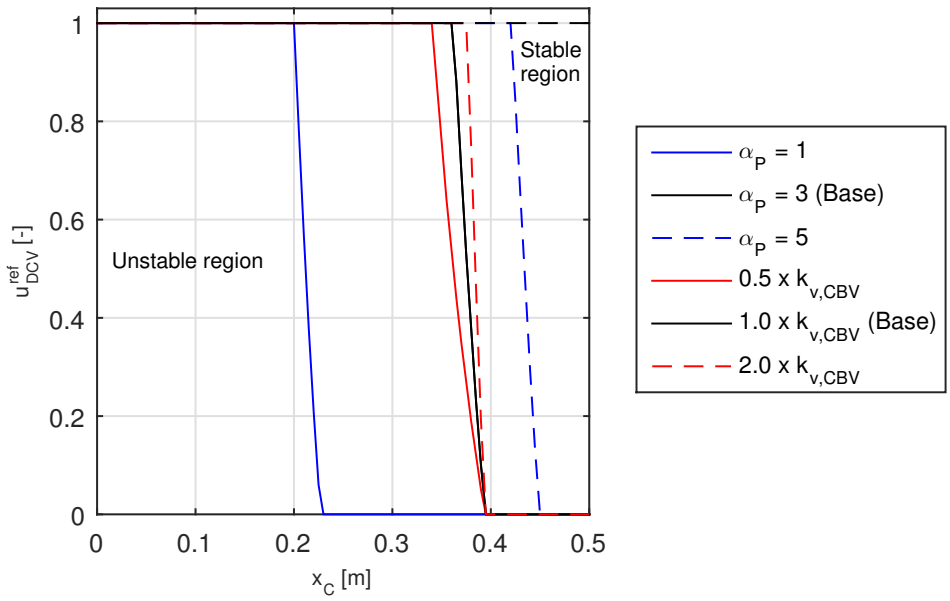

Figure 3.5: Stability of BC when varying the pilot area ratio of the CBV, α_P, and the CBV valve constant $k_{v,CBV}$. The minimum dimensionless opening of the DCV, u^{ref}_{DCV}, that yields a stable system is plotted as a function of the piston position, x_C.

This small parameter study has shown that, even though an optimisation of some parameters definitely can improve the stability of the system, this is not able to make drastic changes. Hence the pursuit of stability is made

elsewhere.

The following chapters focus on two different solutions both able to improve the stability of the system. One is the use of a pressure control valve. The other is a novel concept for addressing the shortcomings of the BC.

Chapter 4

Pressure control valve

A rather well-known way of reducing the oscillations in cranes is by using pressure controlled directional control valves. These have proved efficient in dealing with the oscillations, however there are drawbacks in using them. The investigated valve is a commercially available type PVG32 manufactured by Danfoss A/S. The concept of the valve is definitely not new, since it has been on the market for many years. However, still little theoretical information of its use is available. The focus of paper A was to investigate the valve further.

This valve from Danfoss is interesting because it can be perceived as a cost effective alternative for reducing the oscillations. Furthermore the implementation chosen by Danfoss, where the pressure control is integrated in the main spool, makes it very simple to alter a circuit between pressure control and flow control. This is a practical property if a machine which is already built turns out to be unstable.

A hydraulic diagram showing how the valve in question differs from a classical pressure compensated DCV is shown in figure 4.1. Notice that only the part for lowering motion is presented. The first thing that is noticed with the pressure controlled metering-in (b) is that there is no direct connection to the compensator sensing the load like in (a). This causes the inlet flow to be load dependent, instead of independent. The opening of the compensator and hence the pressure p_C is controlled by the ratio between the two orifices, A_0

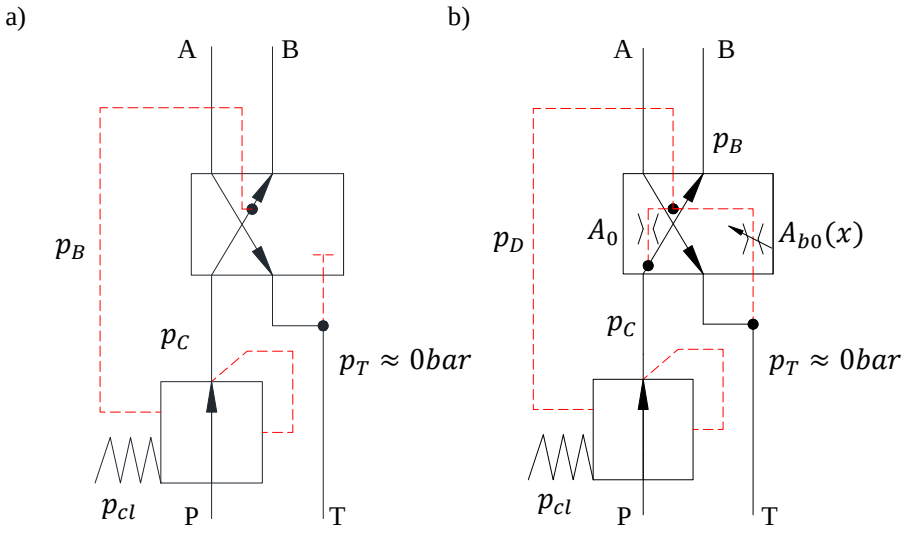

Figure 4.1: Schematic of the DCV valve (only shown for the part of moving downward): a) Pressure compensated metering-in, b) pressure controlled metering-in.

and $A_{b0}(x)$.

$$p_C(x) = \left[\frac{1+\mu(x)^2}{\mu(x)^2}\right] \cdot p_{cl} \tag{4.1}$$

where

$$\mu(x) = \frac{A_{b0}(x)}{A_0} \tag{4.2}$$

By carefully designing the variable orifice discharge area characteristics, $A_{b0}(x)$, an approximately linear pressure characteristic can be obtained, as shown in figure 4.2.

The physical parameters presented in figure 4.2 are given as:

- $p_{DCVPC,max} = 300bar$ is the maximum DCV pressure.
- $S_{PC,max} = 7mm$ is the maximum spool travel.
- $S_{PC,DB} = 0.8mm$ is the spool position at dead band.
- $S_{PC,range} = 4.7mm$ is the spool range in which the pressure varies.

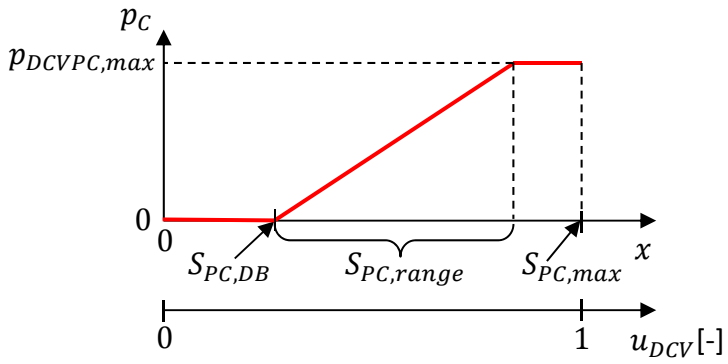

Figure 4.2: Pressure control valve characteristic: pressure p_C as a function of the spool position.

The orifice equation for the BC in equation (3.2), changes in this case to:

$$Q_{P-B} = C_d \cdot A_d(x) \cdot \sqrt{\frac{2}{\rho} \cdot (p_C(x) - p_B)} \tag{4.3}$$

where not only the opening area A_d depends on the main spool position x, but also the pressure before the main spool p_C. One consequence is that the direct relationship between the input signal and the inlet flow disappears. The concept is explained in more detail in paper A and paper B.

To demonstrate the effect of the use of a PCV, an experiment was conducted on experimental setup #1 and the results are compared to the BC, see figure 4.3 and 4.4. The first figure shows the pressures on both sides of the cylinder when a step input ($u_{DCV}^{ref} = 0.10$) is provided to move the cylinder downwards. The stabilising effect is clear as the pressures from the circuit with the PCV (referred to as PCC) quickly settle. Figure 4.4 shows the two cylinder velocities from the same experiment. Both used spools have the same flow rating and the same input. Still, the steady state velocity differs quite a bit, due to the difference in design. The PCV does not utilise the flow controlling capabilities of the CV. If the difference in velocity is undesired, it can be eliminated by implementing closed loop motion control on the PCV.

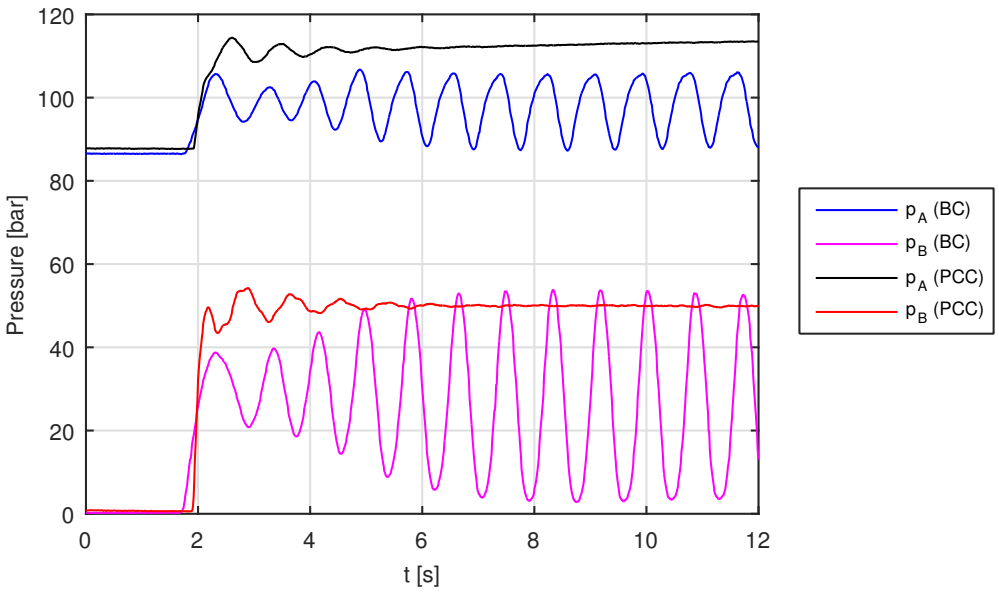

Figure 4.3: Comparison of pressures of the jib cylinder of experimental setup #1 between the BC and the pressure control circuit (PCC) for a step input $u_{DCV}^{ref} = 0.10$.

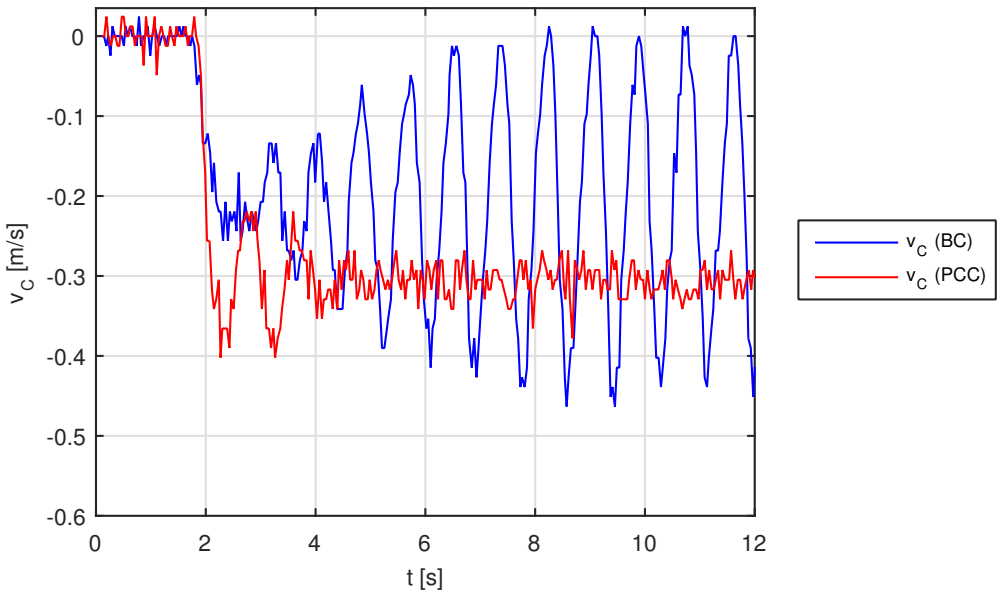

Figure 4.4: Comparison of velocities of the jib cylinder of experimental setup #1 between the BC and the PCC for a step input $u_{DCV}^{ref} = 0.10$.

4.1 Linear stability analysis

The PCC is analysed with respect to stability like the BC in section 3.1. Again experimental setup #2 is used as the reference system. A simplified circuit of the system considered is shown in figure 4.5. Only the lowering motion of the actuator that is subjected to a negative load is treated in this analysis.

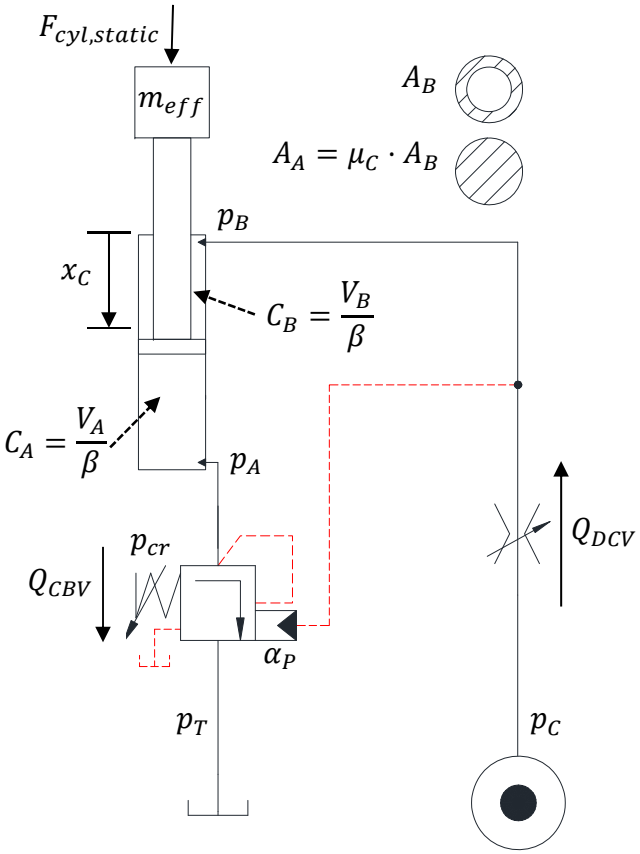

Figure 4.5: Simplified circuit of PCC.

The difference between the two systems is the DCV used, which means that the remaining govering equations are unchanged. Equation (4.3) for the DCV flow can be rewritten to:

$$Q_{DCV} = k_{v,DCVPC} \cdot u_{DCV} \cdot \sqrt{p_C(u_{DCV}) - p_B} \tag{4.4}$$

$p_C(u_{DCV})$ is derived from figure 4.2 as:

$$p_C(u_{DCV}) = \begin{cases} 0 & ,0 \leq u_{DCV} < 0.11 \\ k_{PC1} \cdot u_{DCV} - k_{PC2} & ,0.11 \leq u_{DCV} \leq 0.79 \\ p_{DCVPC,max} & ,0.79 < u_{DCV} \leq 1 \end{cases} \tag{4.5}$$

where the two valve constants k_{PC1} and k_{PC2} are determined as:

$$k_{PC1} = \frac{p_{DCVPC,max} \cdot S_{PC,max}}{S_{PC,range}} \tag{4.6}$$

$$k_{PC2} = \frac{p_{DCVPC,max} \cdot S_{PC,DB}}{S_{PC,range}} \tag{4.7}$$

Linearising equation (4.4), in the region $0.11 \leq u_{DCV} \leq 0.79$, yields:

$$\begin{aligned} \tilde{Q}_{DCV} &= k_{qu,DCV} \cdot \tilde{u}_{DCV} + k_{qp,DCV} \cdot (k_{PC1} \cdot \tilde{u}_{DCV} - \tilde{p}_B) \\ &= (k_{qu,DCV} + k_{qp,DCV} \cdot k_{PC1}) \cdot \tilde{u}_{DCV} - k_{qp,DCV} \cdot \tilde{p}_B \end{aligned} \tag{4.8}$$

where the valve gains are defined as:

$$k_{qu,DCV} = k_{v,DCVPC} \cdot \sqrt{k_{PC1} \cdot u_{DCV}^{ss} - k_{PC2} - p_B^{ss}} \tag{4.9}$$

$$k_{qp,DCV} = \frac{k_{v,DCVPC} \cdot u_{DCV}^{ss}}{2 \cdot \sqrt{k_{PC1} \cdot u_{DCV}^{ss} - k_{PC2} - p_B^{ss}}} \tag{4.10}$$

The expression in equation (4.8) can be recognised as being the same as for a circuit with a constant pressure supply and a servo valve. By combining equation (4.8) with equations (3.9)-(3.11) and (3.19), a third order transfer function is derived:

$$G(s) = \frac{A_B \cdot \tilde{v}_C}{u_{DCV}} = \frac{N_1 \cdot s + N_0}{D_3 \cdot s^3 + D_2 \cdot s^2 + D_1 \cdot s + D_0} \tag{4.11}$$

where

$$N_1 = (k_{qu,DCV} + k_{PC1} \cdot k_{qp,DCV}) \cdot C_A \cdot A_B^2 \tag{4.12}$$

$$N_0 = (k_{qo,CBV} + k_{qp,CBV} + \alpha_P \cdot k_{qo,CBV} \cdot \mu_C) \cdot (k_{qu,DCV} + k_{PC1} \cdot k_{qp,DCV}) \cdot A_B^2 \tag{4.13}$$

$$D_3 = C_A \cdot C_B \cdot m_{eff} \tag{4.14}$$

$$D_2 = (C_A \cdot k_{qp,DCV} + (k_{qo,CBV} + k_{qp,CBV}) \cdot C_B) \cdot m_{eff} \tag{4.15}$$

$$D_1 = (C_A + C_B \cdot \mu_C^2) \cdot A_B^2 + (k_{qo,CBV} + k_{qp,CBV}) \cdot k_{qp,DCV} \cdot m_{eff} \tag{4.16}$$

$$D_0 = (k_{qo,CBV} + k_{qp,CBV} + k_{qp,DCV} \cdot \mu_C^2 + \alpha_P \cdot k_{qo,CBV} \cdot \mu_C) \cdot A_B^2 \tag{4.17}$$

For $0.79 < u_{DCV} \leq 1$, where the valve has reached the upper pressure limit $p_{DCVPC,max}$ equation (4.8) becomes:

$$\tilde{Q}_{DCV} = k_{qu,DCV} \cdot \tilde{u}_{DCV} - k_{qp,DCV} \cdot \tilde{p}_B \tag{4.18}$$

with the valve gains defined as:

$$k_{qu,DCV} = k_{v,DCVPC} \cdot \sqrt{p_{DCVPC,max} - p_B^{ss}} \tag{4.19}$$

$$k_{qp,DCV} = \frac{k_{v,DCVPC} \cdot u_{DCV}^{ss}}{2 \cdot \sqrt{p_{DCVPC,max} - p_B^{ss}}} \tag{4.20}$$

The transfer function for this region has an unchanged denominator while the nominator coefficients in equation (4.12) and (4.13) changes to:

$$N_1 = k_{qu,DCV} \cdot C_A \cdot A_B^2 \tag{4.21}$$

$$N_0 = (k_{qo,CBV} + k_{qp,CBV} + \alpha_P \cdot k_{qo,CBV} \cdot \mu_C) \cdot k_{qu,DCV} \cdot A_B^2 \tag{4.22}$$

The stability of the system is again evaluated numerically by using the Routh-Hurwitz stability criteria. In figure 4.6 is shown the minimum dimensionless opening of the DCV, u_{DCV}^{ref}, that yields a stable system plotted as a function of the piston position, x_C. Notice the physical dead band of the DCV has been compensated, hence $u_{DCV}^{ref} = 0$ is at a spool position at $S_{PC,DB}$, where the pressure begins to rise.

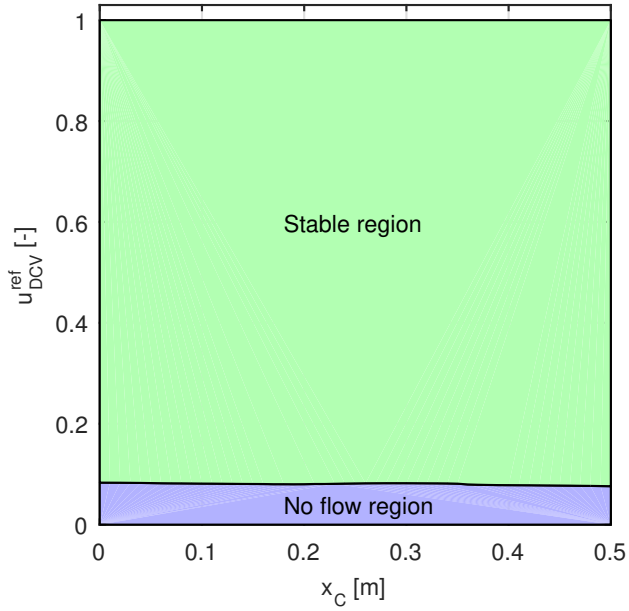

Figure 4.6: Stability of PCC. The minimum dimensionless opening of the DCV, u^{ref}_{DCV}, that yields a stable system is plotted as a function of the piston position, x_C.

The analysis indicates that the PCC is stable in all positions for all valve openings for experimental setup #2. Another observation is the no flow region. When the pressure set by the DCV is less than the required p_B, no oil can flow into the circuit. The limit between the two regions changes as the cylinder extends, hence changing the load on the cylinder.

4.2 Concluding remarks

The use of a pressure control spool in the DCV is a simple and robust solution to the stability problem of the BC. Actually the mobile loader crane used as experimental setup #1 is delivered with one installed on both the main boom and the jib boom.

Drawbacks of using this valve type is the load dependent dead band and load dependent inlet flow as pinpointed in paper A. In order to achieve similar behaviour as the normal pressure compensated DCV a closed loop control system is required. For that purpose control schemes were developed

that give respectively a load independent dead band and a load independent metering-in flow. They are presented in paper B. The performance of each of the schemes was investigated with a varying number of sensors to find the minimum required. In order to address the dead band load dependency a transducer measuring the pressure between the CBV and the piston side of the cylinder was added. This sensor improved the effectiveness of the dead band compensation markedly compared to the alternative without added sensor. A control strategy using a position transducer was presented, capable of emulating the load independent metering-in flow of the pressure compensated DCV of the BC. Again, a better performance can be obtained by adding an additional sensor to the system. The strategy utilises a pressure transducer between the inlet of the DCV and the cylinder together with an experimentally obtained mapping of the steady state valve flow characteristics in a feed forward approach.

Experiments have revealed that below an inlet pressure of approximately 40*bar* the valve acts more unpredictably. The backpressure is not drained, which causes the controller developed in paper B to struggle. Other drawbacks from a crane builders point of view is that only one manufacturer offers this valve type and that the current model assortment is limited.

Chapter 5

Novel concept

This chapter presents a novel concept that significantly reduces oscillations in hydraulic systems containing a CBV in series with a pressure compensated flow supply. The solution is patent pending, see Hansen and Sørensen (2015), and is the main focus of paper C and D.

The hydraulic diagram of the novel concept circuit (NCC) is shown in figure 5.1. The figure only shows the concept in a situation where the flow is metered in to the B-port of the cylinder. With an external compressive force, as indicated in the figure, this corresponds to handling a negative load and is therefore prone to instability.

The underlying idea of the novel concept is to suppress oscillations in the system by detaching the hydraulic pilot line from the B-port pressure to the pressure compensator valve (CV) (the magenta dashed line in figure 5.1) and instead generate the steady state value of the B-port pressure in the secondary circuit (SC). The novel concept encompasses solutions, where the SC is connected only to the CV (option #1) and where the SC is connected to both the CV and the CBV (option #2).

Figure 5.2 demonstrates the effect of the novel solution. It shows the pressures on both sides of the cylinder for the BC and for the NCC when providing a ramp input downwards on experimental setup #2, see section 2.2. For further details see paper C and D.

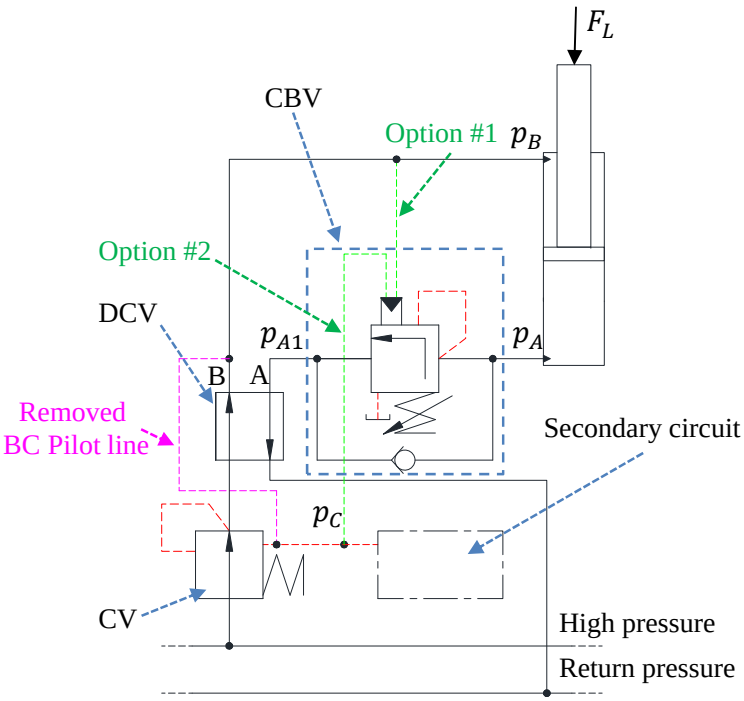

Figure 5.1: Hydraulic diagram of the novel concept circuit (NCC). The figure only shows the lowering case. The pilot line from the BC is removed in the novel concept. Either option #1 or option #2 is chosen.

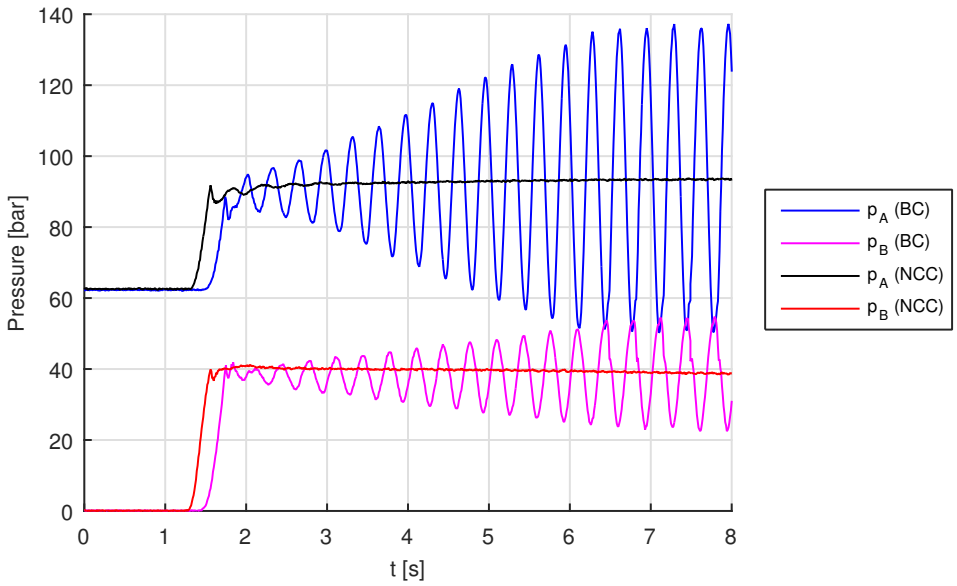

Figure 5.2: Comparison of pressures between the BC and the NCC implemented for a DCV ramp input on experimental setup #2. The data is taken from paper C.

The figure shows that the BC is unstable and the ability of the novel concept to suppress oscillations in a real system is clear.

5.1 Linear stability analysis

This section focuses solely on the differences between the linear model of the NCC and that of the BC. The analysis of the NCC can be found in greater details in paper C. Like it was the case in section 3.1 and 4.1, the experimental setup #2 is employed as the reference system in this section. In figure 5.3 is shown a simplified version of the circuit. Again only the lowering motion is treated in this analysis.

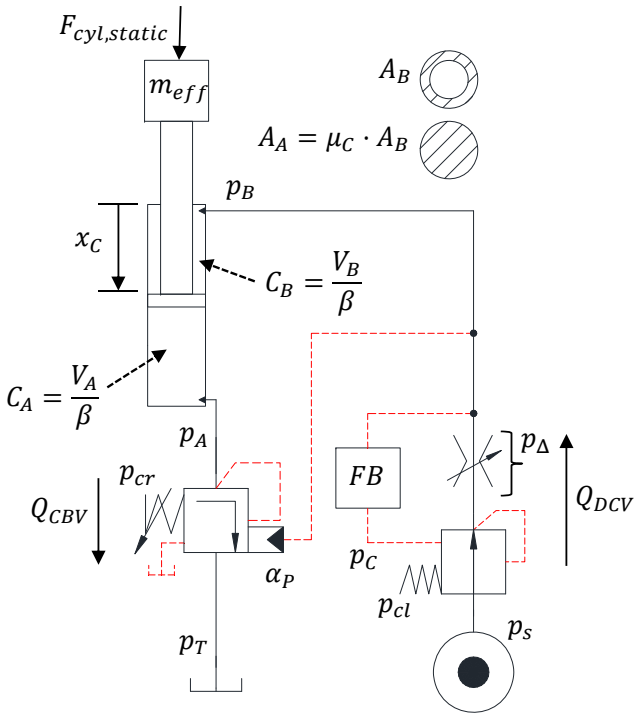

Figure 5.3: Simplified circuit of novel concept.

The addition of the novel concept alters the equation for the pressure drop across the metering-in orifice to:

$$p_\Delta = p_C + p_{CL} - p_B \tag{5.1}$$

where p_C is the filtered version of p_B. The FB block in figure 5.3 contains, in this case, a first order low-pass filter:

$$p_C = \frac{1}{\tau \cdot s + 1} \cdot p_B \tag{5.2}$$

The addition of the filter adds an equation to the governing equations of the system:

$$\tau \cdot \dot{p}_B = p_B - p_C \tag{5.3}$$

and equation (3.6) changes for this system to:

$$Q_{DCV} = k_{v,DCV} \cdot u_{DCV} \cdot \sqrt{p_\Delta} = k_{v,DCV} \cdot u_{DCV} \cdot \sqrt{p_C + p_{CL} - p_B} \tag{5.4}$$

The new set of governing equations is utilised to derive a fourth order transfer function, which is found in paper C. This transfer function is again used together with Routh-Hurwitz's stability criteria to characterise the system. The stability is evaluated in figure 5.4, showing for which values of u_{DCV}^{ref} the system is stable as a function of x_C. The filter constant, τ, is kept constant with a value of $0.32s$. Notice that dead band compensation has been applied on the DCV, see further details in paper D.

Figure 5.4 reveals that the NCC is able to maintain stability in most of the small area of operation, except for a region with piston position below $x_C = 0.4m$ and for valve inputs values, u_{DCV}^{ref}, below 0.035. Compared to the results in figure 3.3, where it was shown that the BC is not able to obtain stability at all if the position is below $x_C = 0.36m$, the improvement created by the NCC is significant.

The influence of the filter time constant τ on system stability is investigated in figure 5.5, showing for which values of u_{DCV}^{ref} the system is stable as a function of x_C. The system is unstable below the lines. A clear relation between τ and stability is seen: higher τ values increase the stable region. The extreme case where $\tau = 0s$ corresponds to the BC. It is also noted that above a certain value of τ the stable region reaches a maximum.

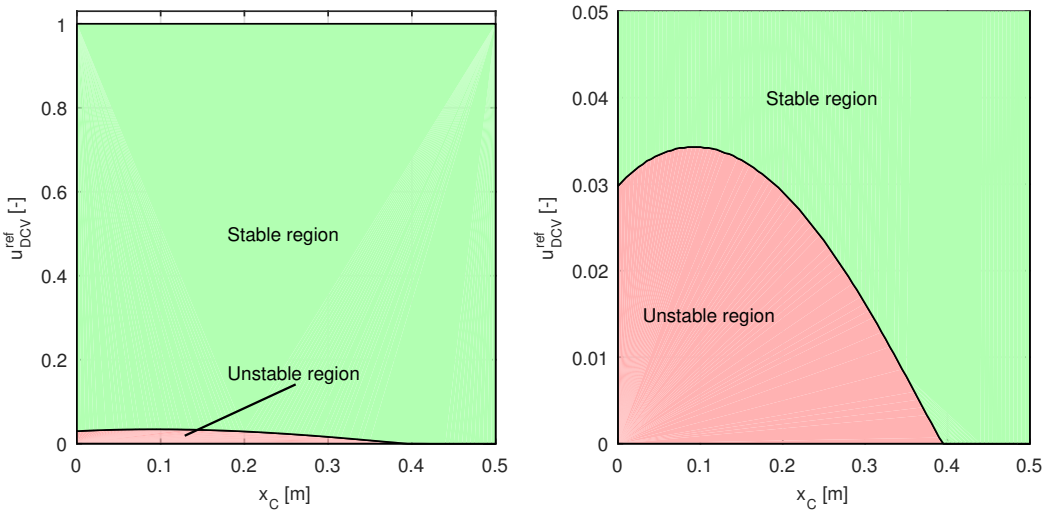

Figure 5.4: Stability of NCC. The minimum dimensionless opening of the DCV, u^{ref}_{DCV}, that yields a stable system is plotted as a function of the piston position, x_C. The figure on the right is a zoom of the left.

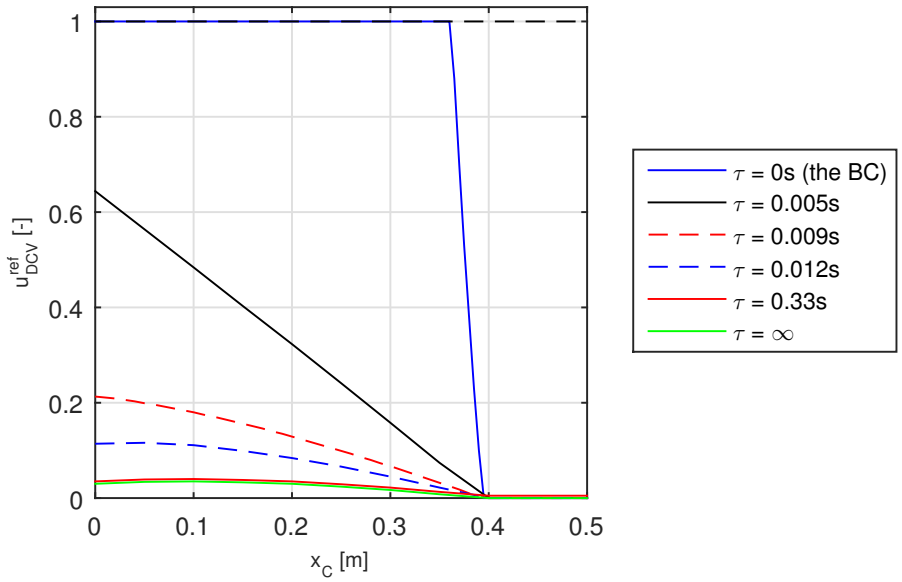

Figure 5.5: Stability of novel concept. The minimum dimensionless opening of the DCV, u^{ref}_{DCV}, which yields a stable system is plotted as a function of the piston position, x_C. The system is unstable for values below the lines.

In figure 5.6 is shown the minimum time constant value that yields a stable system, τ_{min}, plotted as a function of u_{DCV}^{ref} for $x_C = 0.05m$. The figure shows that the stability for high τ values reaches an asymptote, acting as a lower limit.

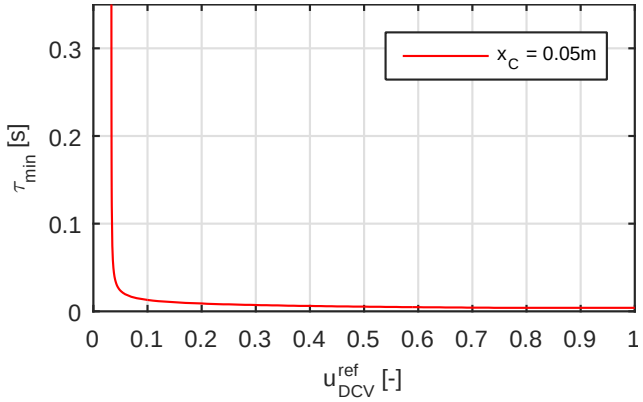

Figure 5.6: Stability of the linear model. The minimum time constant that yields a stable system τ_{min} is plotted vs. the dimensionless opening of the DCV u_{DCV}^{ref} for $x_C = 0.05m$. The figure is also used in paper C.

The region of instability present for small values of u_{DCV}^{ref} at $\tau = \infty$, as seen in figure 5.5, was subject to a further investigation by means of a nonlinear model of the system.

5.2 Parameter study on the nonlinear model

A nonlinear model of the experimental setup #2 is developed, see paper D. The mechanical system is modelled as a multi-body system using the finite segment flexibility method. The hydraulic circuit including the main control components has been modelled using a combination of liquid volumes, variable orifices and 1^{st} and 2^{nd} order transfer functions to resemble the valve dynamics. The eigen frequencies of both the mechanical and the combined mechanical-hydraulic system and the secondary circuit were investigated and validated separately - before being combined to a model of the entire system.

The model confirmed the results from the linear analysis, that there is an elevated risk for instability at small DCV openings for this system. The

model of option #1 shows that an improved system stability can be obtained by either reducing the eigen frequency of the mechanical-hydraulic system or lowering the pilot area ratio of the CBV. Finally, the model of option #2 showed improved stability characteristics compared to option #1. Here it should be recalled that the CBV pilot port is connected to the SC in Option #2. This version would normally be considered less desirable from a reliability point of view because the basic safety features of the CBV are controlled electronically. However, the simulations indicate that it could be an alternative for systems that cannot be stabilised otherwise.

5.3 Concluding remarks

A significant improvement of stability obtained with the NCC has been demonstrated both theoretically and experimentally. The presented NCC shows similar steady state characteristics as the BC but without oscillations. Because the stabilising effect of this solution is created without using the main spool of the DCV, systems with it implemented can still be operated open loop with the operator closing the loop. Alternatively, the solution can be combined with any feedback control strategy using the DCV as the control element for e.g. trajectory control, input shaping or the previous mentioned pressure gradient stabilising control methods. Another advantage of the novel concept is that it is insensitive to the performance of the control system as the ability to suppress oscillations is achieved primarily by the altering of the hydraulic circuit instead of relying on fast feedback control. The chosen filter frequency showed little influence on the ability to reduce oscillations. This makes the solution more robust and saves investments in powerful control systems. The use of the novel concept introduces extra components in the hydraulic circuit and the need for a control system, which of course adds to the cost of the system. However, it has been implemented using commercially available components which both eases the practical implementation and helps to keep down the added cost.

Lastly it is worth mentioning that the novel concept is not limited to the

use of linear actuators as presented in this work, as circuits with rotational actuators and CBV's could also gain from the use of it.

Chapter 6

Conclusions

The objective of this project was to investigate the oscillations created in the hydraulic circuit of knuckle boom cranes and to reduce their severity. The effort has mainly been split two ways:

First, was looked into existing solutions with the focus on the ones not requiring control systems to function. This was done with reliability and robustness in mind. The investigation identified the PCV as the best commercially available solution. The investigation also revealed that the use of a PCV to control the inlet flow in crane applications was rather uncharted territory. The valve, a DCV with a pressure control spool manufactured by Danfoss, has been investigated both theoretically and experimentally. It was the main focus of paper A, paper B and further investigated in the linear stability analysis in chapter 4. This analysis of the valve used together with experimental setup #2 indicates that the combination is stable in all situations. The use of the pressure control spool in the DCV is a simple and robust solution to the stability problem of the BC. However as presented in paper A, drawbacks of its use are the load dependent dead band and load dependent inlet flow. In order to achieve similar behaviour as the normal pressure compensated DCV a closed loop control system is required. These issues are addressed in paper B, where control schemes are proposed to handle them.

In the second part the perspective of the search was broadened to include solutions using control systems. This has lead to the development of a novel,

patent pending, concept that significantly reduces the oscillations of the base circuit. The novel concept were the main focus of paper C and D. The work has demonstrated a significant improvement of stability obtained with the NCC both theoretically and experimentally. The presented NCC has the same steady state characteristics as the BC but without the corresponding oscillatory nature. Because the main spool of the DCV is not used for stabilising the system, the novel concept can be combined with any feedback control strategy. In this project the novel concept is only presented with linear actuators, however its use covers circuits with rotational actuators and CBV's as well.

6.1 Future Work

The presented novel concept has shown some fine results improving the stability, however, there are still areas open for further research. The experiments showed that the pressure capabilities of the SC was limited to a narrow range. As explained in paper C, the range is decided by the used components of the implementation. A different implementation could address this issue.

The controller logic used to create the pressure of the SC influences the performance of the system. The performance is also affected by the low-pass filter used in the SC. So far these two influences have not been investigated. When evaluating the performance the most important areas are stability and response time. The response time is the time from an input is given to the boom starts moving.

References

Bosch Rexroth. Counterbalance valves - introduction. http://apps.boschrexroth.com/products/compact-hydraulics/PiB-Catalogs/, 2016. Accessed: 2016-07-22.

Cristofori, D., Vacca, A., and Ariyur, K. A novel pressure-feedback based adaptive control method to damp instabilities in hydraulic machines. *SAE Int. J. Commer. Veh*, 2012. 5(2):586–596. doi:10.4271/2012-01-2035.

Direct industry. Truck-mounted crane pk 6500. http://www.directindustry.com/prod/palfinger/product-17586-677279.html, 2016. Accessed: 2016-08-22.

European Standard. Cranes - Offshore cranes - Part 1: General-purpose offshore cranes. *NS-EN 13852-1*, 2013.

Handroos, H., Halme, J., and Vilenius, M. Steady-state and dynamic properties of counter balance valves. In *Proc. 3rd Scandinavian International Conference on Fluid Power*. Linköping, Sweden, 1993.

Hansen, M. R. and Andersen, T. O. A design procedure for actuator control systems using optimization methods. In *Proc. 7th Scandinavian International Conference on Fluid Power*. Linköping, Sweden, 2001a.

Hansen, M. R. and Andersen, T. O. Improved functionality and performance of mobile cranes using pressure feedback. In *Proc. Drives and Controls/Power Electronics Conference*. London, UK, 2001b.

Hansen, M. R. and Andersen, T. O. Controlling a negative loaded hydraulic cylinder using pressure feedback. In *Proc. 29th IASTED International Conference on Modelling, Identification and Control*. Innsbruck, Austria, 2010. doi:10.2316/P.2010.675-116.

Hansen, M. R. and Sørensen, J. K. Affiliation National Oilwell Varco. Improvements in the control of hydraulic actuators (pending). 2015. EP15171831.

Huey, J. R. *The Intelligent Combination of Input Shaping and PID Feedback Control*. Ph.D. thesis, Georgia Institute of Technology, 2006.

Kjelland, M. B. and Hansen, M. R. Numerical and experiential study of motion control using pressure feedback. In *Proc. 13th Scandinavian International Conference on Fluid Power*. Linköping, Sweden, 2013.

Kjelland, M. B. and Hansen, M. R. Using input shaping and pressure feedback to suppress oscillations in slewing motion of lightweight flexible hydraulic crane. *International Journal of Fluid Power*, 2015. 16(3):141–148. doi:10.1080/14399776.2015.1089071.

Krus, P. and Palmberg, J.-O. Damping of mobile systems in machines with high inertia loads. In *Proc. JFPS International Symposium on Fluid Power*. page 6370, 1989.

Miyakawa, S. Stability of a hydraulic circuit with a counter-balance valve. *Bulletin of the JSME*, 1978. 21(162):1750–1756.

NEM Hydraulics. Solutions from nem ... for telescopic handlers and loaders. http://www.nem-hydraulics.com/pdf/NEM_Folder_Telescopic_Handlers.pdf, 2016. Accessed: 2016-07-22.

Nordhammer, P., Bak, M. K., and Hansen, M. R. A method for reliable motion control of pressure compensated hydraulic actuation with counterbalance valves. In *Proc. 12th International Conference on Control, automation and systems*. Jeju Island, Korea, 2012.

NOV. National Oilwell Varco. Unpublished, 2014.

Pedersen, H., Andersen, T. O., Hansen, R., and Stubkier, S. Investigation of separate meter-in separate meter-out control strategies for systems with over centre valves. In *Proc. ASME Symposium on Fluid Power and Motion Control*. Bath, UK, 2010.

Persson, T., Krus, P., and Palmberg, J.-O. The dynamic properties of over-center valves in mobile systems. In *Proc. 2nd International Conference on Fluid Power Transmission and Control*. Hangzhou, China, 1989.

Persson, T., Krus, P., and Palmberg, J.-O. The dynamic properties of over-center valves in mobile cranes. In *Proc. 9th AFK Conference for Hydraulics and Pneumatics*. Aachen, Germany, 1990.

Ritelli, G. and Vacca, A. Energetic and dynamic impact of counterbalance valves in fluid power machines. *Energy Conversion and Management*, 2013. 76:701 – 711. doi:http://dx.doi.org/10.1016/j.enconman.2013.08.021.

Ritelli, G. and Vacca, A. A general auto-tuning method for active vibration damping of mobile hydraulic machines. In *Proc. 8th FPNI Ph.D. Symposium on Fluid Power*. Lappeenranta, Finland, 2014.

Zähe, B. Stability of load holding circuits with counterbalance valve. In *Proc. 8th International Bath Fluid Power Workshop*. Bath, UK, 1995.

Zähe, B., Anders, P., and Ströbel, S. A new energy saving load adaptive counterbalance valve. In *Proc. 10th International Fluid Power Conference*. Dresden, Germany, 2016.

Paper A

Boom Motion Control Using Pressure Control Valve

Jesper Kirk Sørensen, Michael Rygaard Hansen and Morten Kjeld Ebbesen.

This paper has been published as:

Jesper Kirk Sørensen, Michael Rygaard Hansen and Morten Kjeld Ebbesen., ”Boom Motion Control Using Pressure Control Valve”, 8^{th} *FPNI Ph.D Symposium on Fluid Power.* Lappeenranta, Finland, June 10-13, 2014.

Boom Motion Control Using Pressure Control Valve

Jesper Kirk Sørensen, Michael Rygaard Hansen and Morten Kjeld Ebbesen.
Department of Engineering Sciences
Faculty of Engineering and Science, University of Agder
Jon Lilletunsvei 9, 4879 Grimstad, Norway.

Abstract — **This paper focuses on the reduction in oscillations created by counterbalance valves by using a proportional pressure control valve. The motion control of a cylinder boom is presented using this valve, which is a 4/3-way directional control valve with the main spool in series with an upstream compensator. The input to the valve control is a main spool position reference and, indirectly, the compensator downstream pressure. This gives a different flow gain and, therefore, a different feedforward scheme as compared to applications with the more common pressure compensated flow control valve.**
The theory behind the pressure control valve is presented and applied to both a theoretical and experimental implementation of closed loop motion control of the jib boom of a commercial vehicle loader crane.

INTRODUCTION

In load carrying applications, counterbalance valves play an important safety role; among the properties are leak tight holding, load holding at pipe burst, and to ensure no drop occurs before lift. It is, however, well known that they tend to introduce instability in a system, especially when the flow supply is pressure compensated. This is the case when the directional control valve that supplies flow to the actuator suspended by the counterbalance valve is equipped with an internal compensator in series with the main spool; a so-called flow control valve or pressure compensated valve. One of the major challenges within hydraulics is to design pressure compensated systems containing counterbalance valves that offer stable handling of negative loads without unnecessarily compromising system efficiency and response Miyakawa (1978); Zahe (1995); Hansen and Andersen (2010); Nordhammer et al. (2012).

In the search for a useful solution, there are different paths to follow. A simple approach is to make changes in the system and remove one of the conflicting components. The counterbalance valve offers a number of advantages such as multiple safety features and the ability to handle a wide variety of actuator loads. Therefore, this paper focuses on the reduction in oscillations by changes in the directional control valve. Specifically, the use of so-called pressure controlled directional control valves in cylinder-boom actuation is investigated. This alternative ensures that flow control can be maintained during cylinder extraction and, simultaneously, be abandoned during cylinder retraction. The investigated valve has been patented until recently Thomsen et al. (1986, 1989, 1991). This represents a cost effective alternative to high bandwidth servo valves. In this paper closed loop motion control of a pressure control valve is introduced with a view to address the major drawbacks of this solution, namely the load dependent deadband and the load dependent metering-in flow.

CONSIDERED SYSTEM

The system used in the current work is a commercial mobile loader crane located at the mechatronics laboratory of the University of Agder. An illustration of the crane is shown in Figure 1. It has a maximum reach of 12m and a load carrying capacity of 1250kg at that reach. The crane is a four-degree of freedom machine consisting of a slewing motion, a main boom, a jib boom, and a telescopic arm system. Only the cylinder controlled rotation of the jib boom relative to the main boom is considered in any detail in this work. Some important data on the jib cylinder are listed in Table 1.

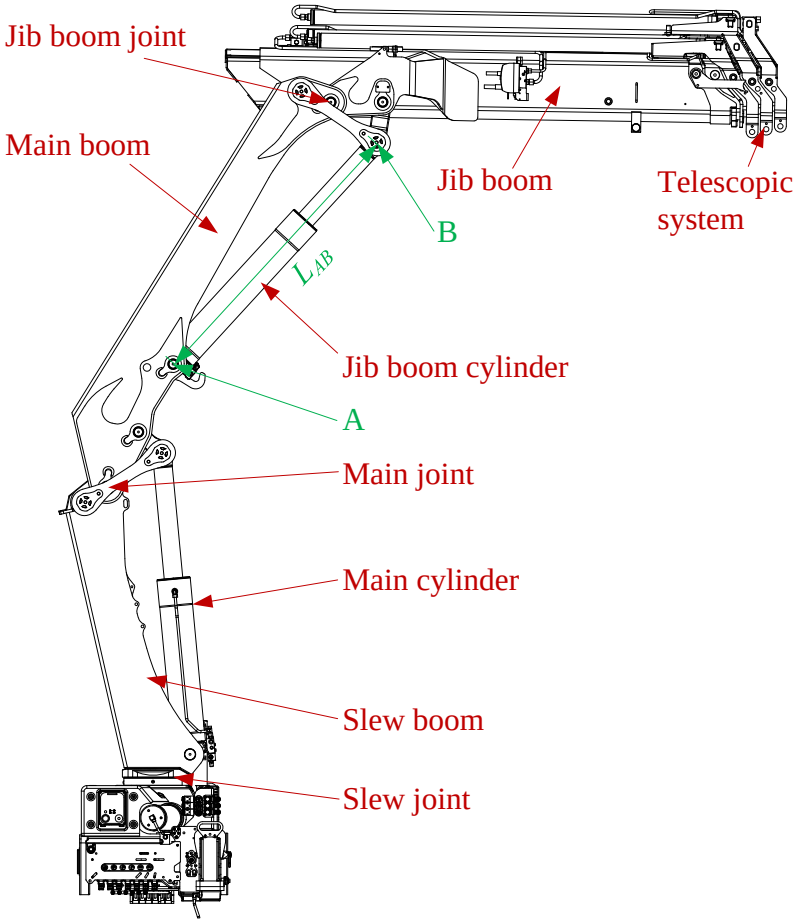

Figure 1: THE MECHANICAL SYSTEM.

The hydraulic circuit of the jib boom motion is shown in Figure 2.
The electrohydraulic control section is part of a typical mobile proportional

valve group that also contains the other degrees of freedom of the crane. The valve group is a PVG32 manufactured by Danfoss A/S. The hydraulic circuit has been somewhat altered from the original one on the crane so the jib boom circuit can be operated with two different standard PVG main spools that have flow control and pressure control of the P-B metering-in, respectively, see Figure 3.

Table 1: JIB CYLINDER DATA.

Parameter	Value
Minimum cylinder length	$L_{AB,min} = 1160\text{mm}$
Maximum cylinder length	$L_{AB,max} = 1980\text{mm}$
Cylinder stroke	$h_C = L_{AB,max} - L_{AB,min} = 820\text{mm}$
Cylinder piston diameter	$D_p = 150\text{mm}$
Cylinder rod diameter	$D_r = 100\text{mm}$
Cylinder area ratio	$\varphi = \frac{D_p^2}{D_p^2 - D_r^2} = 1.8$

The variations in behavior are embedded in the main spool, i.e., the choice of main spool for the 4/3-way directional control valve determines the combination of flow and/or pressure control. Another standardized alternative that is embedded in the block of the control section is simply to avoid the compensator. However, in that case the flow control in the P-A metering-in is abandoned.

A simplified analysis of the two P-B metering-in flows, that assumes fully turbulent flow characteristics and disregards any saturation phenomena and variation in spring compression, yields:

$$Q_{P-B} = C_d \cdot A_d(x) \cdot \sqrt{\frac{2}{\rho} \cdot (p_1 - p_B)} \tag{1}$$

where C_d is the discharge coefficient of the orifice and $A_d(x)$ is the variable discharge area.

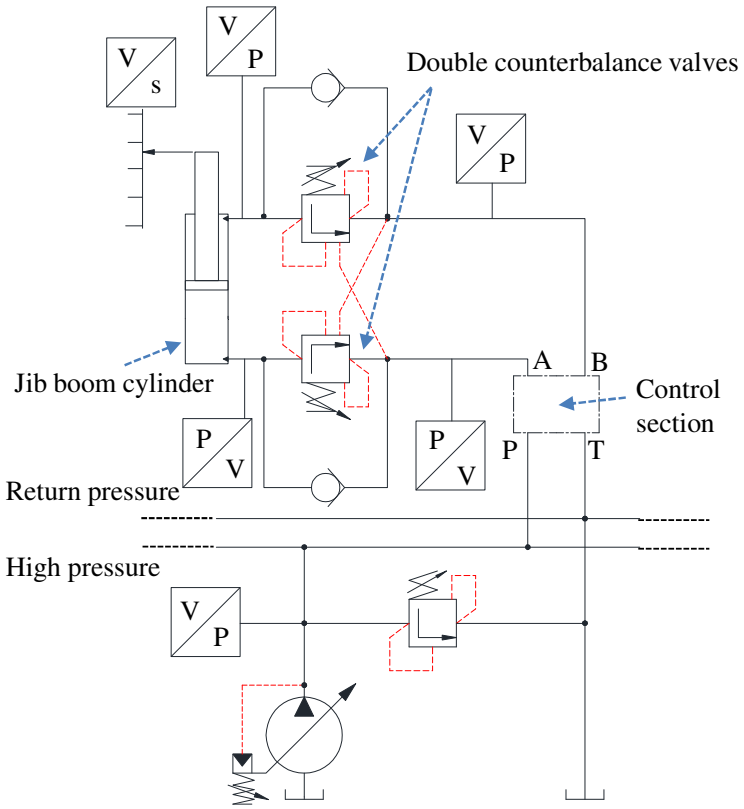

Figure 2: EXPERIMENTAL SETUP FOR CLOSED LOOG MOTION CONTROL OF CRANE JIB.

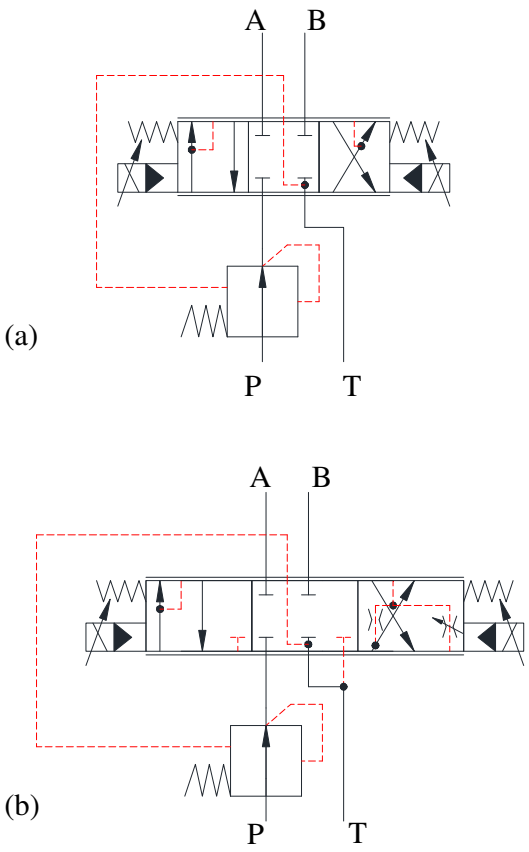

Figure 3: TWO DIFFERENT TYPES OF STANDARD PVG CONTROL SECTIONS, (a) P-A AND P-B BOTH FLOW CONTROL, (b) P-A FLOW CONTROL AND P-B PRESSURE CONTROL.

Situation (a), where P-A and P-B both have flow control, gives:

$$p_1 - p_B \approx p_{cl} = cst. \tag{2}$$

where p_{cl} is the spring setting for the closed compensator and x is the main spool travel.

When looking at the pressure control on P-B, situation (b), the pressure p_1 of equation 1 becomes dependent of x:

$$p_1 = p_1(x) \tag{3}$$

The pressure dependency of the inlet pressure can be derived from the area ratio between the fixed orifice, A_0, and the variable bleed off orifice, $A_{b0}(x)$, see Figure 4.

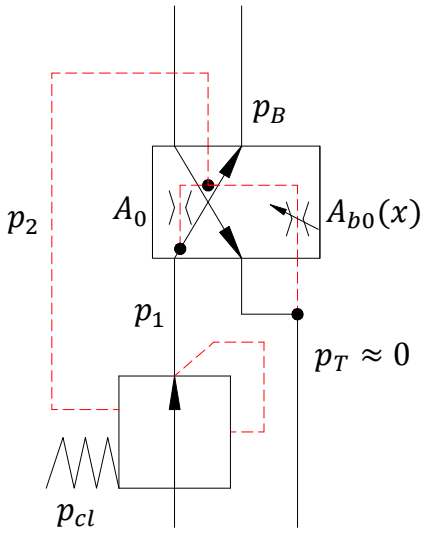

Figure 4: PARAMETERS ASSOCIATED WITH PB PRESSURE CONTROL.

Steady state equilibrium of the compensator and flow continuity in the bleed off line can be formulated as:

$$p_1 = p_2 + p_{cl} \tag{4}$$

Since A_0 and $A_{b0}(x)$ are in series they have the same flow and, consequently, the ratio of the pressure drops are:

$$\frac{\Delta p_{A_0}}{\Delta p_{A_{b0}}} = \frac{p_1 - p_2}{p_2} = \left[\frac{A_{b0}(x)}{A_0}\right]^2 \equiv \mu(x)^2 \tag{5}$$

Combining eq.4 and eq.5 yields:

$$p_1 = \left[\frac{1+\mu(x)^2}{\mu(x)^2}\right] \cdot p_{cl} \equiv \beta(x) \cdot p_{cl} \tag{6}$$

Hence, the bleed off orifice area $A_{b0}(x)$ should close as the main spool opens, however, to avoid saturation it should not close fully. This would yield $p_2 = p_1$ and a fully opened compensator. By careful design, the pressure control of a PVG32 pressure controlled metering-in is linear as deduced from the catalogue Sauer-Danfoss (2012):

$$p_1 = 300bar \cdot \frac{x}{5.5mm} \tag{7}$$

CONTROL STRATEGY

When controlling the jib boom and similar degrees of freedom, there are two basic different types of feedback control:

1. Operator-in-the-loop
2. Sensor feedback

In the first case the operator will adjust the input signal to the valve to meet the target motion based on monitored behavior and in the second case a controller will do the same based on one or more sensor signals. In Figure 5 the two types of feedback control are illustrated by means of block diagrams.

For a sensor feedback system a transfer function, G_{vu}, between a velocity reference, v, and a valve control signal, u, will improve the overall performance,

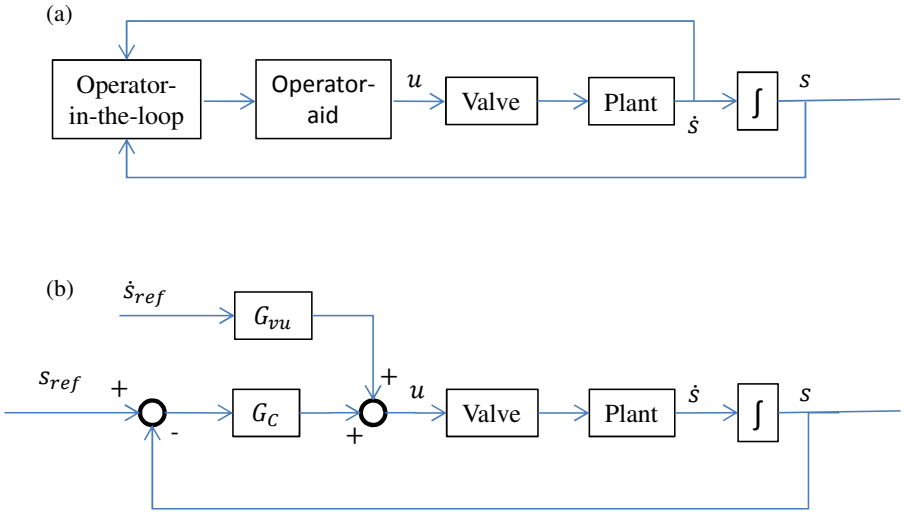

Figure 5: TWO TYPES OF MOTION CONTROL; (a) OPERATOR-IN-LOOP, (b) CONTROLLER BASED ON POSITION SENSOR FEEDBACK AND VELOCITY REFERENCE FEED FORWARD.

by allowing for an efficient feedforward branch that reduces the demands on the controller. With an operator-in-the-loop the operator-aid block could also contain G_{vu}, but also a mapping of the valve performance to change the behavior when operating, like add deadband compensation or minimize load dependency in the metering-in flow.

For a sensor feedback system it requires that both position and velocity references are available continuously, i.e., pre-defined motion. Let us for clarity assume a linear discharge area above a certain deadband and an internal closed loop control on the main spool positioning so that:

$$A_d(x) = w \cdot x \tag{8}$$

$$x = x_{max} \cdot u \tag{9}$$

where x_{max} is the deadband compensated maximum travel of the main spool. In that case the feedforward transfer function for the flow control metering-in is constant independent of load conditions and only changes depending on whether the cylinder is extracting or retracting. For the jib cylinder described

in Table 1 the following transfer function can be obtained when retracting:

$$G_{vu} = \frac{\varphi \cdot A_p}{C_d \cdot w \cdot x_{max} \cdot \sqrt{\frac{2}{\rho} \cdot p_{cl}}} \tag{10}$$

In the absence of linearity the value of G_{vu} may relatively easily be mapped experimentally. In that case the metering-in flow of the valve is measured vs. the input signal.
For the pressure controlled metering-in it is more complicated even though a linear dependency between the spool travel and the inlet pressure is assumed, see also eq. 7:

$$p_1(x) = \beta_0 \cdot x \tag{11}$$

Firstly, the load pressure must be estimated or fed back from the plant. To avoid this a typical or characteristic pressure level in the B-port may be assumed, i.e., $p_B = p_{chr}$. In that case the G_{vu} block corresponds to solving a 3^{rd} order equation. Though the quality of the assumption that $p_B = p_{chr}$, degenerates with large variations of the load.

Combining eq.1, eq.8, eq.9, eq.11 and the fact that the flow also can be described as, $Q = \phi \cdot A_p \cdot \dot{s}_{ref}$, yields:

$$c_3 \cdot u^3 - c_2 \cdot u^2 = c_0 \tag{12}$$

where

$$c_3 = \frac{2}{\rho} \cdot C_d^2 \cdot w^2 \cdot x_{max}^3 \cdot \beta_0 \tag{13}$$

$$c_2 = \frac{2}{\rho} \cdot C_d^2 \cdot w^2 \cdot x_{max}^2 \cdot p_{chr} \tag{14}$$

$$c_0 = \varphi^2 \cdot A_p^2 \cdot \dot{s}_{ref}^2 \tag{15}$$

Obviously, there will be a number of uncertainties accumulating in this type of analysis, and an alternative would be to map the performance of the valve. Preferably, this should be done by measuring the volume flow dependency on

both load pressure, p_B, and input signal, u.

EXPERIMENTAL WORK

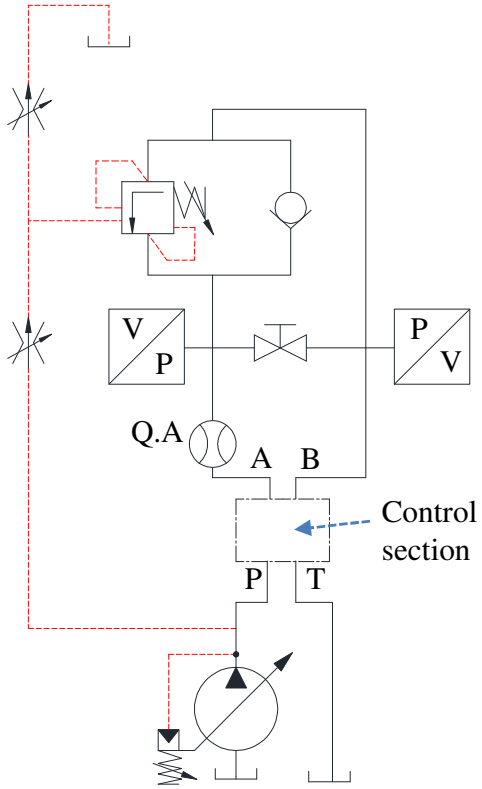

Figure 6: EXPERIMENTAL SETUP FOR MAPPING OF PRESSURE CONTROL SPOOL.

The experimental work has been divided into two parts:

1. Mapping of pressure control spool
2. Implementation of closed loop motion control of pressure control spool on crane jib

The experimental setup for the mapping of the pressure control spool is shown in Figure 6.
The load pressure, p_B, was varied by means of the pilot pressure to the counterbalance valve and in Figure 7 are shown two 2-dimensional traces of the

flow vs. load pressure and main spool travel. The curves display the volume flow vs. spool travel for fixed values of the load pressure.
The experimental setup for the implementation of the closed loop motion control of the pressure control spool on the crane jib is shown in Figure 2.

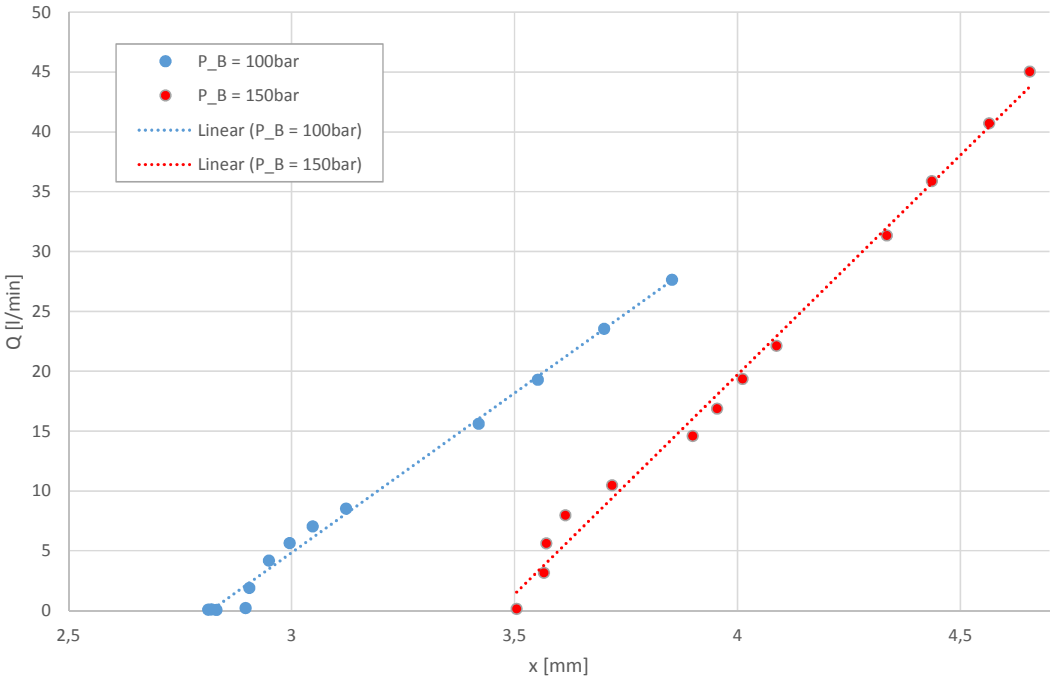

Figure 7: MAPPING OF PRESSURE CONTROL SPOOL.

The reference speed input is shown in Figure 9 and the maximum speed of $\dot{s}_{ref} = 28.6\frac{mm}{s}$ corresponds to a reference flow of $Q_{ref} = 16.4\frac{l}{min}$. With an almost constant load pressure value of $p_B = 150$bar, see Figure 8, a constant feedforward value of $G_{vu} = 13.04\frac{s}{m}$ was determined from the linear approximation in Figure 7. The position controller G_c used in these experiments is a P-controller. In Figure 10 the reference position and the actual position are plotted and in Figure 11 the spool position is shown. The green dashed lines in Figure 8-13 indicate when the velocity ramp is active.

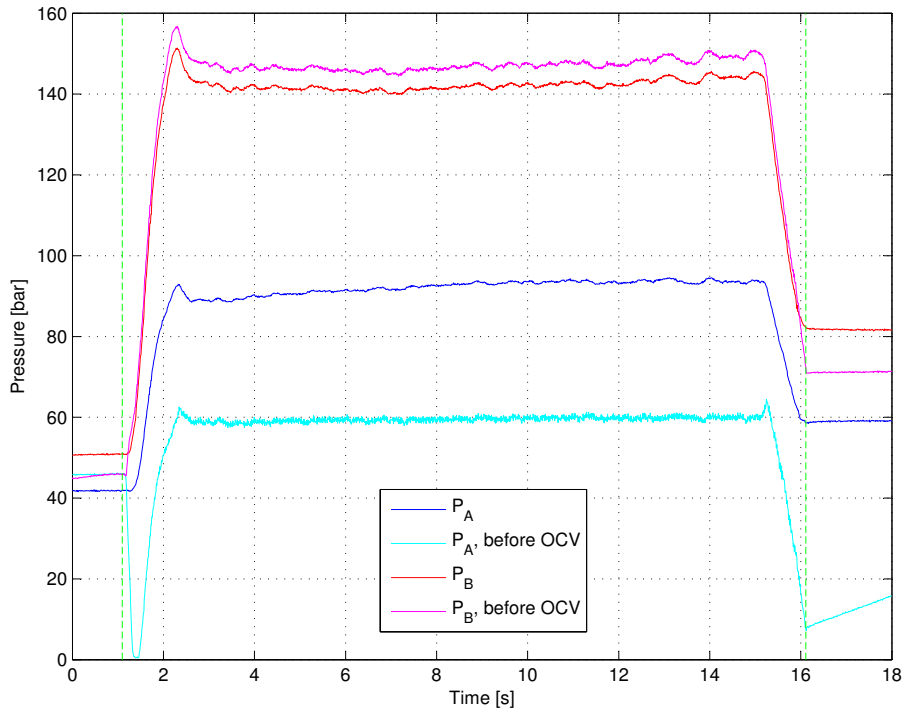

Figure 8: PRESSURES.

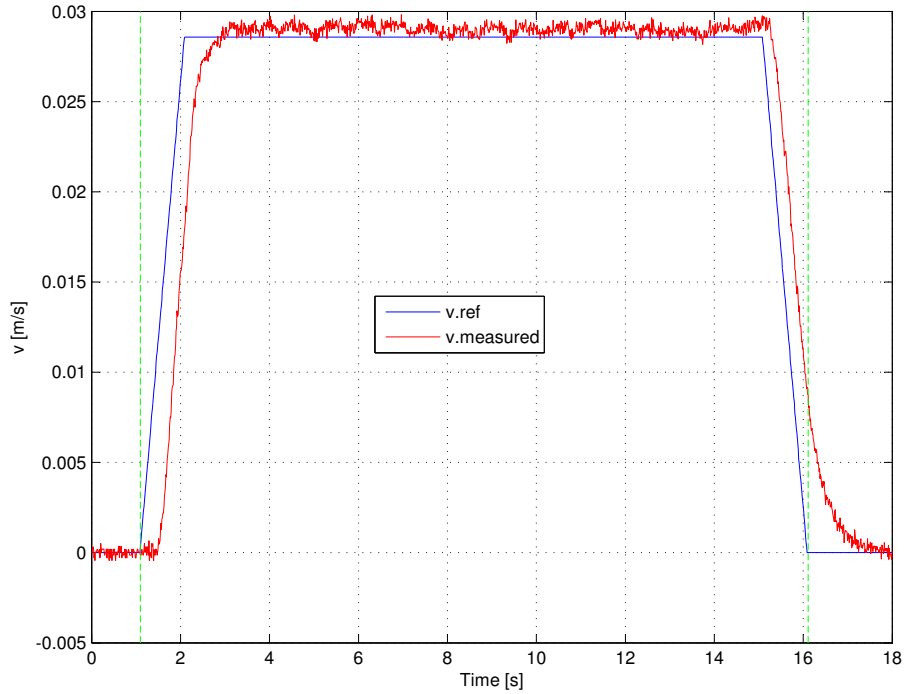

Figure 9: REFERENCE VELOCITY AND ACTUAL VELOCITY.

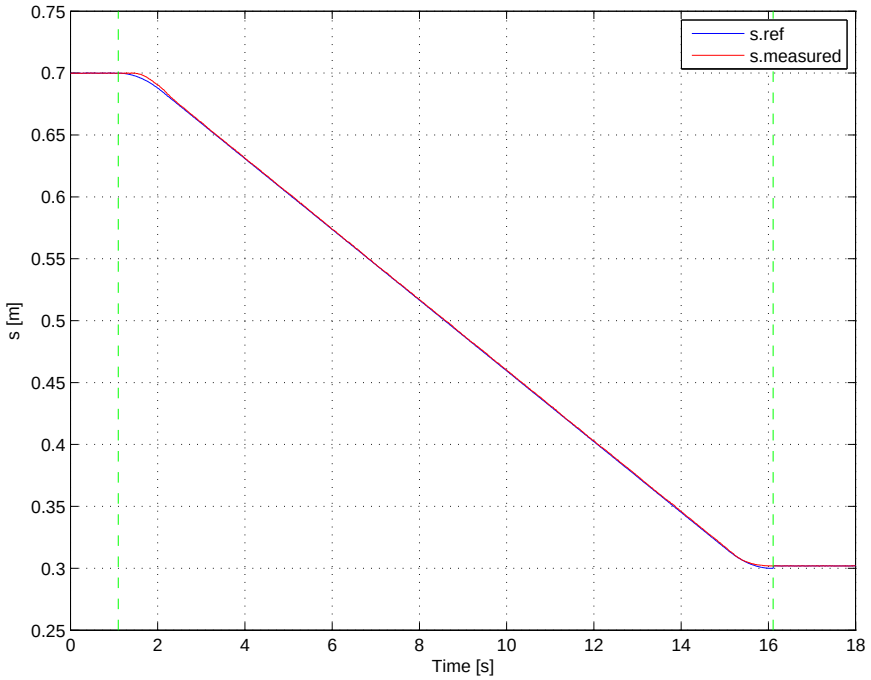

Figure 10: REFERENCE POSITION AND ACTUAL POSITION.

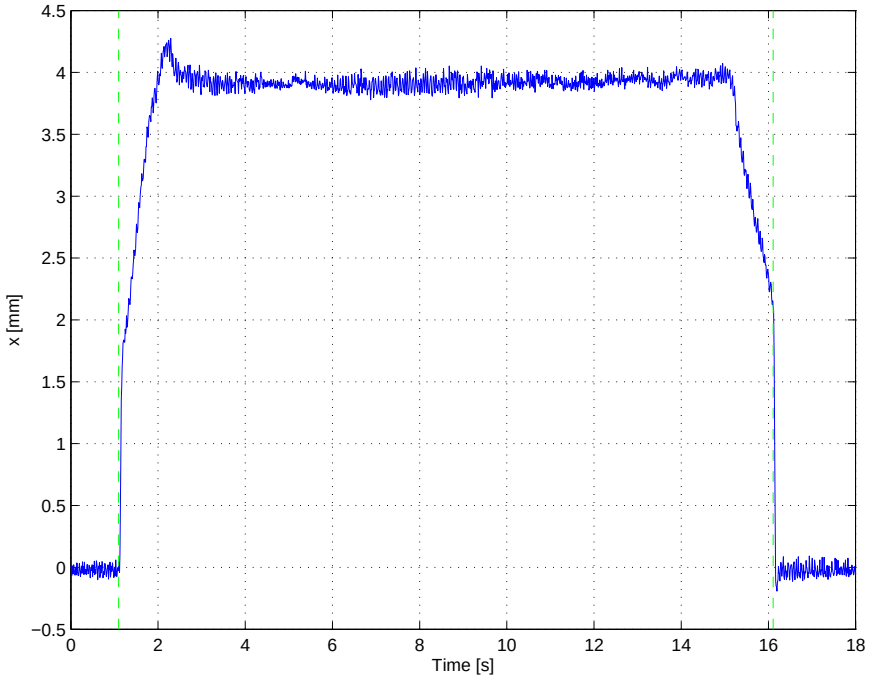

Figure 11: MAIN SPOOL POSITION.

The total control signal to the valve as well as the contributions from the feedback controller and the feedforward term are shown in Figure 12.

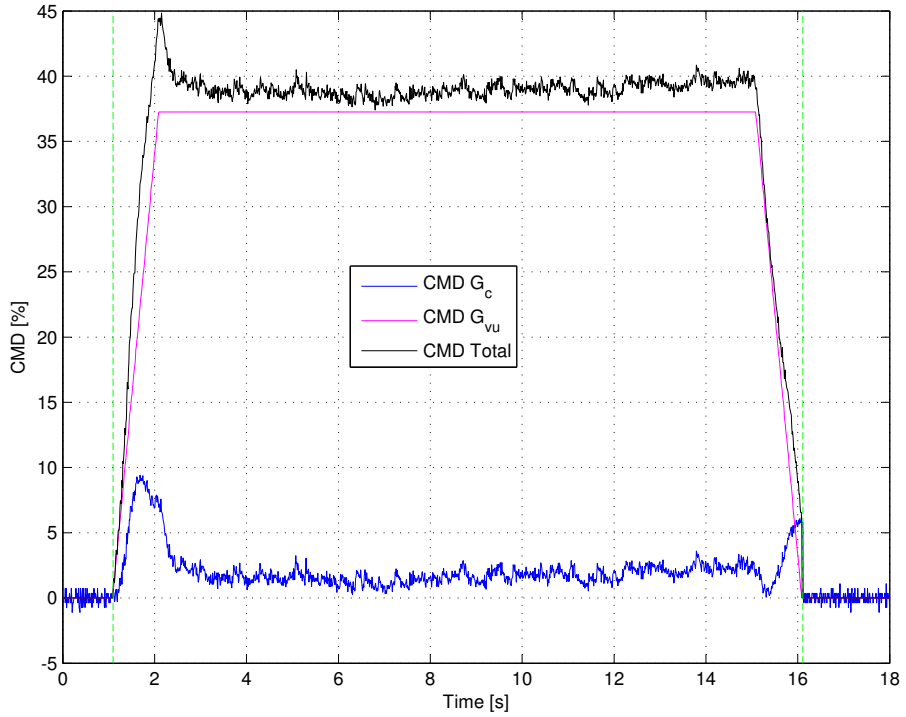

Figure 12: VALVE CONTROL SIGNALS.

Clearly, the overall performance is quite well for a mobile valve with limited bandwidth. Though the proposed control scheme with a single tuned constant in the feedforward branch is sensitive to large load variations. A load pressure p_B of 100bar would for example result in a calculated value for $G_{vu} = 10.30\frac{s}{m}$. The idea of the feedforward branch is that as much of the total command signal as possible origins from it. In figure 13 the two parts of the command signals have been relative to the total signal and compared for the two values of G_{vu}. It shows that the contribution of the feedforward branch drops from approx. 95% to aprrox. 75%, when using G_{vu} calculated for p_B of 100bar instead of the actual p_B of 150bar. Large variations in the B-port pressure for boom cylinders is, however, something that can be avoided by increasing the pilot area ratio of the counterbalance valve. This is possible because the danger of increased oscillations normally accompanied by an increase in pilot area ratio is eliminated by the use of the pressure control spool.

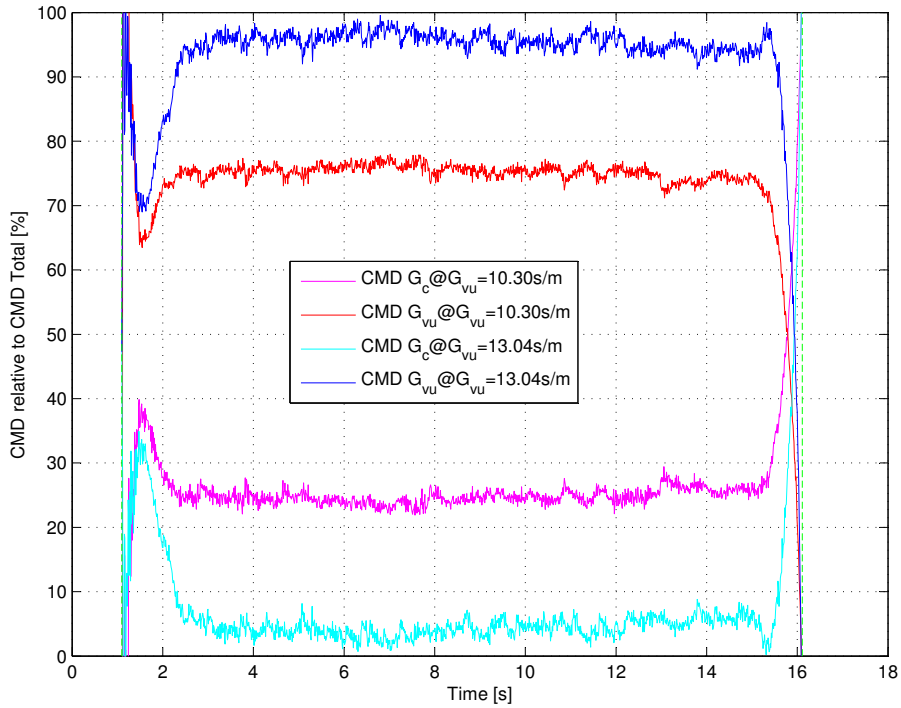

Figure 13: THE EFFECT OF THE FEEDFORWARD BRANCH IN THE TOTAL COMMAND SIGNAL FOR DIFFERENT VALUES OF G_{vu}.

CONCLUSIONS

The pressure control valve associated with the proportional valve group PVG32 of Danfoss A/S is investigated both theoretical and experimental with a view to utilize it in boom control motion. The valve is very suitable for a boom circuit with a counterbalance valve and negative loading during retraction and positive load during extraction. The valve allows for regular pressure compensated metering-in flow when extracting and pressure controlled metering-in flow when retracting. The latter removes the oscillatory nature of the cylinder-counterbalance valve system, however, a closed loop control must be introduced in order to obtain acceptable motion control quality.

Three possible implementations of the feedforward branch of the control scheme are discussed. They include a purely theoretical approach, an approach based on measured flow characteristics of the valve vs. spool position and load pressure as well as a simple manual tuning.

The results are promising, especially since the variations in load pressure during retraction can be minimized for different situations by applying a counterbalance valve with a high pilot area ratio.

References

Hansen, M. and Andersen, T. Controlling a negative loaded hydraulic cylinder using pressure feedback. *29th lASTED International Conference on Modeling, Identification, and Control, Innsbruck, Austria*, 2010.

Miyakawa, S. Stability of a hydraulic circuit with a counterbalance-valve. *Bulletin of the JSME*, 1978. 21(162):1750–1756.

Nordhammer, P., Bak, M., and Hansen, M. A method for reliable motion control of pressure compensated hydraulic actuation with counterbalance valves. *12th International Conference on Control, Automation and Systems, Jeju Island, Korea*, 2012.

Sauer-Danfoss. *PVG 32 Proportional Valve Group - Technical Information*. Sauer-Danfoss, rev hb edition, 2012.

Thomsen, S., Christensen, T., and Zanker, S. *Patentschrift DE 3802672 C2*. Deutsches Patentamt, 1989. Danfoss A/S.

Thomsen, S., Christensen, T., and Zanker, S. *Hydraulic Control Valve With Pressure Sensing Means, Patent Number 4,981,159*. United States Patent, 1991. Danfoss A/S.

Thomsen, S., Eskildsen, C., and Christiansen, P. *Patentschrift DE 3436246 C2*. Deutsches Patentamt, 1986. Danfoss A/S.

Zahe, B. Stability of load holding circuits with counterbalance valves. *8th International Bath Fluid Power Workshop, Bath, UK*, 1995.

Paper B

Load Independent Velocity Control On Boom Motion Using Pressure Control Valve

Jesper Kirk Sørensen, Michael Rygaard Hansen and Morten Kjeld Ebbesen.

This paper has been published as:

Jesper Kirk Sørensen, Michael Rygaard Hansen and Morten Kjeld Ebbesen., ”Load Independent Velocity Control On Boom Motion Using Pressure Control Valve”, 14^{th} *Scandinavian International Conference on Fluid Power.* Tampere, Finland, May 20-22, 2015.

Errata

On page 83 in the list of requirements of the variable dead band compensation (VDC) the pressure transducer should have been p_1. This is also in accordance with figure 5.

Load Independent Velocity Control On Boom Motion Using Pressure Control Valve

Jesper Kirk Sørensen, Michael Rygaard Hansen and Morten Kjeld Ebbesen.
Department of Engineering Sciences
Faculty of Engineering and Science, University of Agder
Jon Lilletunsvei 9, 4879 Grimstad, Norway.

Abstract — **This paper presents a novel scheme for closed loop velocity control of a pressure control valve with attention to the load dependency of both the dead band and the metering-in flow. The control strategy is designed with the use of a minimum of sensors. The only required sensors are position sensors on the cylinders. The performance of the proposed controller is being evaluated both with and without the additional use of pressure transducers. The control scheme is implemented experimentally on a cylinder actuated knuckle boom of a commercial vehicle loader crane.**

Keywords — **Pressure control valve, velocity control, dead band compensation, valve mapping, mobile loader crane, feed forward control.**

1. INTRODUCTION

It is well known that directional control valves with pressure compensated metering-in flow in series with counterbalance valves may introduce instability in a system, see [1-3]. This is especially pronounced when the controlled actuator is subjected to a negative load, i.e., a load that tends to drive the actuator as a pump, because this will require the counterbalance valve to throttle the return flow. The required throttling of the return flow may be handled by the return orifice of the directional control valve as described in [4] thereby eliminating the oscillations. However, this is not a viable solution if the minimum load is 60% or less of the maximum load. In that case, the use of so-called pressure controlled metering-in flow is an alternative that may be put in series with a throttling counterbalance valve without any oscillations. This represents a cost effective alternative to high bandwidth servo valves with the main drawback being the lack of load independent flow, see also [5]. For systems with predominantly positive load on the cylinder during extraction and predominantly negative load during retraction it is possible to combine, the pressure controlled metering in during retraction with pressure compensated metering-in during extraction. That way the flow control offered by the compensator is kept when extracting, however there is a lack of load independent flow, hence velocity of the cylinder, during retraction. In that case, also the dead band of the valve is load dependent. This paper investigates these drawbacks experimentally and the use of position and pressure feedback are introduced with a view to copy the flow control performance of pressure compensated valves except for the oscillatory nature.

2. CONSIDERED SYSTEM

The mobile valve group PVG32 manufactured by Danfoss A/S, Figure 1, is available with pressure controlled metering-in. The controlled pressure is the pressure, p_c, between the compensator and the main spool.

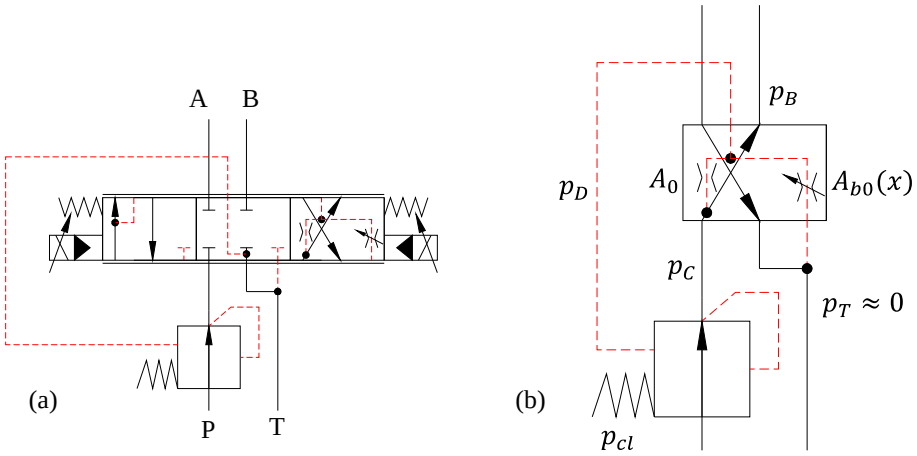

Figure 1. (a) PVG control section with pressure compensated metering-in PA and pressure controlled metering-in PB, (b) Variables associated with pressure controlled metering-in.

The variation in behavior is embedded in the main spool, i.e., the choice of main spool for the 4/3-way directional control valve determines the combination of flow and/or pressure control. A simplified analysis of the PB metering-in flow, that assumes fully turbulent flow characteristics and disregards any saturation phenomena and variation in spring compression, yields:

$$Q_{PB} = C_d \cdot A_d(x) \cdot \sqrt{\frac{2}{\rho} \cdot (p_C(x) - p_B)} \tag{1}$$

Where x is the main spool travel, C_d is the discharge coefficient of the orifice and $A_d(x)$ is the variable discharge area. Steady state equilibrium of the compensator and flow continuity in the bleed off line can be formulated as:

$$p_C = p_D + p_{cl} \tag{2}$$

The spool position dependency of the inlet pressure can be derived from the area ratio, $\mu(x)$, between the fixed orifice, A_0, and the variable bleed off orifice, $A_{b0}(x)$, see Figure 1 (b).

$$\frac{\Delta p_{A0}}{\Delta p_{Ab0}} = \frac{p_C - p_D}{p_D} = \left[\frac{A_{b0}(x)}{A_0}\right]^2 \equiv \mu(x)^2 \tag{3}$$

By combining equation (2) and (3):

$$p_C(x) = \left[\frac{1 + \mu(x)^2}{\mu(x)^2}\right] \cdot p_{cl} \equiv \beta(x) \cdot p_{cl} \tag{4}$$

where $\beta(x)$ is the characteristic of the pilot part of the valve. Hence, the bleed off orifice area $A_{b0}(x)$ should close as the main spool opens, however, to avoid saturation it should not close fully. By careful design the pressure control of a PVG32 pressure controlled metering-in is linear after a certain dead band as deduced from the catalogue [6]:

$$p_C(x) = \begin{cases} 0 & 0 \le x\ [mm] \le 0.8 \\ 300[bar] \cdot \dfrac{x[mm] - 0.8}{4.7} & 0.8 \le x\ [mm] \le 5.5 \\ 300[bar] & 5.5 \le x\ [mm] \le 7 \end{cases} \tag{5}$$

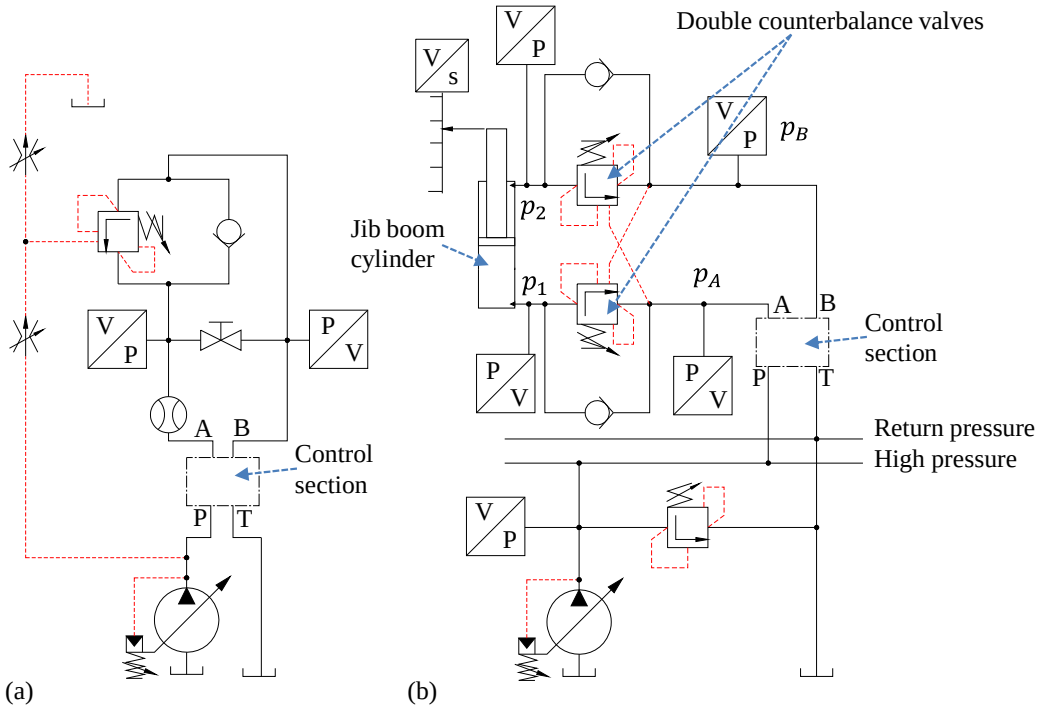

Figure 2. (a) Experimental setup for mapping of pressure control spool. (b) Hydraulic circuit of jib boom.

The performance of the pressure controlled metering-in valve has been obtained experimentally using the setup shown in Figure 2 (a). The load pressure, p_B, was varied by means of the pilot pressure to the counterbalance valve. In Figure 3 (left) are shown three 2-dimensional traces of the flow vs. load pressure and main spool travel. The curves display the volume flow vs. spool travel for fixed values of the load pressure.

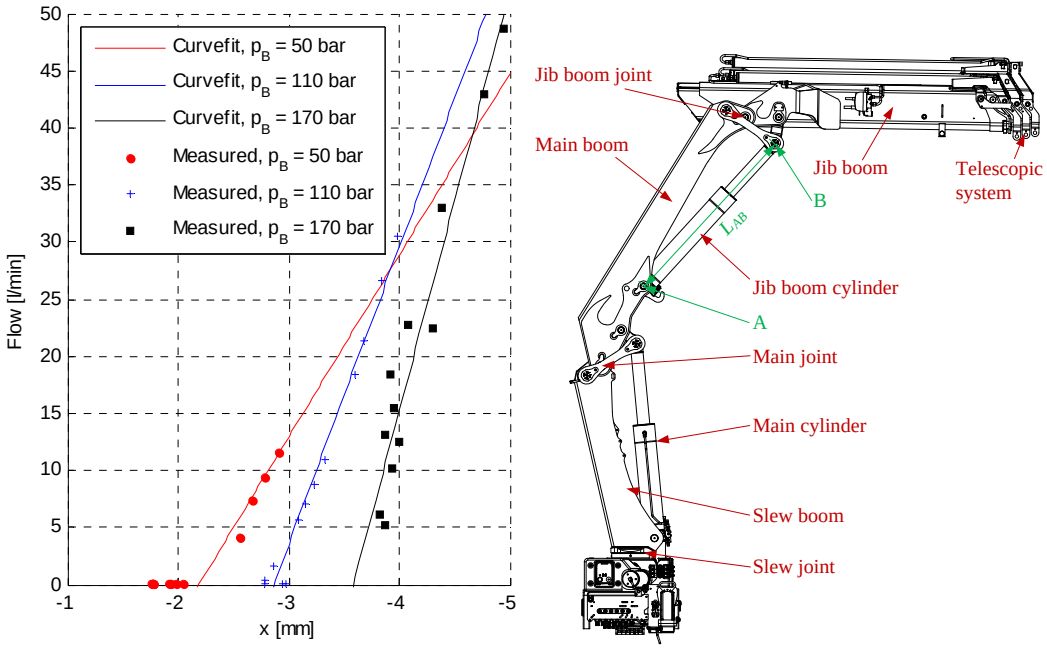

Figure 3. (left) Mapping of pressure control spool. (right) Vehicle loader crane.

A control section with metering-in pressure control was mounted on a commercial mobile loader crane that, basically, is a four-degree of freedom machine consisting of a slewing motion, a main boom, a jib boom and a telescopic arm system, see Figure 3 (right).

The pressure controlled metering-in was applied to the cylinder controlled rotation of the jib boom relative to the main boom. Some important data on the jib cylinder are listed in Table 1.

Table 1. Jib cylinder data

Parameter	Value
Minimum cylinder length	$L_{AB,min} = 1160mm$
Maximum cylinder length	$L_{AB,max} = 1980mm$
Cylinder stroke	$h_c = L_{AB,max} - L_{AB,min} = 820mm$
Cylinder piston diameter	$D_p = 150mm$
Cylinder rod diameter	$D_r = 100mm$
Cylinder area ratio	$\varphi = \frac{D_p^2}{D_p^2 - D_r^2} = 1.8$

The hydraulic circuit of the jib boom motion is shown in Figure 2 (b).

The main spool is electro-hydraulically actuated and an inner closed loop ensures that spool position is proportional to the input signal.

3. CONTROL STRATEGY

The proposed control strategy is shown in Figure 4. The pressure control valve introduces two challenges related to motion control: load dependent dead band and load dependent flow.

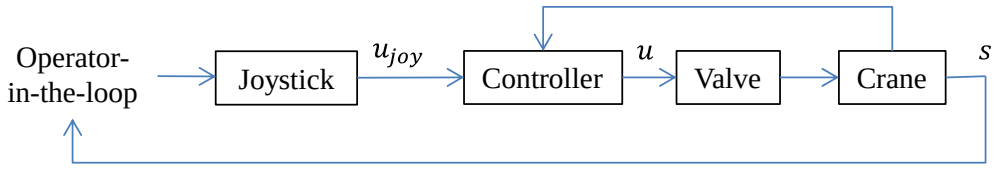

Figure 4. The proposed control strategy.

In the following, the dead band compensation (DC) strategy and the velocity control (VC) are presented.

3.1. A – Dead band compensation

The idea of dead band compensation is to minimize the time from an input have been registered until the system starts moving. Ideally, this is achieved by moving the main spool to the position just before it would make the system move.

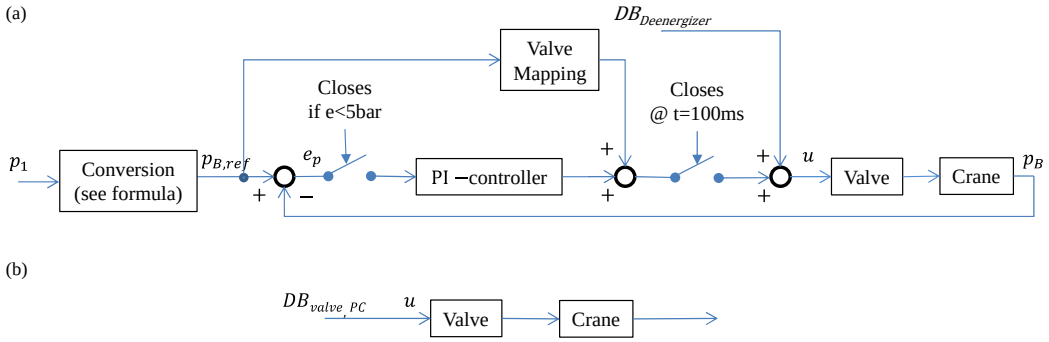

Figure 5. Dead band compensation controller realization. (a) Shows the variable dead band compensation (VDC).(b) Shows the much simpler constant dead band compensation (CDC).

In this paper three types of dead band compensation are evaluated:

- Variable dead band compensation (VDC): VDC is the proposed strategy for a load-independent dead band compensation, see (a) in Figure 5. It consists of a 3-step control strategy.
    1. A feed forward branch with a constant value, $DB_{Deenergizer}$. The effect of the deenergizing part is to remove the backpressure p_A, before increasing the p_B pressure. The deenergizer constant, $DB_{Deenergizer}$ has been found experimentally to a spool position of -1.50mm. This step is given 100ms to move the main spool before activation of the second step.
    2. Step 2 involves a second feedforward branch. The size is determined by sending the calculated reference pressure, $p_{B,ref}$, (see formula below) through a valve mapping to determine the corresponding command signal.

3. The last step consists of a PI-controller working on the difference in pressure p_B between the measured value and the calculated reference. The PI-controller is being activated when the error in pressure is below 5bar, giving the feed forward time to move the spool.

Requirement: Pressure transducer p_1.

- Constant dead band compensation (CDC): The simplest form of dead band compensation, which requires no sensors or knowledge in depth of the system. The controller consists of a feed forward branch moving the spool to the fixed dead band, $DB_{valve,PC}$, described in the datasheet in reference [6], or see part (b) in Figure 5. It has the value for the spool position of -0.80mm, corresponding to a command signal of -11.42%. However, since it does not utilize any sensors, it will not address the issue of the load-dependent dead band. It has been included as a reference for comparison with the VDC.
  Requirement: No sensors
- No dead band compensation (NDC): The spool is in rest.
  Requirement: No sensors

The required pressure for opening the counter balance valve, $p_{B,open}$, can be expressed as:

$$p_{B,open} = \frac{p_{cr} - p_1 + (\alpha + 1) \cdot p_A}{\alpha} \tag{6}$$

The crack pressure, p_{cr}, is set at 350bar and the pilot ratio, α, is 4.25. Due to the use of a 3-port counter balance valve, the backpressure helps closing the counterbalance valve. It is not possible to predict at which pressure p_B it opens, without adding another pressure transducer measuring p_A. However, by adding a deenergizing delay to the dead band compensation the backpressure p_A is drained to tank, hence being negligible. This reduces the above expression to:

$$p_{B,ref} = \frac{p_{cr} - p_1}{\alpha} \leq P_{B,open} \tag{7}$$

where $p_{B,ref}$ is the reference pressure, at which the dead band compensation settles.

3.2. B – Velocity control

Compared to the previously developed control strategy in reference [5] the controller has been expanded to make full use of the valve mapping and utilize a velocity reference as input (joystick). This way the operator closes the control loop.

The proposed controller consists of a position feedback P-controller. The goal is to control the velocity. However, the velocity feedback term derived from the position sensor of the experiments is too noisy to be used in closed loop control. The problem is avoided by generating a position reference, s_{ref}, from integration of the reference velocity obtained from the joystick.

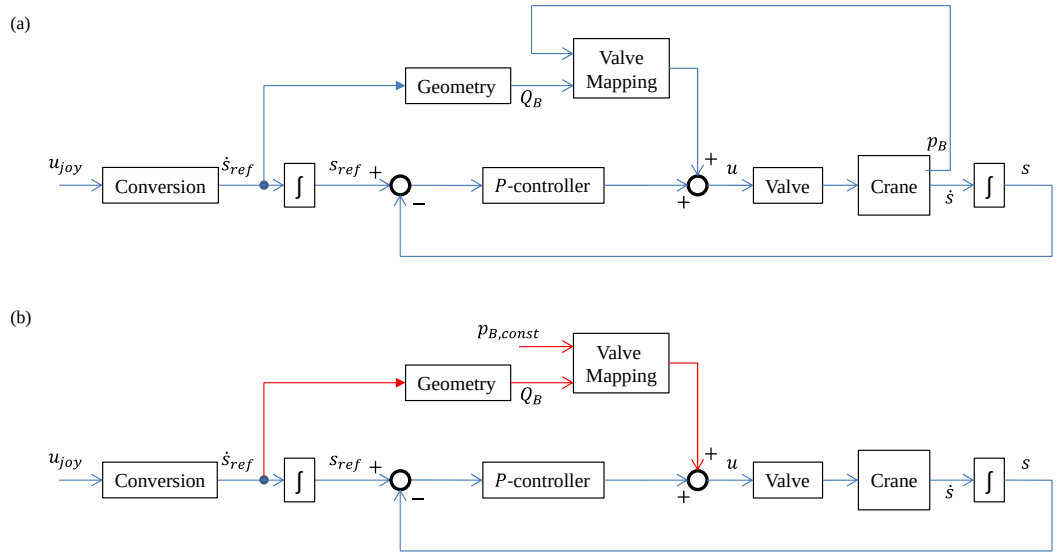

Figure 6. Velocity controller realization, (a) Controller with use of pressure p_B in the feed forward mapping (VM) (b) Controllers without use of pressure p_B. The blue + red part still utilize the valve mapping in the feed

forward, but with p_B constant (CM), whereas the blue part describes a controller without the mapped feed forward branch (NM).

Three versions of the velocity controller were designed, as shown in Figure 6. Each step adds functionality, but increases the complexity at the same time:

- Control strategy no mapping (NM): The simplest controller consists only of the position controller. The advantage is that it is very simple to implement, hence it does not require any knowledge of the system in advance (no mapping). The cost is expected to be a slower system and lower performance.
  Requirement: Position transducer.
- Control strategy constant mapping (CM): CM is a further investigation of the previous presented controller in reference [5]. Adding a feedforward branch with a mapped valve characteristic is expected to increase the performance level. However, it is more troublesome to implement than NM, since the valve must be mapped separately. It still only utilizes the position sensor, why an investigation of the sensitivity for a different load situation is of interest.
  Requirement: Position transducer.
- Control strategy variable mapping (VM): A pressure transducer, p_B, is added to make the controller able to adjust to the current load. Performance wise this is expected to result in the best performance.
  Requirement: Position transducer and pressure transducer to measure p_B.

4. EXPERIMENTAL WORK

The experimental work has been divided into two parts:

- A – Dead band compensation
- B – Velocity control

The proposed control strategies have been implemented on the mobile loader crane and have been evaluated.

4.1. Evaluation

The two different parts of the experimental work is evaluated differently.

- A – Dead band compensation: The focus in this part is to measure the time consumption for:
    1. Settling time, which describes the time from the DC is activated until the spool have settled.
        - Activate the controller and measure.
    2. Dead time, is defined as the time delay between a command signal is given and movement of the boom can be registered.
        - With DC activated and a settled spool, a step input of u_{joy} = -60% is applied.
    3. The ability to adapt to changes of the load situation is being tested by increasing the experienced load by extending the telescope from the standard 0m used in all other experiments to 2m and compare the settling time.
- B – Velocity control: Here the focus is to compare the overall performance of the VC and test the robustness of it.
        - A velocity ramp, see Figure 7, is used as input. The ramp time = 10s is kept constant. The ramp is defined by the rise time, t_r = 0.1s, 0.5s, 1s, 2s, and the desired travel distance, dist = 0.1m, 0.2m, 0.3m.

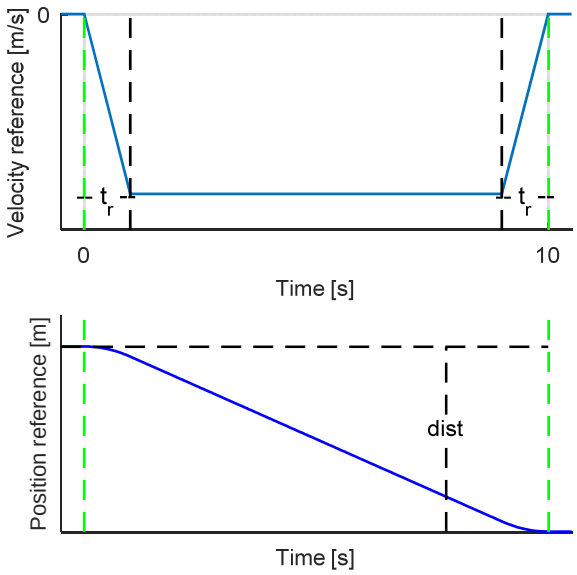

Figure 7. Velocity ramp used in the experimental work (top). At the bottom is shown the corresponding position reference.

The root-mean-square deviation (RMSD) is being used as criterion for the relative evaluation of the two data sets, reference and measured. It is defined as:

$$RMSD, x = \sqrt{\frac{\sum_{t=1}^{n}(x_{reference,t} - x_{measured,t})^2}{n}} \tag{8}$$

The lower the value of RMSD,x the better correspondence between the reference and what actually happens.

In the later, the velocity error is defined as: $\dot{s}_{error} = \dot{s}_{reference} - \dot{s}_{measured}$.

4.2. A – Dead band compensation

Figure 8 shows results of the proposed VDC strategy applied to the experimental setup. The effect of the deenergizing part is clearly seen as the backpressure p_A starts to decrease quickly after applying the controller.

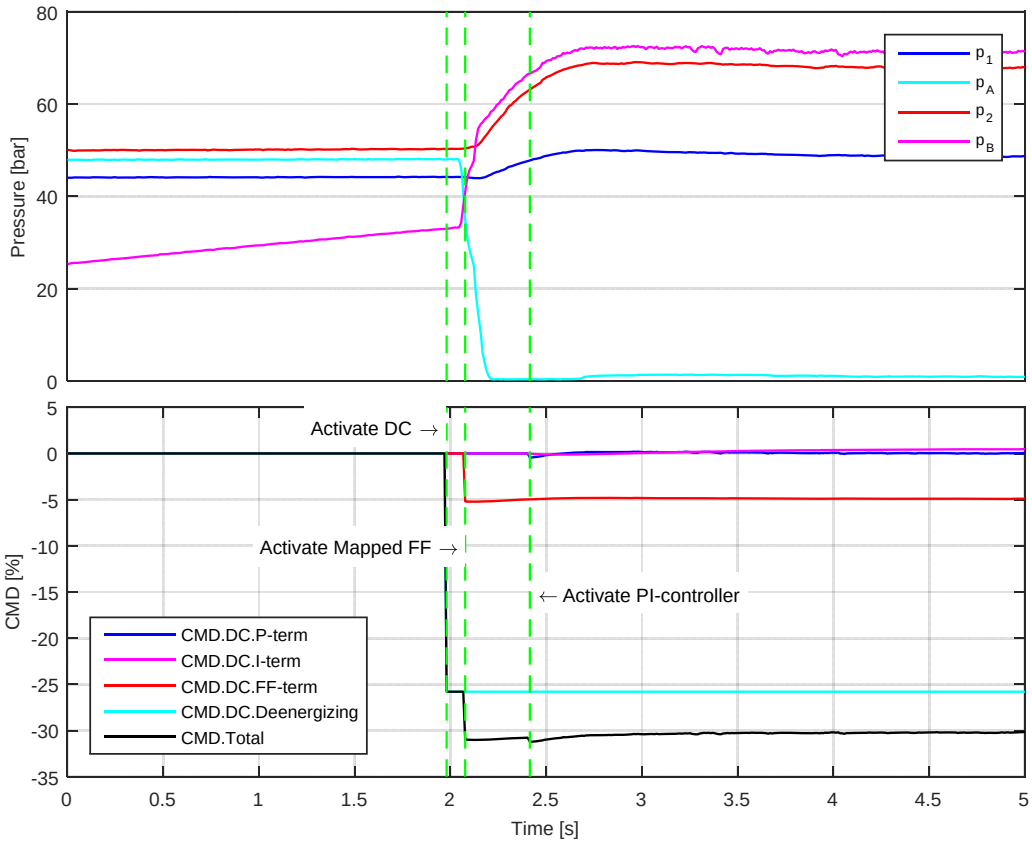

Figure 8. Results of the activation of the VDC. (Top) The pressures over time, (Bottom) The command signal originating from the different parts of the VDC dead band strategy.

The combination of a 3-port counter balance valve and the Danfoss pressure control valve in this application causes the VDC to only work for pressure p_B above approximately 50bar when pressure p_A is drained to tank, see Figure 8 (Top). Alternatively, the counter balance valve could be changed to a 4-port version, where the backpressure does not influence the opening of the valve.

4.2.1. Settling time

Table 2 shows the settling times for both the CDC and the VDC. The different results for the VDC strategy are an outcome of the high variation in pressure

levels in the system when the spool valve is in neutral. As seen, the difference is more than a factor 3 between the ramp up and the ramp down. The settling time for VDC (after moving up), seems a bit high, but it requires only around half the time getting to 90% of the settling pressure, VDC (up, 90%). For practical use the 90% pressure will be sufficient to avoid the operator experiencing the response of the system to be slower. This is because the spool travel required between 90% and 100% settling pressure is minimal.

The settling time for CDC is independent of previous movement since it is a fixed value dead band.

Table 2. Settling time before movement for different strategies

	CDC	VDC (up)	VDC (up, 90%)	VDC (down)
Settling time	110ms	599ms	349ms	196ms

4.2.2. Dead time

Results from the dead time experiments are shown in Figure 9 (top) and the numerical values are presented in Table 3. The effect of the dead band compensation is clearly seen here on the response time with CDC being a little faster than NDC and VDC being clearly faster than the two others.

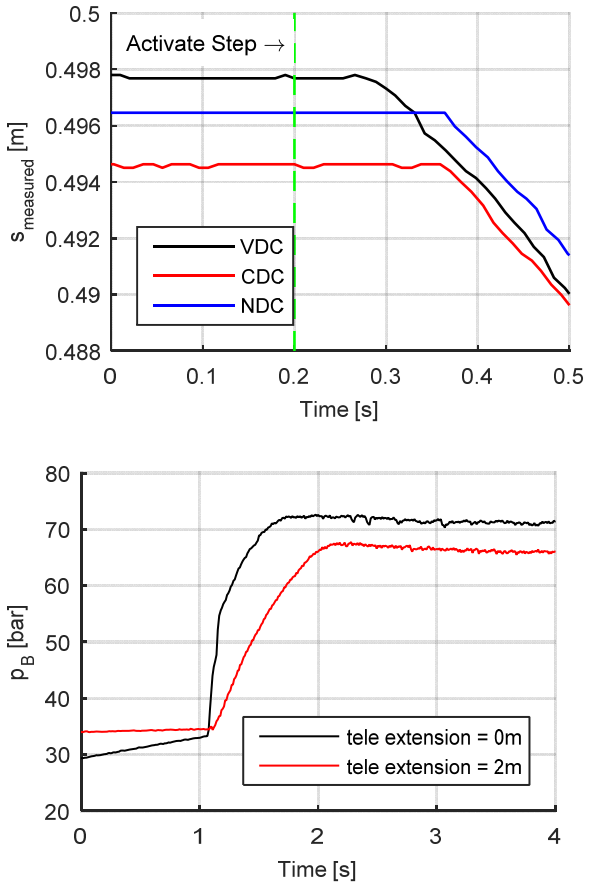

Figure 9. (top) Dead time before movement for different strategies. (bottom) The pressure p_B over time when extending the telescopic system.

Table 3. Dead time before movement for different strategies.

	NDC	CDC	VDC
Dead time	162ms	138ms	89ms

4.2.3. Ability to adapt to load variations

The VDC controller has been tested for two different load cases to see how it reacts. Figure 9 (bottom) shows the pressure p_B for the telescopic system extension at 0m and at 2m. In both cases the VDC lets the pressure p_B settle nicely – ready for moving the crane.

4.3. B – Velocity control

This section shows some results of the VC with VM and VDC using the velocity ramp as input (t_r = 1s and dist = 0.3m). In Figure 10 (top) the total command signal send to the valve is shown. Furthermore, the figure shows the signal from each part of the controller. Due to the correspondence between the signal from the feedforward branch (FF-term) and the total command signal, it is clear that the experimental mapping of the valve used in the feedforward is quite accurate. Figure 10 (bottom) shows how the pressures in the system develop over time when the velocity ramp is used as input.

The green dashed lines in Figure 10 - Figure 13 indicates when the velocity ramp is active.

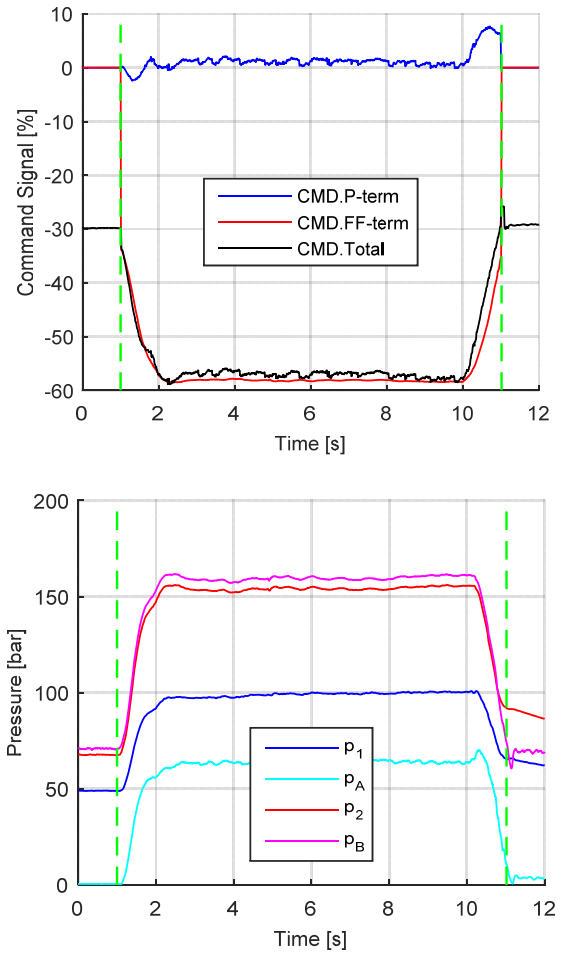

Figure 10. (top) VC with VM and VDC using the velocity ramp as input (t_r = 1s and dist = 0.3m) – command signals. (bottom) The corresponding pressures.

4.3.1. Comparison of different control strategies

The different velocity control strategies – NM, CM, VM - are all tested with CDC, t_r = 1s and dist = 0.3m.

The constant pressure p_B used in the constant mapping strategy have been chosen manually from Figure 10 (bottom) to $p_{B,const}$ = 156bar.

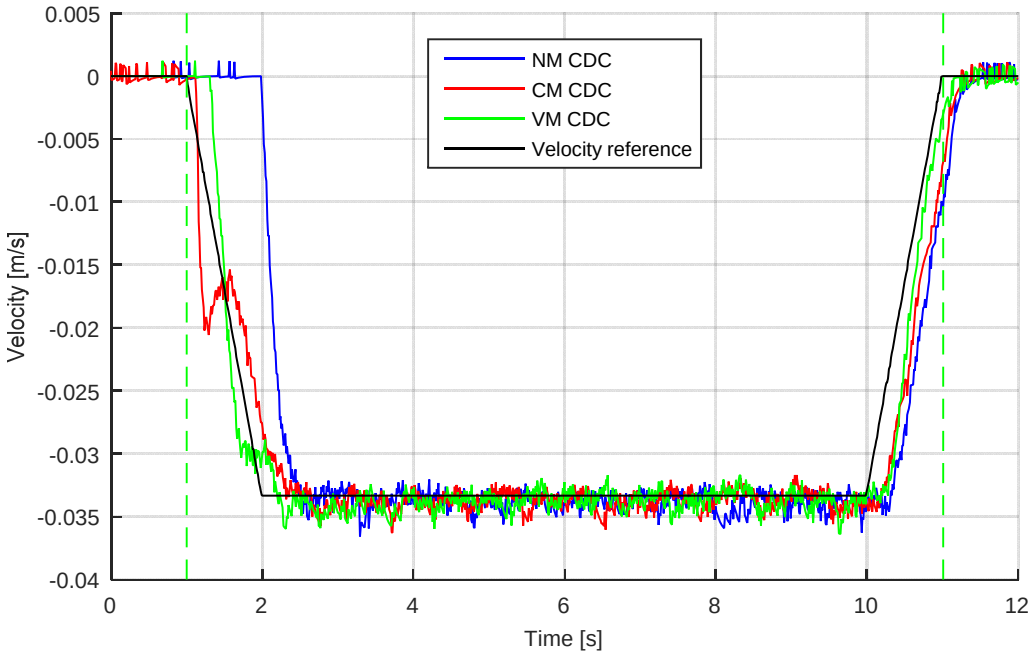

Figure 11. Velocity response for each of the 3 different VC strategies; NM, CM and VM (t_r = 1s and dist = 0.3m).

The velocity responses are compared in Figure 11. As expected, does the VM exhibits the best performance, with the CM not far off and the NM as the slowest. Though the main difference is present when ramping up the velocity, all are capable of moving the cylinder with more or less the desired constant velocity. The peak on the CM curve while ramping up the speed up indicates that the chosen mapping is not very accurate for low velocities, which is confirmed by the results in Figure 13.

Table 4. RMSD-values for different control strategies with the same ramp.

	NM	CM	VM
RMSD Position	0.0176m	0.0012m	0.0009m
RMSD Velocity	0.0075m/s	0.0033m/s	0.0025m/s

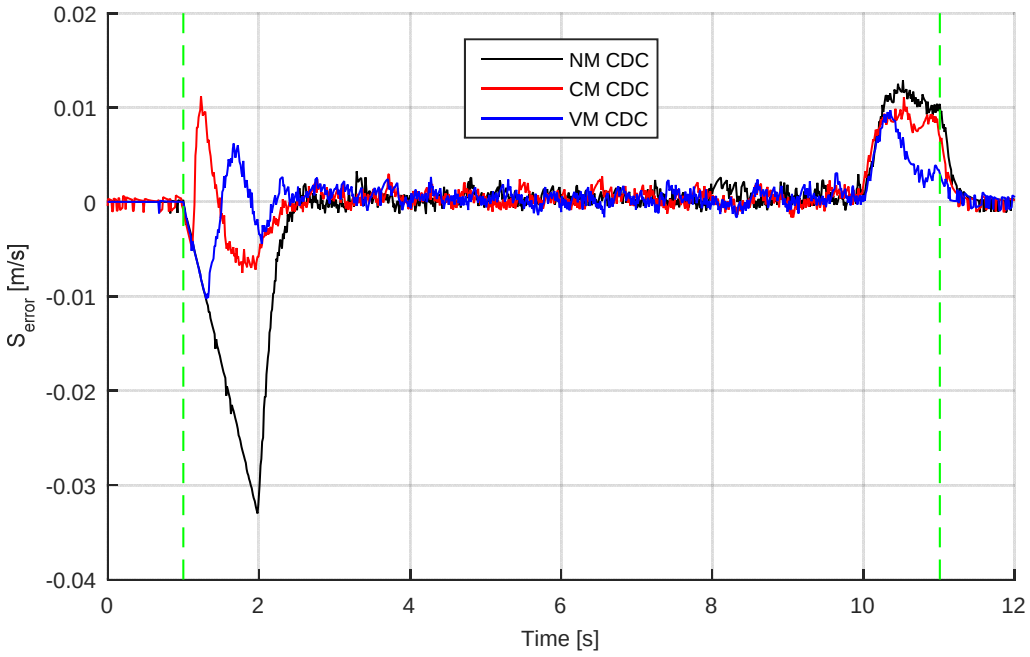

Figure 12. Velocity error of the 3 different VC strategies; NM, CM and VM.

Monitoring the velocity errors compared to the reference velocity, see Figure 12, is another way of assess the performance of the control system. A positive value for the velocity error is a result of the boom going too fast. As already mentioned VM is able to handle the change of velocity better than the others. The RMSD values in Table 4, clearly show the same picture. CM and VM are much better at following the reference input than NM. However, VM also shows a clear improvement over CM, so the addition of the pressure transducer, p_B, pays off performance wise.

4.3.2. The effect of the constant mapping strategy, CM, at different speed

It was shown in the previous section that the constant mapping strategy, CM, could provide usable performance under certain conditions. But since the pressure $p_{B,const}$ is found manually based on knowledge of the specific work cycle is it of interest to see the performance during different conditions. Figure 13 (top) shows how much of the total command signal origins from the feed forward running the velocity ramp using two different values of dist

(0.1m and 0.3m) in order to alter the velocity obtained during the operation. A percentage higher than 100% means that the valve mapping returns too high flow demands and the P-controller needs to do more work to compensate. The red curve show a good compliance of the valve mapping to what actually would be required by the system running steady state with a value around 103% opposite approximately 126% for the black. However, both show problems handling velocity variations at the beginning and at the end of the ramp. This imply that changing the velocity at which the crane operates, hence the pressure levels, the mapping becomes less accurate. Indicating CM would be less effective at dist = 0.1m.

Table 5. CM: Different values of dist with t_r = 1s.

	dist = 0.1m	dist = 0.3m
RMSD Position	0.0037m	0.0012m
RMSD Velocity	0.0023m/s	0.0033m/s

The RMSD vales for both position and velocity have been found, see Table 5. The position error (the RMSD value), has increased by more than a factor 3 as a result of a load case the controller is not designed for. The RMSD value for the velocity is higher for dist 0.3m than for 0.1m which is surprising. The explanation can be found by looking at the velocity response for dist 0,1m in Figure 13 (bottom) where a high peak can be observed when accelerating. The inaccurate mapping returns too high command signals. Due to this, the system will in reality experience a step input when the controller is activated. This creates the peak. The controller handles well getting the speed back at the reference which is why the RMSD velocity value is fine. However, there is no compensation position wise for the distance travelled during the peak, that can cause the RMSD value to be more than a factor 3 larger than for dist = 0.3m. The CM can be concluded not to be well suited for an application like this, where the load situation changes much during operation.

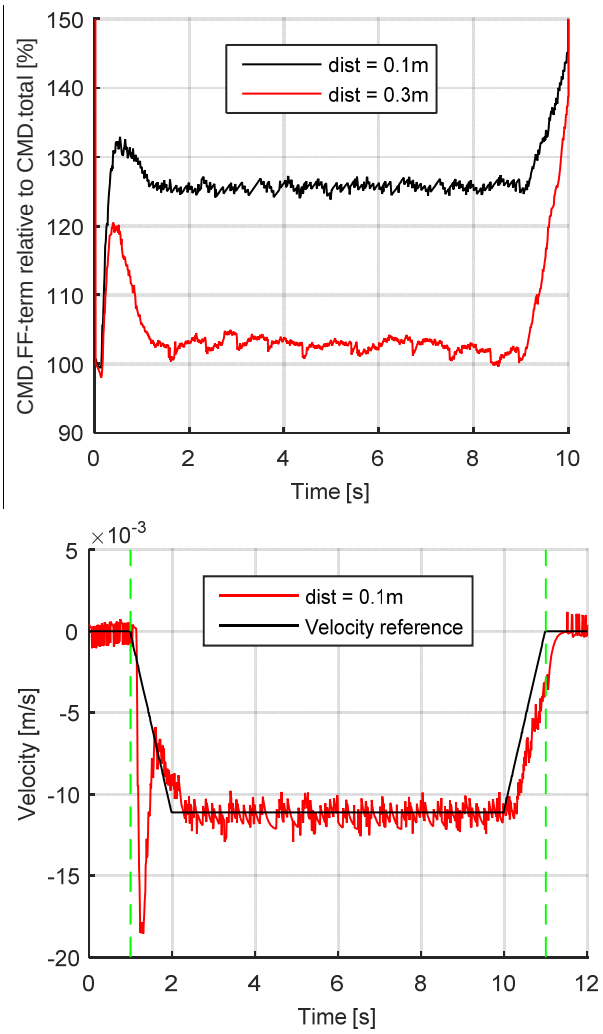

Figure 13. (top) The effect of feedforward compared to the total command signal using the constant mapping strategy, CM, with $p_{B,const}$ = 156bar, for dist = 0.1m and 0.3m. (bottom) Velocity response of CM CDC with t_r = 1s and dist = 0.1m.

4.3.3. VM at different speeds

In this section the VM strategy is investigated further. In Table 6 RMSD values for experiments with different values for dist (0.1m, 0.2m and 0.3m) are shown. These experiments were carried out using VDC instead of CDC as in section 4.3.1. The improvement in the overall performance for the VM

strategy, when using VDC, can be seen when comparing the RMSD values for dist = 0.3m, with the corresponding results in Table 4. Both RMSD values are smaller but it is most significant for the RMSD Position. The RMSD position values for dist=0.1m, 0.2m and 0.3m are approximately equal and the RMSD velocity values gradually decrease from the already fine values at dist=0.3m. It can therefore be concluded that the controller adapts well to changes of the load scenario.

Table 6. VM: different values of dist with t_r = 1s.

	dist = 0.1m	dist = 0.2m	dist = 0.3m
RMSD Position	0.0010m	0.0011m	0.0007m
RMSD Velocity	0.0008m/s	0.0014m/s	0.0025m/s

To assess the quality of the mapping used in VM at different speeds the feed forward's share of the total command signal is shown in Figure 14. The mapping is accurate for dist = 0.3m, accounting for approximately 98% of the control signal when running steady state. The results for dist = 0.1m and dist = 0.2m are not quite as impressive as the one for dist = 0,3m but with a feedforward branch accounting for around 94% of the total signal the mapping still is good.

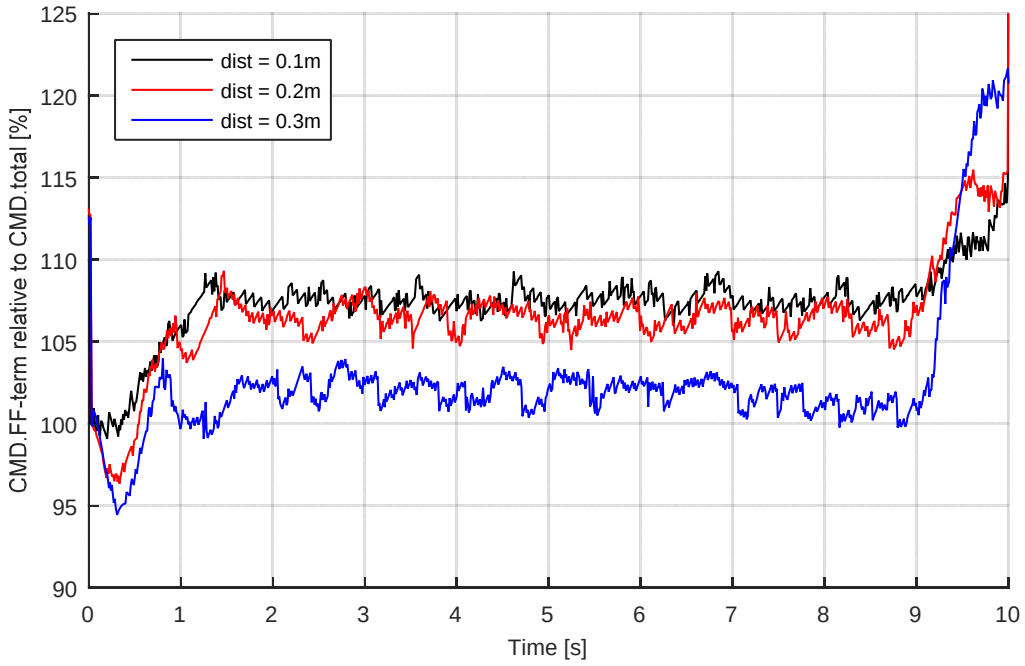

Figure 14. The effect of the variable mapping strategy, VM, with 3 different speeds (different values of dist).

4.3.4. VM for different values of rise time, t_r

The final investigating is to test the controller with control inputs with different rise times, t_r. In Table 7 is listed RMSD values for rise times; 0.1s, 0.5s, 1s, and 2s. The values for the slower rise times of 1s and 2s are quite similar and gradually increasing in size the faster the rise time become. Rise time 0.1s have a RMSD velocity value nearly twice the size of the one for t_r = 2s. This indicates that the system is not fast enough to handle these accelerations properly. A rate limiter could be considered to solve this issue.

Table 7. VM: different values of t_r with dist = 0.3m.

	t_r = 0.1s	t_r = 0.5s	t_r = 1s	t_r = 2s
RMSD Position	0.0009m	0.0009m	0.0007m	0.0007m
RMSD Velocity	0.0047m/s	0.0035m/s	0.0025m/s	0.0021m/s

5. CONCLUSIONS

Two issues caused by the use of pressure control valves were addressed: the load-dependent dead band and the load-dependent metering-in flow.

A variable 3-step dead band compensation routine (VDC) was developed. Experiments showed that it is capable of reducing the time until movement can be detected from 162ms with no dead band compensation to 89ms with the controller activated. Furthermore the VDC was tested in different load situations and showed to be able to adjust to the varying load – until 50bar, which represents the lower limit of valve mapping. However in order to function the VDC requires that pressure p_A is measured. The VDC was also compared to a constant dead band compensation (CDC), based on the dead band specified in the datasheet for the valve. Experiments show a dead time of 139ms on this, which is some improvement compared to the result with no compensation and it is easy to implement. However since it is a fixed value in all cases it does not address the load dependency of the valve, and higher pressure levels will result in longer dead times. Of course a custom-made compensation which does not need any sensors could be designed for a specific work-cycle, but that was not in the scope of this paper.

To address the issue of the load-dependent metering-in flow a feedback control scheme was investigated. It used the integrated operator velocity (joystick) input as position reference and a feed forward based on the current metering-in pressure level and an a-priori experimental mapping of the pressure control valve. It is referred to as VM (Variable Mapping) because it computes the feedforward term based on the measured pressure. This compares to CM (Constant Mapping) that was also investigated where the feed forward term is constant. Finally, a pure feedback controller with no mapping (NM) was also subjected to the same experiments as VM and CM. The results were rather unanimously in the favor of VM with respect to velocity and position accuracy in general. Also, it showed to be well suited to handle variations in load and velocity reference.

REFERENCES

[1] Miyakawa, S., 1978. “Stability of a hydraulic circuit with a counterbalance-valve”. Bulletin of the JSME, 21(162), pp. 1750–1756.

[2] Zahe, B., 1995. “Stability of load holding circuits with counterbalance valves”. 8th International Bath Fluid Power Workshop, Bath, UK.

[3] Hansen, M., and Andersen, T., 2010. “Controlling a negative loaded hydraulic cylinder using pressure feedback”. 29th lASTED International Conference on Modeling, Identification, and Control, Innsbruck, Austria.

[4] Nordhammer, P., Bak, M., and Hansen, M., 2012. “A method for reliable motion control of pressure compensated hydraulic actuation with counterbalance valves”. 12th International Conference on Control, Automation and Systems, Jeju Island, Korea, Oct.

[5] Sørensen J.K., Hansen, M.R. and Ebbesen, M.K., 2014, “Boom Motion Control Using Pressure Control Valve”, 8th FPNI Ph.D Symposium on Fluid Power, Lappeenranta, Finland

[6] Sauer-Danfoss, 2014. PVG 32 Proportional Valve Group - Technical Information, rev HE ed. Sauer-Danfoss.

Paper C

Novel concept for stabilising a hydraulic circuit containing counterbalance valve and pressure compensated flow supply

Jesper Kirk Sørensen, Michael Rygaard Hansen and Morten Kjeld Ebbesen.

This paper has been published as:

Jesper Kirk Sørensen, Michael Rygaard Hansen and Morten Kjeld Ebbesen., ”Novel concept for stabilising a hydraulic circuit containing counterbalance valve and pressure compensated flow supply”, *International Journal of Fluid Power.* Publisher: Taylor & Francis, 2016. 17(3):152-162.

This is an Accepted Manuscript of an article published by Taylor & Francis in International Journal of Fluid Power on 19 April 2016, available online: http://www.tandfonline.com/10.1080/14399776.2016.1172446.

Novel concept for stabilising a hydraulic circuit containing counterbalance valve and pressure compensated flow supply

Jesper Kirk Sørensen, Michael Rygaard Hansen and Morten Kjeld Ebbesen.
Department of Engineering Sciences
Faculty of Engineering and Science, University of Agder
Jon Lilletunsvei 9, 4879 Grimstad, Norway.

Abstract — **In this paper, a novel concept for stabilising a hydraulic system containing a counterbalance valve and a pressure compensated flow supply is presented. The concept utilizes a secondary circuit where a low-pass filtered value of the load pressure is generated and fed back to the compensator of the flow supply valve. The novel concept has been investigated theoretically and experimentally. A linear model has been developed to verify the improved stability conditions. The novel concept has been implemented on a single boom actuated by a cylinder. The results show that the pressure oscillations in an otherwise unstable system can be suppressed with the novel concept. This happens without any compromise on the load independence of the flow supply but with some limitations on response time.**

Keywords — **oscillations, counterbalance valve, pressure compensated valve, instabilities in hydraulic systems, load-holding application.**

1 Introduction

For safety reasons, hydraulic load carrying applications are required by law to contain a load holding protection device. The most widely used device is the counterbalance valve (CBV). It is multi-functional and provides leak tight load holding, load holding at hose/pump failure as well as shock absorption, overload protection, and cavitation prevention at load lowering.

However, it is well known that a series connection of a pressure compensator (CV), a directional control valve (DCV) and a CBV tends to introduce instability in a system, see Miyakawa (1978), Persson et al (1989), Handroos et al (1993), Zähe (1995) and Hansen and Andersen (2010). This is mainly a problem when the controlled actuator is subjected to a negative load, i.e., a load that tends to drive the actuator as a pump, because this will require the counterbalance valve to throttle the return flow, see Figure 1. This system will be referred to as the base circuit.

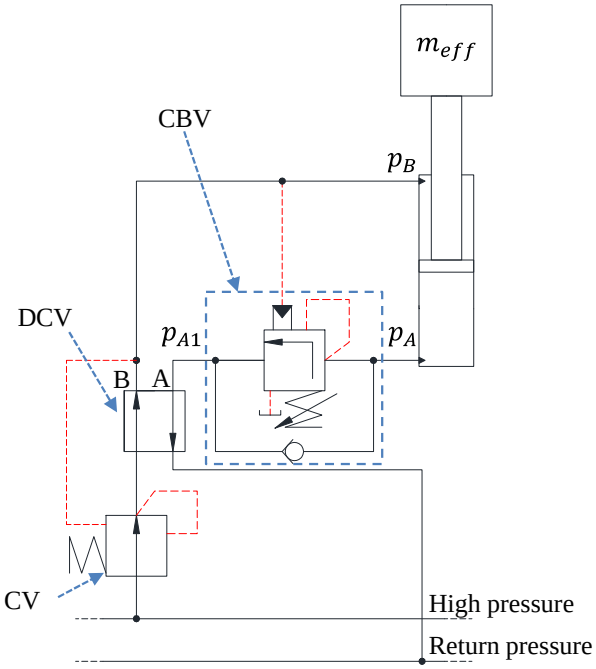

Figure 1. The base circuit consisting of a pressure compensator (CV), a directional control valve (DCV), and a counterbalance valve (CBV).

It is a major challenge within hydraulic system design to find solutions that offer stable handling of negative loads together with pressure compensated metering-in flow. Typically, practical solutions will

compromise either the load independency, the response time or the level of oscillations (Nordhammer et al, 2012). The consequences of the oscillatory nature of such systems are reduced safety, reduced productivity as well as added fatigue load on both the mechanical and hydraulic system. The severity of oscillations is affected by a wide variety of parameters some of which are hard to predict or change: external load on the actuator, the damping and hysteresis of the CBV, the operator input as well as volumes and restrictions in the hydraulic lines.

The efforts to minimize the oscillatory nature of the base circuit can be divided into three groups:

- Parameters variations (pilot area ratio of CBV, pilot line orifices, etc.) on the circuit using same main components.
- Feedback control of DCV.
- Replace either the CBV or the pressure compensated DCV with alternatives.

The parameters most influential on the stability are the damping of the system and the pilot ratio of the CBV (Hansen and Andersen, 2001). A more stable operation when lowering the load can be achieved by reducing the pilot ratio of the CBV. This will come at the expense of a higher pressure level and thereby cause a higher energy consumption - especially with small external loads.

Another approach is to add damping when designing the hydraulic circuit. Many ways of doing this have been tried over the years; adding volumes, adding orifices, adding logic valves, etc. Especially, interest has been focused on the pilot line to the CBV. By manipulating the pressure towards the CBV pilot port in different ways; add delays, create a difference in the path back and forth, positive effects can be achieved. Different commercial solutions are available, as for example the ones shown in Figure 2, from Bosch Rexroth (Bosch, 2015) and NEM Hydraulic (NEM, 2014). Common for these is that they are application and condition sensitive, especially towards temperature variations.

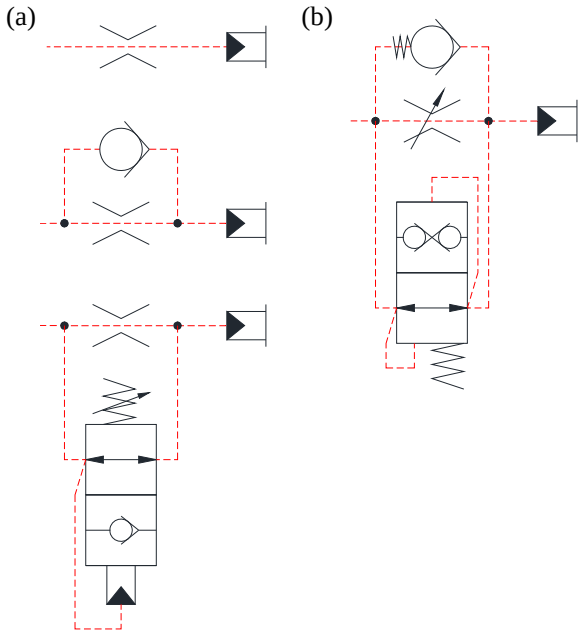

Figure 2. Examples of current solutions for damping the pilot line of the CBV. a) is from Bosch Rexroth (Bosch, 2015) and b) is from NEM Hydraulic (NEM, 2014).

A different approach is to actively compensate for the oscillations by applying closed-loop control strategies that involve the input signal to the DCV and some kind of pressure feedback (Hansen and Andersen, 2010, Cristofori et al, 2012 and Ritelli and Vacca, 2014). The most important limitation in these strategies is the bandwidth limitation in typical DCVs. Alternatively, the pressure compensator (CV) can be removed and the DCV replaced by a servo valve which is a proven and reliable method for motion control. The weakness here are in the investment costs and the difficulties in handling disturbances in the supply pressure caused by neighbouring circuits. Separate meter-in separate meter-out (SMISMO) techniques are also a possibility. These utilise two or more actively controlled valves that opens up for the combination of flow and pressure control in the inlet and outlet ports. However these systems are, inherently, less reliable and their performance is sensitive to parameter variations (Pedersen et al, 2010).

The author has investigated the use of a DCV with compensated supply pressure, see Sørensen et al (2014) and Sørensen et al (2015). This is a commercially available alternative that is characterized by low cost but also load dependent flow. Another example is described in Nordhammer et al,

(2012), where the main throttling ability is moved from the CBV to the return orifice of the DCV, thereby eliminating the oscillations. However, this is not a viable solution if the minimum load is 60% or less of the maximum load, which strongly minimizes the applicability.

All of the approaches have certain drawbacks as compared to the base circuit. In this paper, a novel concept is presented. It has the same steady state characteristics as the base circuit only without the corresponding oscillatory nature.

2 Novel concept

In Figure 3 a hydraulic diagram of the proposed novel concept is shown, patent pending (Hansen and Sørensen, 2015). It is shown in a situation where the actuator is subjected to a negative load, i.e., a lowering motion of some gravitational payload.

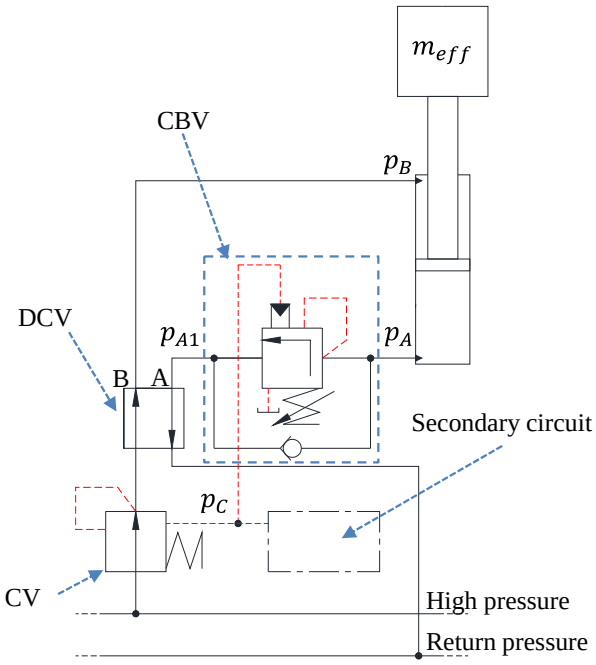

Figure 3. Hydraulic diagram of novel concept. Both the CBV and the CV are connected to the secondary circuit.

When compared to the base circuit in Figure 1, it can be seen that the pilot connections of both the CV and CBV are supplied by the secondary circuit rather than by the B-port pressure. The underlying idea is to suppress

oscillations in the system by generating the steady state value of the B-port pressure in the secondary circuit.

The novel concept also encompasses solutions where the secondary circuit only is connected to the CV or the CBV. In fact, the solution where only the CV is connected to the secondary circuit, see Figure 4, is preferred from a reliability point of view because the CBV and the related safety functions are activated as usual.

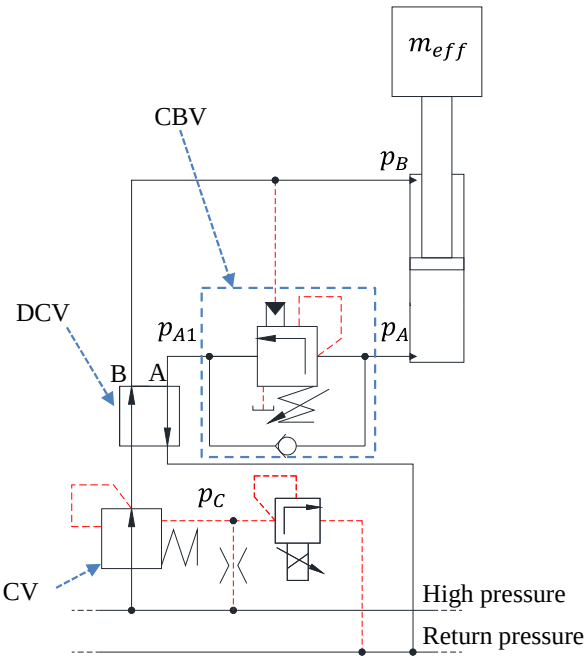

Figure 4. Hydraulic diagram of novel concept where only the CV is connected to the secondary circuit. The secondary circuit is shown in more detail.

The concept can, because the system works passively from the operators point of view, be combined with any closed loop control strategies on the DCV. In this paper, the concept presented is with a linear actuator, but the method will also work for rotational actuators in circuits with counterbalance valves.

In Figure 4 the secondary circuit is shown in more detail. It is realized with an orifice and a proportional pressure relief valve (PPRV) in series. The intermediate pressure, p_C, will be referred to as the compensator pressure and it is connected to the CV.

The overall target is that p_C shall be the steady state value of p_B thereby suppressing oscillations of the compensator and, subsequently, in the entire system. For that purpose, a control strategy is suggested that requires the measurement of p_B, a low-pass filtering yielding a reference value for the compensator pressure, $p_{C,ref}$ and a measurement of said pressure, p_C. This allows for a closed loop control where the pressure setting of the proportional pressure relief valve is adjusted by means of a voltage signal, U, in order to continuously meet the reference value of the compensator pressure.

A block diagram of the used control strategy is shown in Figure 5.

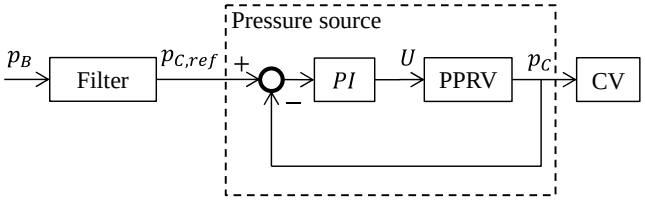

Figure 5. The proposed control strategy.

Clearly, a hydraulic filter circuit connecting p_B with p_C could be considered as an alternative, however, the concept of a closed loop control minimizes the uncertainties on parameters associated with small orifices and liquid dynamics.

In this setup, a PPRV instead of a proportional pressure reducing valve is chosen. The main reason for this is to minimize the pressure drop across the proportional unit because the compensator pressure typically will be 10-20% of the supply pressure.

3 Considered system

In order to examine the novel concept in more detail both linear stability analyses and experiments have been carried out. These investigations have been conducted on the same setup in the mechatronics laboratory at the University of Agder, see Figure 6. The setup consists of a hydraulically actuated boom and a control system.

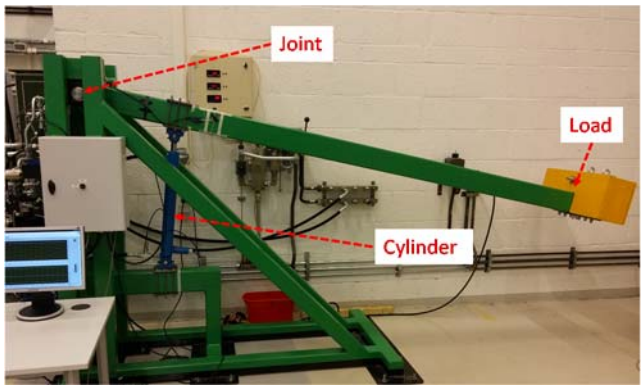

Figure 6. Hydraulic arm test setup.

The hydraulic diagram of the setup corresponds to the one in Figure 4.

The novel concept has been implemented using commercially available components. The DCV and CV are embedded in a pressure compensated 4/3-way directional control valve group from Danfoss (Model: PVG32). It has an electrohydraulic actuation with linear flow vs. input signal characteristics with a maximum value of $Q_{max,DCV} = 25\ \frac{L}{min}$. The 4-port CBV is from Sun Hydraulics (Model: CWCA) with a 3:1 pilot area ratio and a rated flow of $Q_{r,CBV} = 60\ \frac{L}{min}$. The PPRV is from Bosch Rexroth (Model: DBETE) and has a crack pressure that varies linearly with the voltage input. At maximum signal, $U_{max} = 10\ V$, the valve cracks open at $p_{C@0L/min} = 280\ bar$ and has a rated value at $p_{C@0.8L/min} = 315\ bar$.

In Table 1 are listed some other important data for the experimental setup.

Table 1. Important data of the experimental setup.

Parameter	Value
Distance from main hinge to mass centre of boom + load.	$L = 3570\ mm$
Mass of boom + load	$m = 410\ kg$
Cylinder stroke	$H_c = 500\ mm$
Cylinder piston diameter	$D_p = 65\ mm$
Cylinder rod diameter	$D_r = 35\ mm$
Cylinder area ratio	$\mu_C = \frac{D_p^2}{D_p^2 - D_r^2} = 1.41$
Supply pressure	$p_S = 180\ bar$
Eigen frequency of mechanical hydraulic system (cylinder mid stroke)	$f_{mh} = 2.9\ Hz$
Fixed orifice, pressure drop at a flow $Q = 2\ \frac{L}{min}$	$\Delta p\vert_{@2L/min} = 220\ bar$
PPRV, pressure drop at a flow $Q = 2\ \frac{L}{min}$ and fully open	$\Delta p\vert_{@2L/min} = 6.1\ bar$
CBV pilot ratio	$\alpha_P = 3$

A real-time I/O system is used to control the hydraulic valves on the crane with a loop time of 10ms. The control system can record sensor information from all the position and pressure sensors mounted on the crane.

The primary circuit is simply activated in a regular way by continuously supplying the directional control valve with an input signal.

The purpose of the controller on the secondary circuit is to keep the compensator pressure p_C, in accordance with the reference pressure $p_{C,ref}$, in Figure 5. The filter box uses the actual p_B value as input and returns $p_{C,ref}$. The choice of filter frequency should of course reflect both the dominant lowest eigen frequency of the mechanical hydraulic system as well as the demand for a certain response time of the system. The role of the low-pass filter is to remove oscillations, however if it is chosen overly conservative then the system reacts too slowly. Therefore, some logic has been added so

that the compensator reference pressure, $p_{C,ref}$, never goes below a certain minimum value, p_{min}, see equation (1).

$$p_{C,ref} = \begin{cases} p_{min} & p_B < p_{min} \\ p_{B,LPF} & p_B \geq p_{min} \end{cases} \quad (1)$$

where $p_{B,LPF}$ is the low-pass filtered value of p_B.

$$\dot{p}_{B,LPF} = \frac{1}{\tau} \cdot \left(p_B - p_{B,LPF}\right) \quad (2)$$

The PI-controller has the classical outlook

$$U = K_P \cdot \left(p_{C,ref} - p_C\right) + \int K_I \cdot \left(p_{C,ref} - p_C\right) \cdot dt \quad (3)$$

where saturation and corresponding anti-windup measures (integrated effort not accumulated at saturation) are implemented so that $0 \leq U \leq 10\ V$.

Basically, only four parameters need to be set: p_{min}, τ, K_P and K_I.

More advanced control strategies can be implemented if required from a performance point of view. As an example, the use of a feed-forward technique could have been investigated, however the scope of this paper is to present the novel concept rather than pursuing an optimal controller.

The experimental work showed some clear limitations in the chosen implementation of the secondary pressure circuit, which influences the achievable compensator pressure range listed in Table 2.

Table 2. Compensator pressure range for secondary circuit connected to the CV and disconnected.

p_S [bar]	$p_{C,min}$ PPRV fully open [bar]	$p_{C,max}$ PPRV closed [bar]
180	3	75
180*	5*	180*

*disconnected from CV

In the experimental work done in this paper the p_C value did not rise above 55 bar, hence, no attempt was made to increase $p_{C,max}$.

The performance obtained indicates that the circuit in reality looks like the one shown in Figure 7 and that it is somewhat component (CV) dependent.

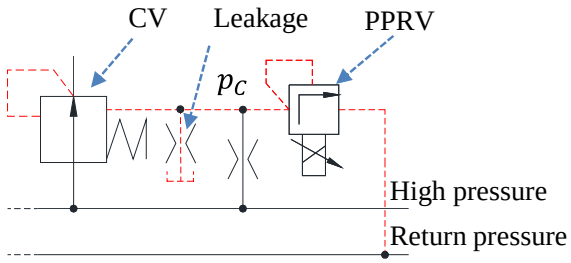

Figure 7. Actual secondary circuit including leakage in the load sensing system of the proportional valve group.

Measurements revealed that the internal leakage of the load sensing system of the proportional valve group has the same order of magnitude as the fixed orifice.

An estimate of the internal leakage yielded a pressure drop at $Q = 2\,\frac{L}{min}$ of $\Delta p|_{@2L/min} = 160\ bar$, i.e., slightly less resistance as compared to the fixed orifice, see Table 1. Internal leakage must be expected across the CV and other places in the load sensing system of the valve group, and this must be taken into account when choosing a PPRV and a fixed orifice. Basically, the fixed orifice shall not be too small relative to internal leakage since this will limit the maximum obtainable compensator pressure. Simultaneously the fixed orifice shall not be too large relative to the PPRV since this will limits the minimum obtainable compensator pressure. Therefore, the secondary circuit components shall be designed based on expected minimum and maximum steady state values of p_B and an estimate of the internal leakage of the valve group. Alternatively, a proportional pressure reducing valve could be connected to the high pressure line and in series with the internal leakage yielding a $p_{C,max}$ close to p_S.

4 Linear stability analysis

A linearised stability analysis can help characterise the novel concept. In Figure 8 is shown a simplified circuit of the considered system including the core components and parameters.

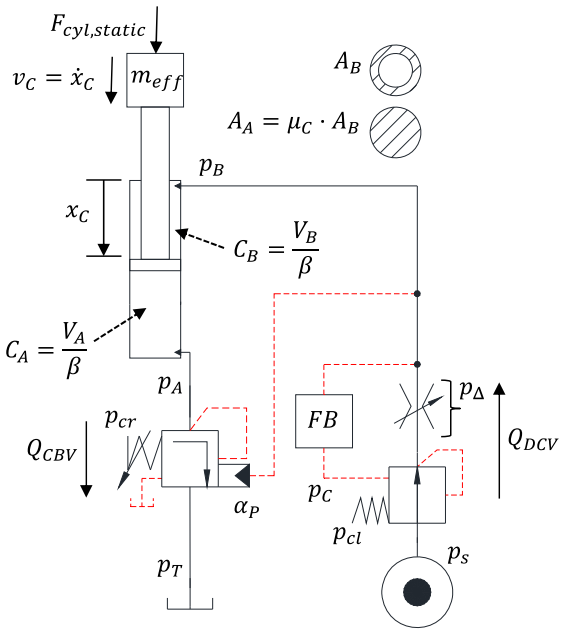

Figure 8. Simplified circuit.

The pressure drop across the metering-in orifice is

$$p_\Delta = p_C - p_B + p_{cl} \tag{4}$$

where p_{CL} is the set pressure of the compensator spring that relates to the fully closed position. The box, FB, is the first order low-pass filter that has been used:

$$p_C = \frac{1}{\tau \cdot s + 1} \cdot p_B \tag{5}$$

The extreme values of the time constant τ of the filter yields:

$$\tau = 0 \qquad p_\Delta = p_{cl} \tag{6}$$

$$\tau = \infty \qquad p_\Delta = p_S - p_{cl} - p_B - p_{C0} \tag{7}$$

Which reduces the system to either the base circuit, see Figure 1, without any filtering or a system with constant compensator pressure, $p_C = p_{C0}$.

The governing equations for the system are:

$$m_{eff} \cdot \dot{v}_C = p_B \cdot A_B - p_A \cdot \mu_C \cdot A_B + F_{cyl,static} \quad (8)$$

$$C_A \cdot \dot{p}_A = \mu_C \cdot A_B \cdot v_c - Q_{CBV} \quad (9)$$

$$C_B \cdot \dot{p}_B = Q_{DCV} - A_B \cdot v_c \quad (10)$$

$$\tau \cdot \dot{p}_C = p_B - p_C \quad (11)$$

$$Q_{DCV} = k_{v,DCV} \cdot u_{DCV} \cdot \sqrt{p_\Delta} \quad (12)$$

$$Q_{CBV} = k_{v,CBV} \cdot u_{CBV} \cdot \sqrt{p_A} \quad (13)$$

$$u_{CBV} = \frac{\alpha_P \cdot p_B + p_A - p_{cr}}{\Delta p_{op,CBV}} \quad (14)$$

In the above, a number of assumptions have been made including: no backpressure, no friction or damping in the cylinder and in the valves, no valve dynamics, no flow forces, and a linear discharge characteristic of the counterbalance valve. The value $\Delta p_{op,CBV}$ is the extra pressure required to fully open the counterbalance valve.

Linearising and denoting any parameter variation relative to the steady state solution with a tilde yields the following expressions in the Laplace domain:

$$m_{eff} \cdot s \cdot \tilde{v}_C = A_B \cdot \tilde{p}_B - \mu_C \cdot A_B \cdot \tilde{p}_A \quad (15)$$

$$C_A \cdot s \cdot \tilde{p}_A = \mu_C \cdot A_B \cdot \tilde{v}_C - \tilde{Q}_{CBV} \quad (16)$$

$$C_B \cdot s \cdot \tilde{p}_B = \tilde{Q}_{DCV} - A_B \cdot \tilde{v}_C \quad (17)$$

$$\tau \cdot s \cdot \tilde{p}_C = \tilde{p}_B - \tilde{p}_C \quad (18)$$

$$\tilde{Q}_{DCV} = k_{qu,DCV} \cdot \tilde{u}_{DCV} + k_{qp,DCV} \cdot (\tilde{p}_C - \tilde{p}_B) \quad (19)$$

$$\tilde{Q}_{CBV} = k_{qu,CBV} \cdot \tilde{u}_{CBV} + k_{qp,CBV} \cdot \tilde{p}_A \quad (20)$$

$$\tilde{u}_{CBV} = \frac{\alpha_P \cdot \tilde{p}_B + \tilde{p}_A}{\Delta p_{op,CBV}} \quad (21)$$

In equation (19) and (20) the valve gains are:

$$k_{qu,DCV} = k_{v,DCV} \cdot \sqrt{p_\Delta^{(ss)}} \quad (22)$$

$$k_{qp,DCV} = \frac{k_{v,DCV} \cdot u_{DCV}^{(ss)}}{2 \cdot \sqrt{p_{\Delta}^{(ss)}}} \tag{23}$$

$$k_{qu,CBV} = k_{v,CBV} \cdot \sqrt{p_{A}^{(ss)}} \tag{24}$$

$$k_{qp,CBV} = \frac{k_{v,CBV} \cdot u_{CBV}}{2 \cdot \sqrt{p_{A}^{(ss)}}} \tag{25}$$

Specifically, equation (19) is of interest since it reveals the influence of the filtering. With no filtering, $\tau = 0$, the DCV flow is:

$$\tilde{Q}_{DCV} = k_{qu,DCV} \cdot \tilde{u}_{DCV} \tag{26}$$

which corresponds to the base circuit without any damping of the inlet flow. With maximum filtration, $\tau = \infty$, it becomes

$$\tilde{Q}_{DCV} = k_{qu,DCV} \cdot \tilde{u}_{DCV} - k_{qp,DCV} \cdot \tilde{p}_{B} \tag{27}$$

where the negative term automatically introduces damping in the system. In practice, a finite time constant is present, which leads to the flow being described by equation (19). It should be noted that when the steady state opening of the directional control valve becomes zero, $\tilde{u}_{DCV} = 0$, then equation (27) becomes (26). In practice, there will be some leakage in the zero position so that $k_{qp,DCV}$ never becomes exactly zero as discussed by (Merritt, 1967) on servo valves in neutral position, however, the novel concept will have less impact for small valve openings.

From equations (15)...(21) the closed loop transfer function for valve opening $\tilde{u}_{DCV}$ as input and the cylinder displacement flow $A_B \cdot \tilde{v}_C$ as output can be derived. The transfer function is of the fourth order and the denominator is expressed by:

$$D(s) = D_4(\tau) \cdot s^4 + D_3(\tau) \cdot s^3 + D_2(\tau) \cdot s^2 + D_1(\tau) \cdot s + D_0 \tag{28}$$

where the coefficients are:

$$D_4 = C_A \cdot C_B \cdot m_{eff} \cdot \tau \tag{29}$$

$$D_3 = \left(C_A \cdot k_{qp,DCV} + C_B \cdot k_{qo,CBV} + C_B \cdot k_{qp,CBV}\right) \cdot m_{eff} \cdot \tau + C_A \cdot C_B \cdot m_{eff} \tag{30}$$

$$D_2 = \left(A_B^2 \cdot C_A + A_B^2 \cdot C_B \cdot \mu_C^2 + k_{qo,CBV} \cdot k_{qp,DCV} \cdot m_{eff} + k_{qp,CBV} \cdot k_{qp,DCV} \cdot m_{eff}\right) \cdot \tau + \left(k_{qo,CBV} + k_{qp,CBV}\right) \cdot C_B \cdot m_{eff} \tag{31}$$

$$D_1 = \left(k_{qo,CBV} + k_{qp,CBV} + k_{qp,DCV} \cdot \mu_C^2 + \alpha_p \cdot k_{qo,CBV} \cdot \mu_C\right) \cdot A_B^2 \cdot \tau + \left(C_B \cdot \mu_C^2 + C_A\right) \cdot A_B^2 \tag{32}$$

$$D_0 = \left(\left(1 + \alpha_p \cdot \mu_C\right) \cdot k_{qo,CBV} + k_{qp,CBV}\right) \cdot A_B^2 \tag{33}$$

In the above equations the term

$$k_{qo,CBV} = \frac{k_{qu,CBV}}{\Delta p_{op,CBV}} = \frac{k_{v,CBV} \cdot \sqrt{p_A^{(ss)}}}{\Delta p_{op,CBV}} \tag{34}$$

has been introduced in order to simplify the notation.

The Routh-Hurwitz stability criteria states that the system is stable if the following three inequalities are fulfilled:

$$D_i > 0, for\ i = 1..4 \tag{35}$$

$$D_3 \cdot D_2 - D_4 \cdot D_1 > 0 \tag{36}$$

$$D_3 \cdot D_2 \cdot D_1 - D_4 \cdot D_1^2 - D_3^2 \cdot D_0 > 0 \tag{37}$$

Inequality in equation (35) is always satisfied. The other two inequalities must be investigated numerically because the expressions are not easily interpreted. The cylinder position is chosen as almost fully extracted with $x_C = 0.05\,m$, or 90% extracted, avoiding singularities caused by zero capacitance in the B-volume. It is well known that a combination of the fully extracted position and small openings of the counterbalance valve is critical with respect to stability.

Table 3. Parameters of linearised analysis.

Parameter	Value
External cylinder load	$F_{cyl,static} = 2.10 \cdot 10^4 N$
Effective mass	$m_{eff} = 1.50 \cdot 10^4\ kg$
Capacitance of A volume	$C_A = 1.13 \cdot 10^{-4} \frac{L}{bar}$
Capacitance of B volume	$C_B = 2.45 \cdot 10^{-5} \frac{L}{bar}$
Directional control valve constant	$k_{v,DCV} = 9.34 \frac{L}{min \cdot \sqrt{bar}}$
Counterbalance valve constant	$k_{v,CBV} = 15 \frac{L}{min \cdot \sqrt{bar}}$
Counterbalance valve fully open pressure difference	$\Delta p_{op,CBV} = 250 bar$

Without maximum filtering, see equation (27), the minimum steady state opening that is stable is $u_{DCV}^{(ss)} = 0.033$. Without any filtering, see equation (26), the system is unstable for any value of $u_{DCV}^{(ss)}$. In Figure 9 the minimum time constant value that yields a stable system, τ_{min}, is plotted vs. $u_{DCV}^{(ss)}$. It is clear that the correlation is strongly nonlinear allowing very small time constants until the critical steady state opening is approached.

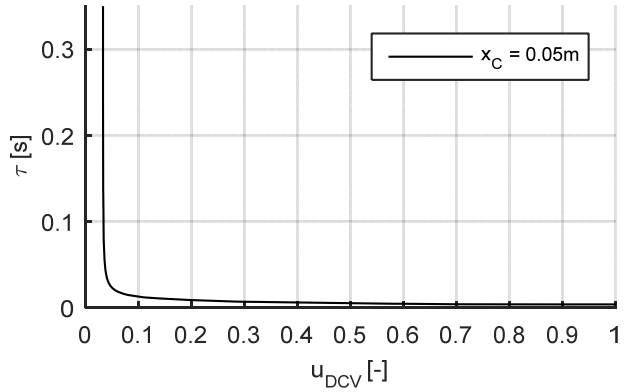

Figure 9. Stability of the linear model. The minimum time constant value that yields a stable system is plotted vs. the dimensionless opening of the directional control valve u_{DCV}.

The linear analysis reveals that the novel concept can improve stability. However, for very small openings of the DCV and, subsequently, small openings of the CBV the novel concept will become increasingly similar in

behaviour to the base circuit that is inherently unstable. The linear analysis has some limitations at the small openings. Leakage in the DCV as well as damping in the compensator and CBV will greatly improve the ability of the novel concept to suppress oscillations even at small flows.

5 Experimental investigation

The investigation is divided in two parts: one for the secondary circuit alone and one for the total system.

5.1 Secondary circuit

In order to be able to evaluate the performance of the novel concept the secondary circuit is analysed first. To do so a reference step input, $p_{C,ref}$, of 40 bar is applied to the secondary circuit alone. With $p_{min} = 5\ bar$, the gains were adjusted to: $K_P = 0.01\frac{V}{bar}$ and $K_I = 0.04\frac{V}{bar \cdot s}$. The results are shown in Figure 10.

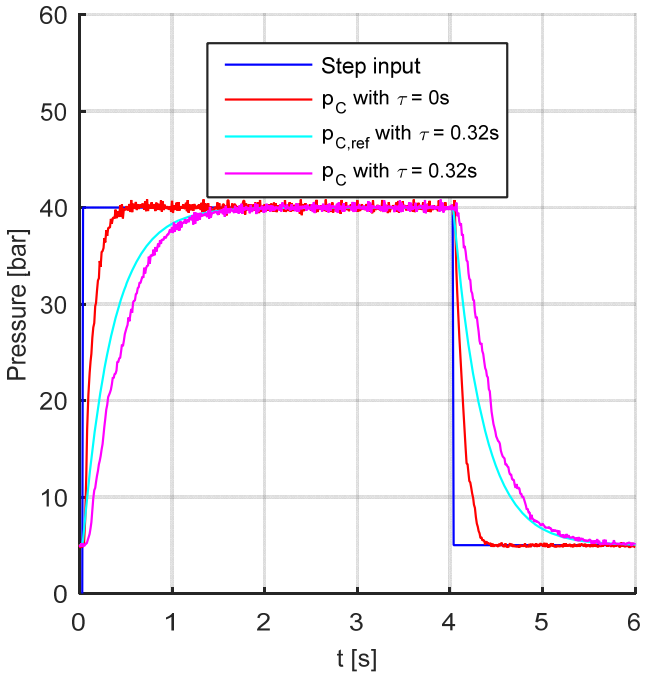

Figure 10. Pressure performance of secondary circuit.

The blue curve shows the reference input. The ability of the closed-loop control system to follow this reference is shown in red. It takes approximately

0.3s to reach the wanted reference. This curve is obtained without any filtration, i.e., $\tau = 0\ s$, The remaining curves, the cyan and magenta ones demonstrate the effect of the low-pass filter in the system, where the curves show the filtered reference $p_{C,ref}$ and how p_C follows it. The cut-off frequency is set to approximately 20% of the mechanical hydraulic eigen frequency, i.e., $\tau = 0.32s$.

5.2 Total system

To achieve a uniform evaluation of the total system a standard actuation of the DCV is used, see Figure 11. Only situations where the cylinder is retracting are investigated.

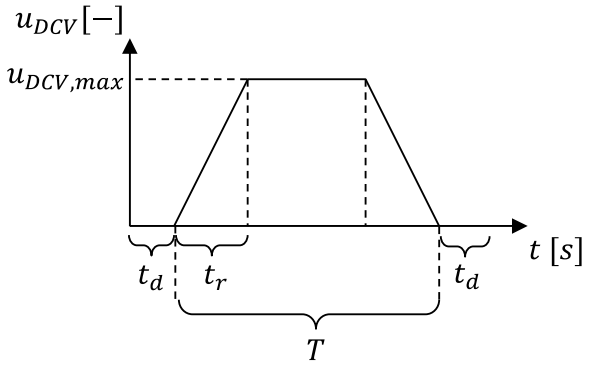

Figure 11. Work cycle - actuation function.

The actuation is defined by the cycle time, T, a delay time to ensure static conditions, t_d, the ramp time, t_r, and the wanted steady state DCV input $u_{DCV,max}$. The time parameters are similar for all tests, see Table 4.

Table 4. Common parameters for all actuation.

Cycle time, T	Ramp time, t_r	Time delay, t_d
8 s	1 s	1 s

5.2.1 Demonstration of novel concept

The effect of the novel concept is shown in Figure 12 where the system is subjected to an actuation of $u_{DCV,max} = 0.15$. The controller was implemented with $p_{min} = 35\ bar$, and the same gains as in section 5.1.

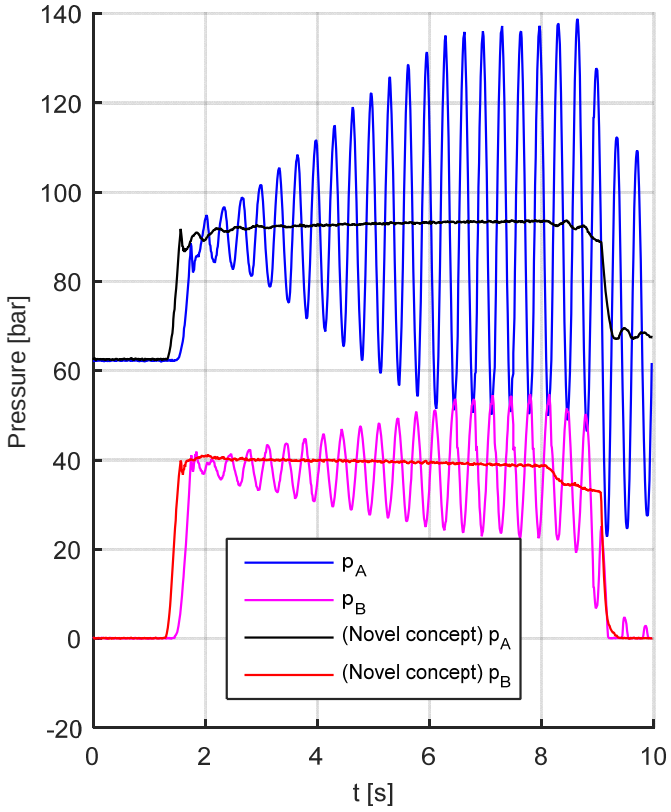

Figure 12. Comparison of pressures between the base circuit and the system with the novel concept implemented ($u_{DCV,max} = 0.15$).

The base circuit should be unstable and the novel concept stable according to the linear analysis which is also what can be observed. Further, the ability of the novel concept to suppress oscillations in a real system is demonstrated. The corresponding behaviour of the secondary circuit is shown in Figure 13.

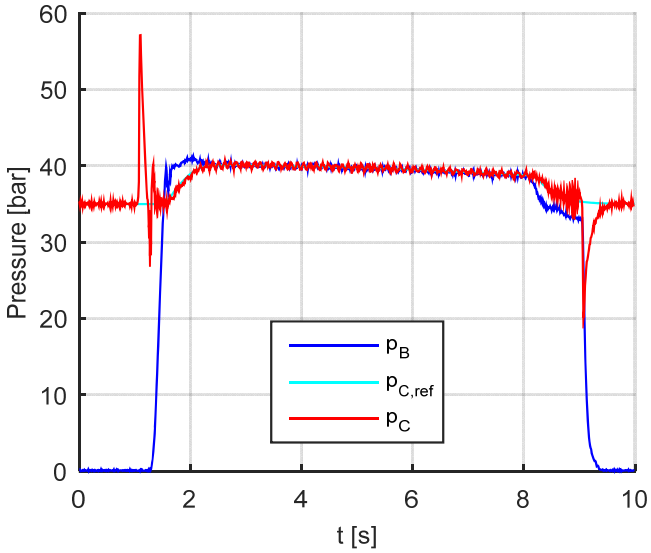

Figure 13. Pressure response of the novel concept's secondary circuit during work cycle ($u_{DCV,max} = 0.15$).

It is clear, that as the DCV is actuated at $t = t_d$ the secondary circuit is subjected to disturbances. The disturbances are probably caused by the motion of the main spool and the related variations in leakage paths as well as the pumping effect of the CV spool. As an example, the increase in p_C to approximately 55 bar at $t = 1.2\ s$ will remain if the PPRV is not actively controlled. Investigations show that the disturbances are DCV related and should be expected when using a standard valve for this system. However, the PI-controller of the secondary circuit manages these disturbances before the DCV reaches its deadband and the motion of the cylinder is not affected.

5.2.2 Stability for small DCV openings

The stability analysis of the linear model predicted instability for small openings of the DCV. To verify this the work cycle was executed with $u_{DCV,max} = 0.05$. This was done for the base circuit and the novel concept, see Figure 14.

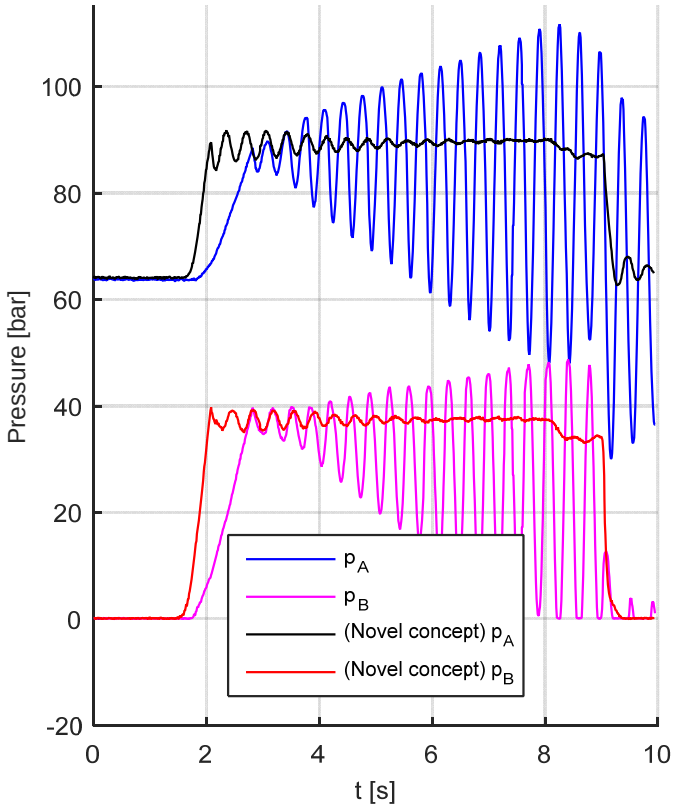

Figure 14. Comparison of pressures between the base circuit and the system with the novel concept implemented ($u_{DCV,max} = 0.05$).

Experiments show that in reality the novel concept seems able to suppress oscillations for small valve openings as well although a certain variation is observed in both pressures. Obviously, the inherent damping of the system as well as the fact that the cylinder is stroking in and thereby moving towards a more stable position means that the system oscillations are suppressed.

5.2.3 Handling different DCV openings

An important feature of the novel concept is that it shall be able to maintain the load independent flow capability of the DCV. Experiments using the work cycle function for eight different values of $u_{DCV,max}$ for both the base circuit and the novel concept were conducted and the steady state cylinder velocities can be compared.

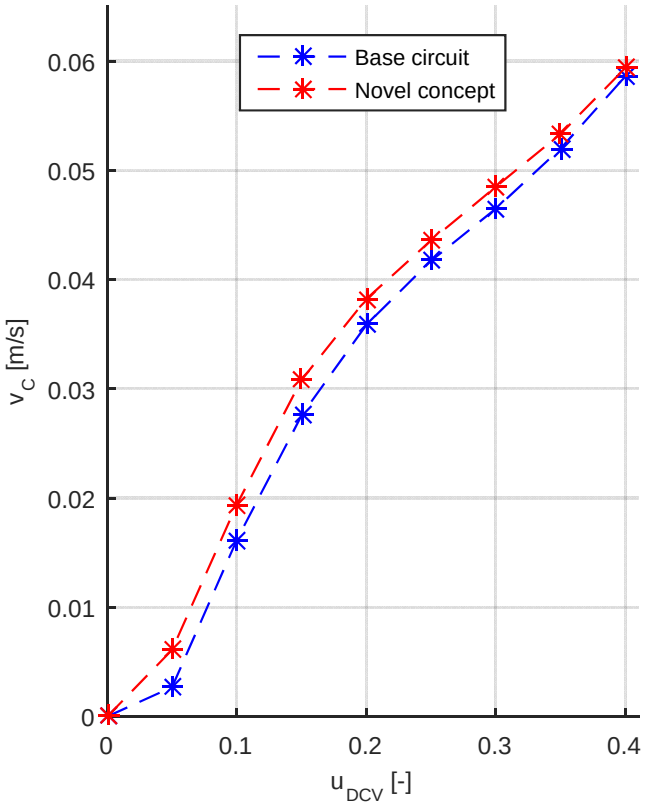

Figure 15. Steady state cylinder velocities for different valve openings for both the base circuit and the novel concept.

The results of these experiments are shown in Figure 15. The shape of the curves for the two systems are similar indicating that the flow control is intact. It can be seen that the novel concept has a slightly higher flow rate. A possible explanation is that the pressure experienced by the CV in the base circuit, due to small orifice effects in the LS-paths, is actually slightly smaller than the p_B value. Unlike for the novel concept where such a reduction in pilot pressure is automatically compensated.

5.2.4 Handling load variations

This section continues with experiments demonstrating the ability of the novel concept to handle load variations. These experiments were conducted using the work cycle with $u_{DCV,max} = 0.15$. Experiments for three different load cases were chosen with required p_B-pressures of 40, 47 and 55 bar corresponding to different loads mounted on the boom.

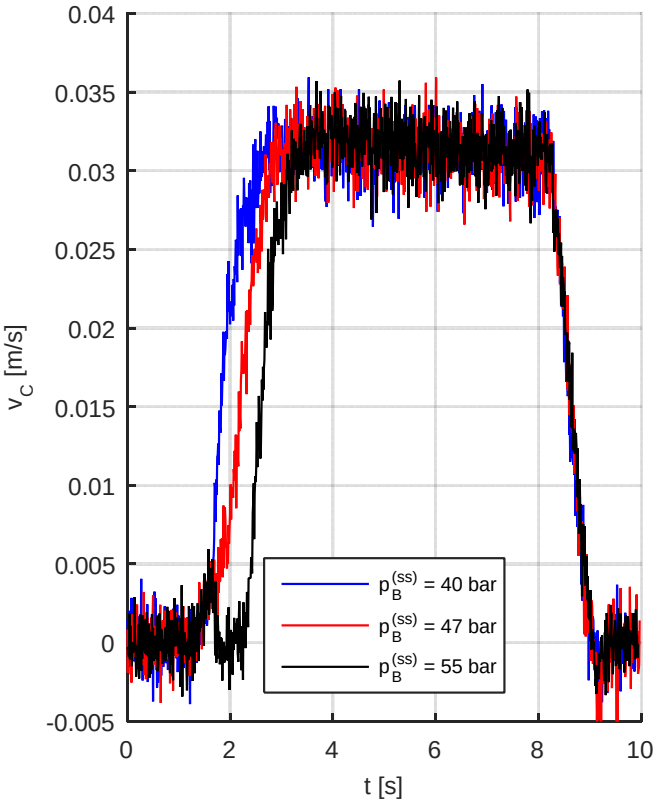

Figure 16. Comparison of cylinder velocities – different pressure levels.

Figure 16 shows that the steady state speed is load independent when using the novel concept, however, the response time is increased when the difference between the standby pressure and the steady state pressure level is increased. This is caused by the low-pass filter and the effect can probably be reduced by improving the closed loop control of the secondary circuit.

6 Conclusions

A novel concept for suppressing oscillations in hydraulic systems containing a counterbalance valve and a pressure compensated flow supply is presented. The concept utilizes a secondary circuit where a low-pass filtered value of the load pressure is generated and fed back to the compensator of the flow supply valve.

Stability of the novel concept has been investigated on a linearized model and has been experimentally verified. The results show a significant

reduction of the pressure oscillations when lowering the boom on an otherwise unstable system

The stability analysis indicates that for DCV openings below 3.3% instability will still be an issue. However, this is not observed experimentally which can be explained by a lack of damping in the linear model.

Experiments comparing the steady state cylinder velocity for different DCV openings and different load pressure levels also show that the load independent flow of the base circuit is kept when using the novel concept. From the operator point of view, the behaviour is left unaltered and hence eliminating the need for additional velocity control of the actuator.

6.1 Future work

In the present paper some issues have not been investigated deeply and require more work. Amongst other, this includes the following:

- Deeper analysis of the relation between component properties and system performance utilising the novel concept
- Further investigation of the consequences of load variations on the boom
- Investigation of system performance using different pilot ratios of the CBV
- Try different filtering algorithms in the filter box in order to reduce the response time of the system

Acknowledgements

The authors wish to thanks Rune Husveg, Sondre Nordås, Christian Solvik and Thomas Børseth for their contribution during their master thesis studies assembling the test setup and doing preliminary experiments.

Funding

The work is funded by the Norwegian Ministry of Education & Research and National Oilwell Varco.

References

Bosch. 2015. Counterbalance valves. http://apps.boschrexroth.com/products/compact-hydraulics/PiB-Catalogs/. Bosch Rexroth Oil Control S.p.A.

Cristofori, D., Vacca, A., and Ariyur, K.. 2012. A Novel Pressure-Feedback Based Adaptive Control Method to Damp Instabilities in Hydraulic Machines, SAE Int. J. Commer. Veh. 5(2):586-596, 2012, doi:10.4271/2012-01-2035.

Handroos, H., Halme, J. and Vilenius, M.. 1993. Steady-state and Dynamic Properties of Counter Balance Valves. *3rd Scandinavian International Conference on Fluid Power*. Linköping, Sweden.

Hansen, M. and Andersen, T., 2001. A Design Procedure for Actuator Control Systems Using Optimization Methods. 7th Scandinavian International Conference on Fluid Power, Linköping, Sweden.

Hansen, M. and Andersen, T.. 2010. Controlling a negative loaded hydraulic cylinder using pressure feedback. 29th IASTED International Conference on Modelling, Identification and Control, Innsbruck, Austria, doi: http://dx.doi.org/10.2316/P.2010.675-116.

Hansen, M. and Sørensen, J.. 2015. Improvements in the control of hydraulic actuators. EP15171831 (Pending)

Merritt, H.E.. 1967. Hydraulic Control Systems. John Wiley & Sons, New York..

Miyakawa, S.. 1978. Stability of a Hydraulic Circuit with a Counter-balance Valve. *Bulletin of the JSME*, Vol. 21, No. 162 pp. 1750-1756.

NEM. 2014. Solutions from NEM ... for Telescopic Handlers and Loaders. Edition 11/2014, NEM hydraulics. Available from: http://www.nem-hydraulics.com/pdf/NEM_Folder_Telescopic_Handlers.pdf

Nordhammer, P., Bak, M., and Hansen, M.. 2012. A method for reliable motion control of pressure compensated hydraulic actuation with counterbalance valves. 12th International Conference on Control, automation and systems (ICCAS), Jeju Island, Korea.

Pedersen, H., Andersen, T., Hansen, R. and Stubkier, S.. 2010. Investigation of Separate Meter-In Separate Meter-Out Control Strategies for Systems

with Over Centre Valves. ASME Symposium on Fluid Power and Motion Control, FPMC 2010, Bath, UK

Persson, T., Krus, P. and Palmberg, J-O.. 1989. The Dynamic Properties of Over-Center Valves in Mobile Systems. *2nd International Conference on Fluid Power Transmission and Control*. Hangzhou, China.

Ritelli, G. and Vacca, A.. 2014. A General Auto-Tuning Method For Active Vibration Damping of Mobile Hydraulic Machines. 8th FPNI Ph.D. Symposium on Fluid Power, Lappeenranta, Finland.

Sørensen, J., Hansen, M. and Ebbesen, M.. 2014. Boom Motion Control Using Pressure Control Valve. 8th FPNI Ph.D. Symposium on Fluid Power, Lappeenranta, Finland.

Sørensen, J., Hansen, M. and Ebbesen, M.. 2015. Load Independent Velocity Control On Boom Motion Using Pressure Control Valve. 14th Scandinavian International Conference on Fluid Power, Tampere, Finland.

Zähe, B.. 1995. Stability of Load Holding Circuits with Counterbalance Valve. *8th International Bath Fluid Power Workshop*. Bath, UK.

Authors

Jesper K. Sørensen graduated in 2010 from Aalborg University with a M.Sc. in Electric Mechanical System Design. He worked two years in the Wind Turbine industry, before beginning as a Ph.D. student in the Mechatronics group at University of Agder, Norway, in 2012. The topic of his research is boom movement in hydraulic cranes, with main focus on the hydraulic actuation.

Michael R. Hansen received his M.Sc. in mechanical engineering from Aalborg University in Denmark in 1989 and his Ph.D. in computer-aided design of mechanical mechanisms from the same institution in 1992. He is currently holding a position as professor in fluid power in the mechatronics group at the Department of Engineering Sciences at the University of Agder in Norway. His research interests mainly include fluid power, multi-body dynamics and design optimization.

Morten K. Ebbesen is affiliated with the Department of Engineering Sciences, University of Agder, Norway, as associate professor in the Mechatronics group. He received his M.Sc. (2003) and Ph.D. (2010) in mechanical engineering from the University of Aalborg, Denmark. His interests are in the field of dynamics, flexible multibody systems, time domain simulation, hydraulics and optimization.

Paper D

Numerical and Experimental Study of a Novel Concept for Hydraulically Controlled Negative Loads

Jesper Kirk Sørensen, Michael Rygaard Hansen and Morten Kjeld Ebbesen.

This paper has been submitted as:

Jesper Kirk Sørensen, Michael Rygaard Hansen and Morten Kjeld Ebbesen., ”Numerical and Experimental Study of a Novel Concept for Hydraulically Controlled Negative Loads”, *Modeling, Identification and Control.* Publisher: Norwegian Society of Automatic Control, expected 2016.

Numerical and Experimental Study of a Novel Concept for Hydraulically Controlled Negative Loads

Jesper Kirk Sørensen, Michael Rygaard Hansen and Morten Kjeld Ebbesen.
Department of Engineering Sciences
Faculty of Engineering and Science, University of Agder
Jon Lilletunsvei 9, 4879 Grimstad, Norway.

Abstract — **This paper presents a numerical and experimental investigation of a novel concept that eliminates oscillations in hydraulic systems containing a counterbalance valve in series with a pressure compensated flow supply. The concept utilizes a secondary circuit where a low-pass filtered value of the load pressure is generated and fed back to the compensator of the flow supply valve. The novel concept has been implemented on a single boom actuated by a cylinder. A nonlinear model of the system has been developed and an experimental verification shows good correspondence between the model and the real system. The model is used for a parameter study on the novel concept. From the study it is found that the system is stable for large directional valve openings and that for small openings a reduction of the oscillatory behaviour of the system can be obtained by either lowering the eigen frequency of the mechanical-hydraulic system or by lowering the pilot area ratio of the counterbalance valve.**

Keywords — **counterbalance valve, pressure compensated valve, instabilities in hydraulic systems, nonlinear model, load-holding application.**

1 Introduction

For safety reasons, hydraulic load carrying applications are required by law to contain a load holding protection device. The most widely used device is the counterbalance valve (CBV). It is multi-functional and provides leak tight load holding, load holding at hose/pump failure as well as shock absorption, overload protection, and cavitation prevention at load lowering. However, it is well known that a series connection of a pressure compensator (CV), a directional control valve (DCV), and a CBV tends to introduce instability in a system, see Miyakawa (1978), Persson et al. (1989), Handroos et al. (1993), Zähe (1995) and Hansen and Andersen (2010). This is mainly a problem when the controlled actuator is subjected to a negative load, i.e., a load that tends to drive the actuator as a pump, because this will require the counterbalance valve to throttle the return flow, see Figure 1. The system in Figure 1 will be referred to as the base circuit.

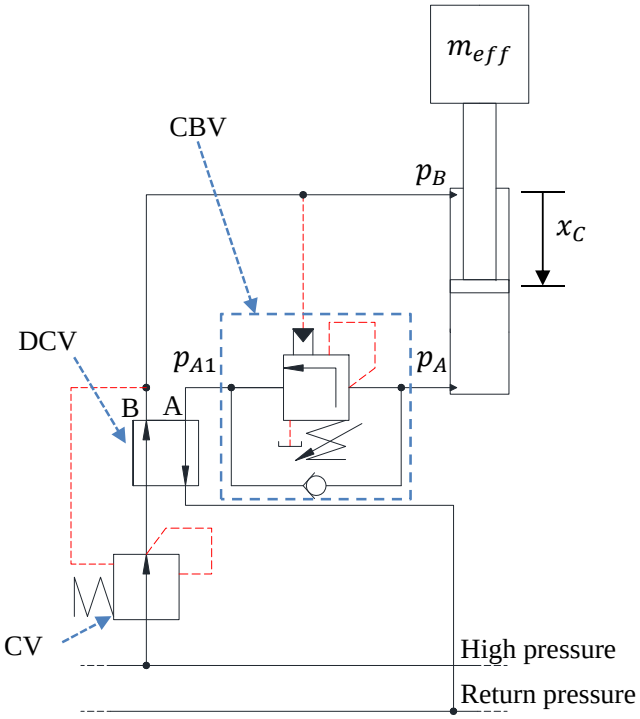

Figure 1: The base circuit consisting of a pressure compensator (CV), a directional control valve (DCV), a counterbalance valve (CBV), and a cylinder subjected to a compressing load.

It is a major challenge within hydraulic system design to find solutions that offer stable handling of negative loads together with pressure compensated metering-in flow. Typically, practical solutions will compromise either the load independency, the response time or the level of oscillations (Hansen and Andersen (2001) and Nordhammer et al. (2012)). The consequences of the oscillatory nature of such systems are reduced safety, reduced productivity as well as added fatigue load on both the mechanical and hydraulic system. The severity of oscillations is affected by a wide variety of parameters some of which are hard to predict or change: the external load on the actuator, the properties of the mechanical structure, the friction in the cylinder, the damping and hysteresis of the CBV, the operator input as well as volumes and restrictions in the hydraulic lines. The efforts to minimize the oscillatory nature of the base circuit can be divided into three groups: Parameters variations (pilot area ratio of CBV, pilot line orifices, etc.) on the circuit using the same main components. The parameters with most influence on the stability are the damping of the system and the pilot ratio of the CBV (Hansen and Andersen, 2001). However lowering the pilot ratio of the CBV to minimize the oscillations will increase pressure levels and hence increase power consumption – especially with small external loads. Another approach is to add damping when designing the pilot line leading in to the CBV. However, no unique solution has emerged that is useful across applications and working conditions. A different approach is to actively compensate for the oscillations by applying closed-loop control strategies that involve the input signal to the DCV and some kind of pressure feedback (Hansen and Andersen (2010), Cristofori et al. (2012) and Ritelli and Vacca (2014)). The most important limitation in these strategies is the bandwidth limitation in typical DCVs. Alternatively, the pressure compensator (CV) can be removed and the DCV replaced by a servo valve which is a proven and reliable method for motion control. The weaknesses here are in the investment costs and the difficulties in handling disturbances in the supply pressure caused by neighbouring circuits. The author have investigated the use of a DCV with compensated supply pressure, see Sørensen et al. (2014) and Sørensen et al. (2015). This is a commercially

available alternative that is characterized by low cost but also load dependent flow. Another example is described in Nordhammer et al. (2012), where the main throttling ability is moved from the CBV to the return orifice of the DCV, thereby eliminating the oscillations. However, this is not a viable solution if the minimum load is 60% or less of the maximum load, which strongly minimizes the applicability. All of the approaches have certain drawbacks as compared to the base circuit. The authors have previously presented a novel concept for addressing this stability issue (Sørensen et al., 2016). It has the same steady state flow characteristics as the base circuit only without the corresponding oscillatory nature. The novel concept was implemented on an experimental setup and its ability to suppress oscillations was experimentally verified. This paper is devoted to the nonlinear modelling of the new concept with a view to investigate and predict the performance of the novel concept with special emphasis on stability.

2 Novel concept

In Figure 2 a hydraulic diagram of the proposed novel concept is shown, patent pending (Hansen and Sørensen, 2015). It is shown in a situation where the actuator is subjected to a negative load, i.e., a lowering motion of some gravitational payload.

When compared to the base circuit in Figure 1, it can be seen that the pilot pressure connection of the CV is supplied by the secondary circuit rather than by the B-port pressure. The underlying idea is to suppress oscillations in the system by generating the steady state value of the B-port pressure in the secondary circuit, filtering out any oscillations. The novel concept also encompasses solutions where the secondary circuit is connected to the CBV or both the CV and the CBV. The version used in this paper where only the CV is connected to the secondary circuit, is however the preferred one from a reliability point of view. This is because the CBV and the related safety functions are activated independent of any electrical system. Since the concept is passive as seen from the operator's point of view it can be

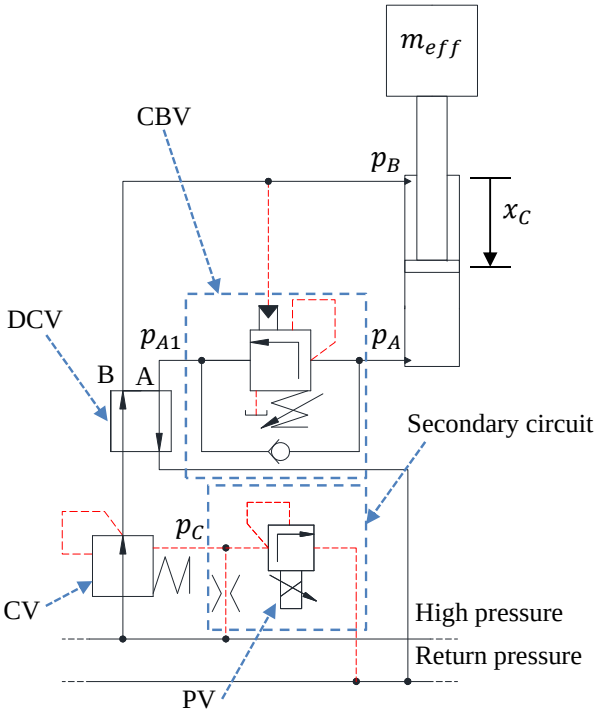

Figure 2: Hydraulic diagram of novel concept where the CV is connected to the secondary circuit.

combined with any closed loop control strategies on the DCV. In this paper, the concept presented is with a linear actuator, but the method will also work for rotational actuators in circuits with counterbalance valves.

The novel concept employs an orifice and a proportional pressure relief valve (PV) in series. The intermediate pressure, p_C, is connected to the CV and will be referred to as the compensator pressure. The overall target is that p_C shall be the steady state value of p_B thereby suppressing oscillations of the compensator and, subsequently, in the entire system. For that purpose, a control strategy is suggested that requires the measurement of p_B, a low-pass filtering yielding a reference value for the compensator pressure, p_C^{ref} and a measurement of pressure, p_C. This allows for a closed loop control where the pressure setting of the proportional pressure relief valve is adjusted by means of a control signal, u_{PV}, in order to continuously meet the reference value of the compensator pressure. A block diagram of the used control strategy is shown in Figure 3.

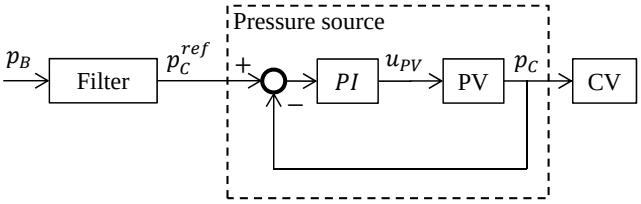

Figure 3: The proposed control strategy.

Figure 4 demonstrates the effect of the novel solution. It compares the pressures on both sides of the cylinder for the base circuit and the novel concept when providing a ramp input downwards to a simple load-carrying boom, see further details in section 3. The base circuit is unstable and the ability of the novel concept to suppress oscillations in a real system is clear.

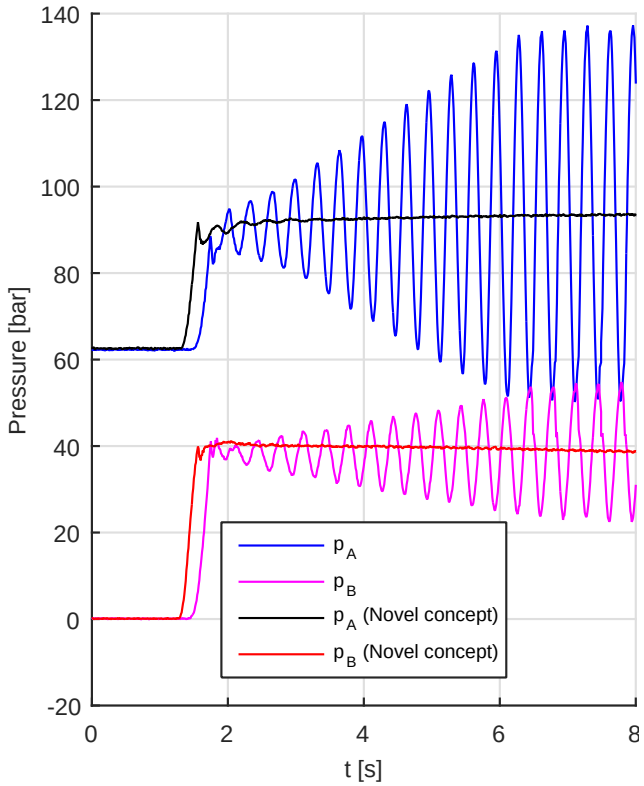

Figure 4: Comparison of pressures between the base circuit and the system with the novel concept implemented for a DCV ramp input.

3 Considered system

In order to examine the novel concept in more detail investigations have been conducted on a setup in the mechatronics laboratory at the University of Agder, see Figure 5. The setup consists of a hydraulically actuated boom and a control system.

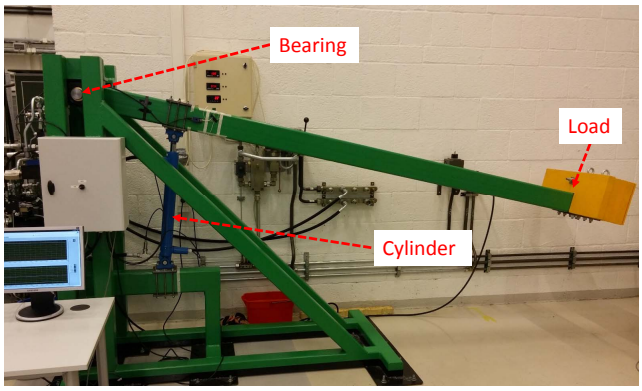

Figure 5: Hydraulic boom experimental setup.

The hydraulics can easily be altered from the novel concept in Figure 2 to the base circuit in Figure 1. The novel concept has been implemented using commercially available components. The DCV and CV are embedded in a pressure compensated 4/3-way directional control valve group from Danfoss (Model: PVG32). It has an electrohydraulic actuation with linear flow vs. input signal characteristics with a maximum value of $Q_{DCV}^{max} = 25L/min$. The 4-port CBV is from Sun Hydraulics (Model: CWCA) with a 3:1 pilot area ratio and a rated flow of $Q_{CBV}^{r} = 60L/min$. The PV is from Bosch Rexroth (Model: DBETE) and has a crack pressure that varies linearly with the voltage input. At maximum signal, $u_{PV}^{max} = 1$, the valve cracks open at $p_{C@0L/min} = 185bar$ and has a rated pressure $p_{PV}^{r} = p_{C@0.8L/min} = 200bar$. In Table 1 are listed some other design parameters of the experimental setup.
A real-time I/O system is used to control the hydraulic valves on the boom with a loop time of 10ms. The control system can record sensor information from all the position and pressure sensors mounted on the test setup. The primary circuit is activated by supplying the directional control valve with an input signal. The purpose of the controller on the secondary circuit is to keep

Table 1: Design parameters of the experimental setup.

Parameter	Value
Distance from bearing to mass centre of boom + load.	$L = 3570mm$
Mass of boom + load	$m = 410kg$
Cylinder stroke	$H_c = 500mm$
Cylinder piston diameter	$D_p = 65mm$
Cylinder rod diameter	$D_r = 35mm$
Cylinder area ratio	$\mu_C = \frac{D_p^2}{D_p^2 - D_r^2} = 1.41$
Supply pressure	$p_S = 180bar$

the compensator pressure, p_C, in accordance with the reference pressure p_C^{ref}, in Figure 3. The filter box uses the actual p_B value as input and returns p_C^{ref}. The choice of filter frequency should of course reflect both the dominant lowest eigen frequency of the mechanical-hydraulic system as well as the demand for a certain response time of the system. The role of the low-pass filter is to remove oscillations, however if it is chosen overly conservative then the system reacts too slowly. Therefore, some logic has been added so that the compensator reference pressure, p_C^{ref}, never goes below a certain minimum value, p^{min}:

$$p_C^{ref} = \begin{cases} p^{min} & , p_B < p^{min} \\ p_{B,LPF} & , p_B \geq p^{min} \end{cases} \tag{1}$$

where $p_{B,LPF}$ is the low-pass filtered value of p_B:

$$\dot{p}_{B,LPF} = \frac{1}{\tau} \cdot (p_B - p_{B,LPF}) \tag{2}$$

The PI-controller has the classic form:

$$u_{PV} = K_P \cdot (p_C^{ref} - p_C) + \int K_I \cdot (p_C^{ref} - p_C) \cdot dt \tag{3}$$

where saturation and corresponding anti-windup measures (integrated effort

not accumulated at saturation) are implemented so that $0 \leq u_{PV} \leq 1$. Basically, only four parameters need to be set: p^{min}, τ, K_P and K_I.

4 Nonlinear model

A nonlinear model of the system, both with and without the novel concept implemented, is developed using the commercial simulation software SimulationX. This section describes how the different parts of this model are modelled.

4.1 Mechanical system

The mechanical system used in the investigation of the concept for stabilizing the hydraulic circuit comprises a boom, a payload, a base, and a double acting hydraulic actuator – see Figure 6.

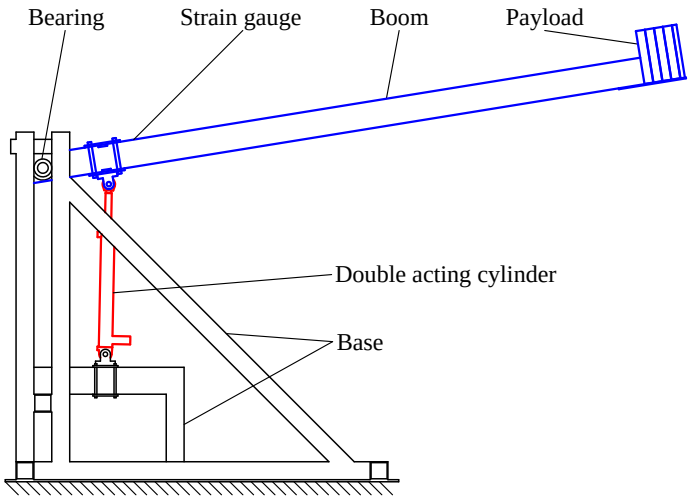

Figure 6: Mechanical system.

In the time domain simulation of the system the boom is modelled to be flexible using the finite segment method as described by Huston and Wang (1994). The method is now well tested for modelling the dynamic behaviour of flexible beam systems in a relatively simple way. In the finite segment

method a beam is replaced with a number of smaller beam segments connected to each other with extension and/or torsional springs. With this method it is possible to model both bending, extension, and torsion of a beam. The system at hand is considered to be a planar mechanism and only bending is taken into account. The flexibility in the longitudinal direction of the beam is omitted as its influence on the dynamic behaviour of the system can be neglected. Therefore the segments in the present model are connected by revolute joints and torsional springs. Due to the segmented nature of the model it does not describe the deformed shape of the beam smoothly but this is not required for the problem at hand where the key point of interest is system oscillations. The segmented structure is illustrated in Figure 7.

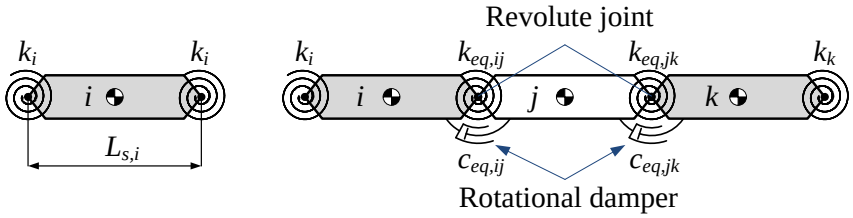

Figure 7: Illustration of torsional springs and dampers between segments in the finite segment method.

The torsional spring between two segments has the stiffness of two springs mounted in series. The stiffness k_i of the spring related to segment number i can be written as:

$$k_i = \frac{2 \cdot E \cdot I_z}{L_{s,i}} \tag{4}$$

where E is the bulk modulus of the beam material, I_z is the 2$^{\text{nd}}$ moment of inertia for the cross section of the prismatic beam, and $L_{s,i}$ is the length of the segment. The equivalent spring stiffness $k_{eq,ij}$ between two segments can then be written as two springs in series:

$$k_{eq,ij} = \frac{k_i \cdot k_j}{k_i + k_j} \tag{5}$$

The number of segments in the model is a compromise between accuracy

and computational time. To obtain a sufficiently good approximation of the eigen frequency of the boom the model contains four segments between the bearing and cylinder and five segments between the cylinder and the payload. The base is considered to be rigid even though observations during the experimental work have revealed that the base also contributes to the flexibility in the system. To accommodate the flexibility of the base a tuning factor has been applied to the stiffnesses of the segments to tune the dynamic behaviour to experimental data. The payload is considered to be a rigid point mass. As illustrated in Figure 7 a rotational damper is also included in the connection between two segments. The value of the damping coefficient, c_{eq}, is found through tuning to the experimental data.

4.2 Hydraulic system

The description of the hydraulic system is only developed for downwards motion of the boom.

4.2.1 Directional control valve

The directional control valve unit consists of a directional control valve in series with a pressure compensator valve. The valve has been modelled as two variable orifices as shown in Figure 8. The opening of these are controlled by a set of function blocks, including valve dynamics.

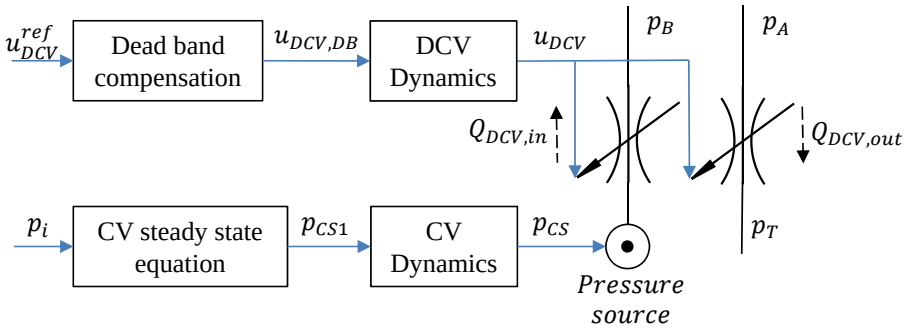

Figure 8: Structure of DCV model.

The blue lines are signal lines and the black lines are hydraulic lines. Assum-

ing constant density and using the orifice flow equation then the flow across the DCV can be computed as:

$$Q_{DCV,in} = k_{CS-B} \cdot u_{DCV} \cdot \sqrt{p_{CS} - p_B} \tag{6}$$

$$Q_{DCV,out} = k_{A-T} \cdot u_{DCV} \cdot \sqrt{p_A - p_T} \tag{7}$$

where $Q_{DCV,in}$ and $Q_{DCV,out}$ are the compensated metering-in flow and metering-out flow, p_T is the tank pressure, u_{DCV} is the dimensionless opening of the valve. The parameters k_{CS-B} and k_{A-T} are valve constants. The compensated supply pressure, p_{CS}, is calculated by the compensator equation, which is implemented like:

$$p_{CS1} = \begin{cases} p_S & , p_i \geq p_S - p_{DCV,cl} \\ p_i + p_{DCV,cl} & , p_i < p_S - p_{DCV,cl} \end{cases} \tag{8}$$

where p_i is the input pressure to the CV, p_S is the supply pressure and $p_{DCV,cl}$ is the nominal pressure drop across the main spool (setting of CV spring). The dynamics of the CV is added to account for the valve not being a perfect flow source. It is described by a first order transfer function:

$$\frac{p_{CS}}{p_{CS1}}(s) = \frac{1}{\tau_{CV} \cdot s + 1} \tag{9}$$

A difference between the model of the base circuit and the novel concept is the input pressure, p_i, to the CV:

$$p_i = \begin{cases} p_B & \text{, for Base Circuit} \\ p_C & \text{, for Novel Concept} \end{cases} \tag{10}$$

Experiments showed a slightly higher flow output of the DCV utilising the novel concept than of the base circuit. This indicates that equation (10) in

reality looks like:

$$p_i = \begin{cases} p_B - \Delta p_{LS}^{BC}(u_{DCV}) \\ p_C - \Delta p_{LS}^{NC}(u_{DCV}) \end{cases} \tag{11}$$

where Δp_{LS} is the pressure drop internally in the DCV's load sensing system before the CV which is a function of u_{DCV}. The difference between the two systems occurs because pressure p_C is obtained by connecting the secondary circuit to an external port on the DCV, while pressure p_B is handled internally in the DCV. The experiments indicate that $\Delta p_{LS}^{BC} > \Delta p_{LS}^{NC}$. The pressure drop Δp_{LS}, is combined with k_{CS-B} in an equivalent valve characteristic L_{CS-B}, changing equation (6) to:

$$Q_{DCV,in}^{BC} = L_{CS-B}^{BC}(u_{DCV}) \cdot \sqrt{p_{CS} - p_B} \tag{12}$$

$$Q_{DCV,in}^{NC} = L_{CS-B}^{NC}(u_{DCV}) \cdot \sqrt{p_{CS} - p_B} \tag{13}$$

In Figure 9 is shown L_{CS-B} for both systems as a function of u_{DCV}.

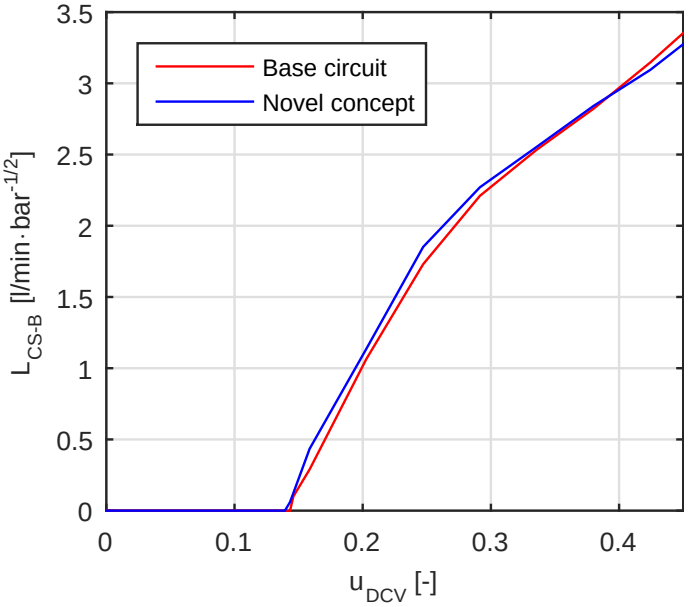

Figure 9: Equivalent valve characteristic, L_{CS-B}, as function of u_{DCV}.

The spool is open-centre, hence, it has no dead band on the outlet. For the

inlet a dead band compensation is implemented as follows, where σ_{DB} is the dimensionless dead band:

$$u_{DCV,DB} = \begin{cases} 0 & , u_{DCV}^{ref} = 0 \\ \sigma_{DB} + (1 - \sigma_{DB}) \cdot u_{DCV}^{ref} & , u_{DCV}^{ref} > 0 \end{cases} \tag{14}$$

The dynamics of the DCV is implemented using a second order transfer function:

$$\frac{u_{DCV}}{u_{DCV,DB}}(s) = \frac{1}{\frac{s^2}{\omega_{DCV}^2} + 2 \cdot \zeta_{DCV} \cdot \frac{s}{\omega_{DCV}} + 1} \tag{15}$$

where ω_{DCV} is the natural eigen frequency of the valve and ζ_{DCV} is the damping ratio. Values for the parameters used in the modelling work can be found in Table 2.

Table 2: DCV model parameters.

Parameter	Value
k_{A-T}	$2.3 \frac{L}{min\sqrt{bar}}$
$p_{DCV,cl}$	$7bar$[a]
τ_{CV}	$0.0064s$
σ_{DB}	0.14
ω_{DCV}	$30 \frac{rad}{s} (4.8Hz)$
ζ_{DCV}	0.8[a]

[a] Bak and Hansen (2013)

4.2.2 Counterbalance valve

The valve is a 4-port vented valve from Sun Hydraulics. The counterbalance valve consists of two parts: a check valve and a pilot operated relief valve as shown in Figure 1 and Figure 2. Only the relief valve is modelled by means of a variable orifice as shown in Figure 10. The opening is controlled by a set of function blocks, including valve dynamics. The blue lines are signal lines and the black lines are hydraulic lines.

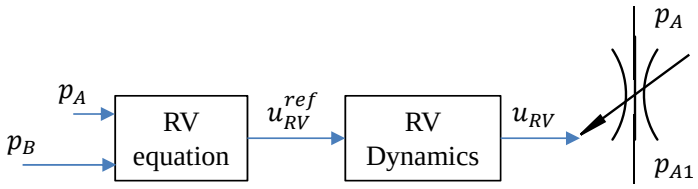

Figure 10: Structure of CBV model.

The flow, Q_{CBV}, through the valve is defined by the orifice equation:

$$Q_{CBV} = k_{v,CBV} \cdot u_{RV} \cdot \sqrt{p_A - p_{A1}} \tag{16}$$

where $k_{v,CBV}$ is the counterbalance valve constant, and u_{CBV} is the dimensionless opening of the relief valve. Assuming no back pressure from tank, the normalised reference opening, $0 \leq u_{RV}^{ref} \leq 1$, is defined as:

$$u_{RV}^{ref} = \frac{\alpha_P \cdot p_B + p_A - p_{cr,RV}}{\Delta p_{op,RV}} \tag{17}$$

where α_P is the CBV pilot area ratio, $p_{cr,RV}$ is the crack pressure of the relief valve and $\Delta p_{op,RV}$ is the extra pressure required to open the CBV fully. The dynamics of the relief valve poppet is described by a first order transfer function:

$$\frac{u_{RV}}{u_{RV}^{ref}}(s) = \frac{1}{\tau_{RV} \cdot s + 1} \tag{18}$$

where τ_{RV} is the time constant. Values for the CBV parameters can be seen in Table 3.

Table 3: CBV model parameters.

Parameter	Value
$k_{v,CBV}$	$1.90 \frac{L}{min\sqrt{bar}}$
$p_{cr,RV}$	$196bar$
$\Delta p_{op,RV}$	$350bar$
α_P	3
τ_{RV}	$0.089s$

4.2.3 Hydraulic cylinder

The model of the hydraulic cylinder is based on the one presented by Bak and Hansen (2013). The cylinder force, F_{cyl}, is defined as:

$$F_{cyl} = F_P - \tanh(v_C \cdot C_{th}) \cdot F_{fr} \tag{19}$$

It consists of the pressure induced force, F_P, and a friction component, F_{fr}. The hyperbolic tangent function is used to avoid numerical difficulties at zero velocity, however, the shape factor C_{th} is chosen sufficiently high to ensure that stiction between the piston and the cylinder can be simulated from negligible velocity fluctuation. The pressure induced force is defined as:

$$F_P = p_A \cdot \mu_C \cdot A_B - p_B \cdot A_B \tag{20}$$

The friction force is defined as:

$$F_{fr} = F_S + C_P \cdot |F_P| \tag{21}$$

where F_S describes the force required to overcome the static friction and C_p is a scaling factor for the pressure dependent friction. The friction parameters for the cylinder can be found in Table 4.

Table 4: Hydraulic cylinder model parameters.

Parameter	Value
C_{th}	$10300\frac{s}{m}$
F_S	$\mu_C \cdot A_B \cdot 1 \cdot 10^5 m^2 Pa$
C_p	0.02

4.2.4 Secondary circuit

The performance of the chosen implementation of the secondary circuit depends to a large extent on the used PV. However, experiments have shown that the internal leakage cannot be neglected, whether it is across the CV or

other places in the load sensing system of the valve group. The leakage is modelled as a fixed orifice and the circuit is shown in Figure 11.

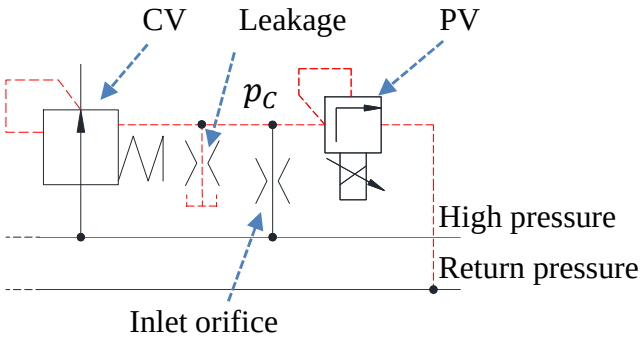

Figure 11: Actual secondary circuit including leakage in the load sensing system of the proportional valve group.

The orifice parameters are estimated from experiments, and they are listed in Table 5. The PV has its own factory set closed loop control aiming at linearising the flow-pressure characteristics. Based on measurements the following model for the flow has been identified.

$$Q_{PV} = k_{PV} \cdot \sigma_{PV} \cdot \sqrt{p_C} \tag{22}$$

where k_{PV} is the PV constant and σ_{PV} is the dimensionless opening of the orifice internally in the PV. It is linked to the dimensionless input reference, u_{PV}, by the following equation:

$$\sigma_{PV} = \begin{cases} \frac{p_C - u_{PV} \cdot p_{PV}^r}{\Delta p_{op,PV}} & , u_{PV} > \sigma_1 \\ \frac{p_C - u_{PV} \cdot p_{PV}^r}{\Delta p_{op,PV}} \cdot \frac{\theta_1}{(u_{PV})^2} & , \sigma_0 < u_{PV} < \sigma_1 \\ 1 & , u_{PV} = \sigma_0 \end{cases} \tag{23}$$

where σ_0 and σ_1 select the intervals of the piecewise function. θ_1 is a constant to adjust the curvature. The range of pressure, p_C, available from the secondary circuit goes from $p_C^{min} = 3bar$ to $p_C^{max} = 75bar$.

Table 5: Secondary circuit model parameters

Parameter	Value
Inlet orifice, pressure drop at a flow $Q = 2\frac{L}{min}$	$\Delta p\|_{@2L/min} = 220bar$
Leakage, pressure drop at a flow $Q = 2\frac{L}{min}$	$\Delta p\|_{@2L/min} = 160bar$
k_{PV}	$0.791\frac{L}{min\sqrt{bar}}$
$\Delta p_{op,PV}$	$40bar$
p^r_{PV}	$200bar$
θ_1	0.0081
σ_0	0
σ_1	0.09
p^{min}_C, PV fully open	$3bar$
p^{max}_C, PV closed	$75bar$

5 Experimental verification of nonlinear model

In this section the nonlinear model is verified against experimental results. First the behaviour of the parts of the system are verified before the model for the total system is. In general, when tuning/verifying the nonlinear model, it is being evaluated for four parameters: General tendency of the curves, peak sizes, the frequencies of the oscillations and finally the steady state values.

In this section, the following abbreviations are used:
Sim = Data from the nonlinear simulation model.
Exp = Data from experiments.

5.1 Cylinder friction

Figure 12 shows the cylinder load as a function of piston position, with and without friction in the cylinder both from simulation and experiments (the curve without friction is calculated from the up and down curves). When moving the boom downwards the friction causes the experienced cylinder force of the cylinder to drop with the magnitude of the friction force and vice versa when moving upwards.

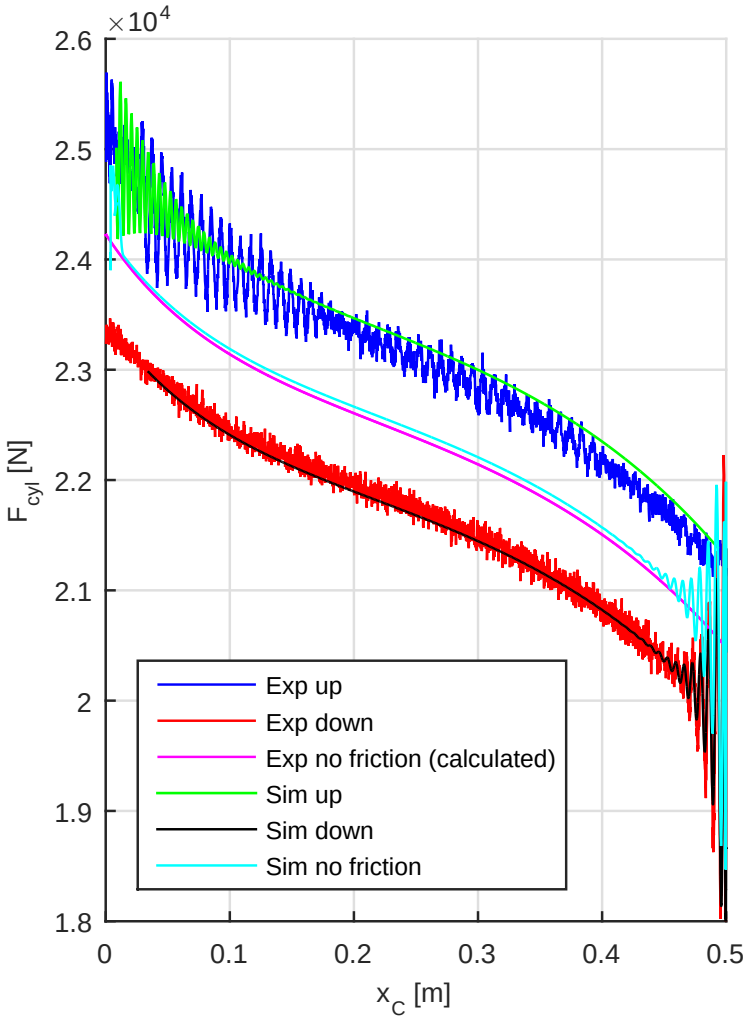

Figure 12: Load curves with and without friction.

The curves in Figure 12 are obtained by doing a full up-down cycle with constant cylinder velocity. The method used to model the cylinder seems to be a good fit in this case, since all three curves (up, down, and no friction) show a similar pattern as the measured ones. This also shows that the mechanical loads in the model are a good approximation of the real system.

5.2 Eigen frequency

The pure mechanical eigen frequency, f_m, and damping are found in the top and bottom position of the boom. In both of these experiments the piston is preloaded so that it is mechanically fixed to the relevant cylinder end plate. Next, the boom is excited manually and the motion is recorded. In Figure 13 the oscillations from the experiments are compared to the ones achieved from the simulation. From the experimental setup, strain is measured in the boom, see Figure 6, and from the simulation, the deflection of the nearby spring is used. The two data sets have been normalised to have the same amplitude at time $t = 0s$, see Figure 13. The comparison of strain and deflection respectively is considered to be acceptable.

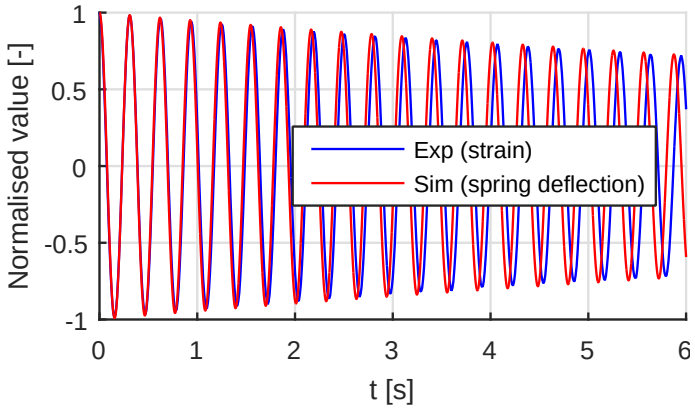

Figure 13: Normalised values of oscillations in top position ($x_C = 0m$).

The curves show a good correspondence between simulation and experiments. The model has a slightly higher eigen frequency. Due to the fact that the base is not included directly as a flexible part in the modelling of the mechanical structure but only as a tuning factor, the mechanical eigen frequency

from the model does not match the experiments perfectly over the entire span of operation. However, the difference is acceptable, see Table 6. The curves in Figure 13 also show that the mechanical damping is in accordance.

Table 6: Mechanical eigen frequencies, f_m.

Position	f_m (Sim)	f_m (Exp)
Top	$3.2Hz$	$3.2Hz$
Bottom	$3.1Hz$	$3.2Hz$

The next step is to look at the combined mechanical-hydraulic eigen frequency, f_{mh}, when the piston is suspended by two oil column springs in parallel. For that purpose investigations are carried out for two characteristic piston positions, $x_C = 0.10m$ and $x_C = 0.25m$, respectively. Figure 14 (upper) shows the normalised values of oscillations when the boom is placed with the piston at $x_C = 0.10m$ and a similar external force as before is applied to verify the spring effect of the hydraulic system. As it can be seen, the oscillations show a nice fit, including the damping. However, a variance in eigen frequency is noticed. During the first second, the curves coincide, then the oscillations of the simulation are slowing down compared to the measured values before finally ending a bit faster than the experimental ones. To illustrate this, the frequency of each period is shown as a function of time in Figure 14 (lower), where the mentioned difference is visible. This varying eigen frequency of the boom is a result of the friction. As time elapses and the oscillatory motion dampens out then the stiction period where the piston and the cylinder are locked together increases until it covers the entire oscillation time. In that period, the eigen frequency increases from the mechanical-hydraulic to the pure mechanical that can also be found in Table 6. Because of the small deviations from the experiments and the good correlation in how the stiction influences the overall motion, the model is considered useful for a parameter study.

For $x_C = 0.25m$ the same tendency is observed, see Figure 15. It is also noticed that the damping rate is lower in this position, due to the change in cylinder volumes.

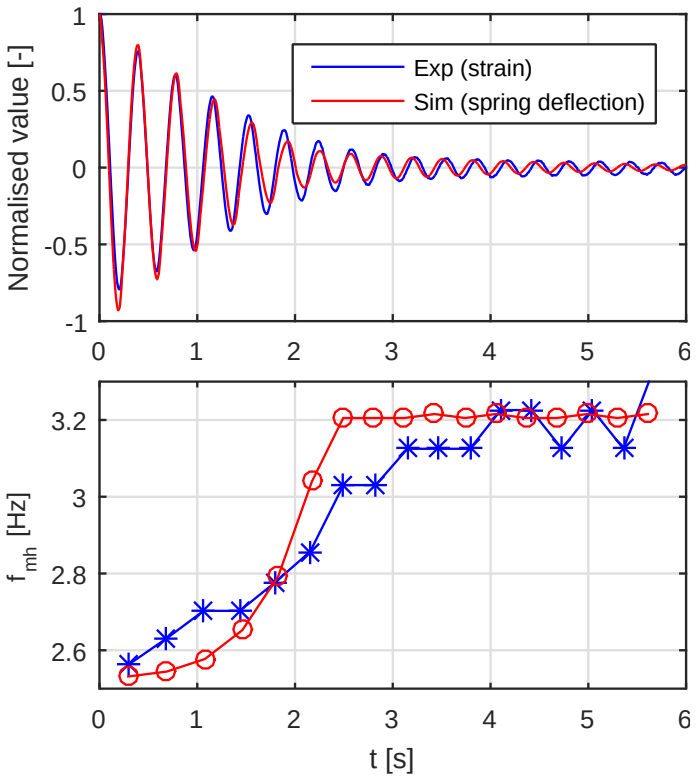

Figure 14: (Upper) Normalised values of oscillations at $x_C = 0.10m$. (Lower) Mechanical-hydraulic eigen frequency f_{mh}, showing the frequency between each downwards zero crossing of the upper figure.

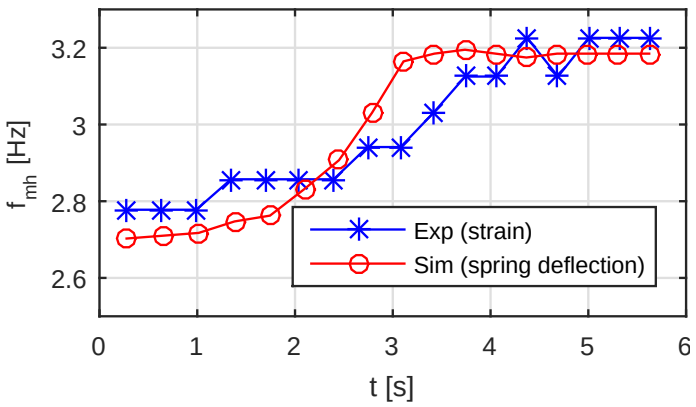

Figure 15: Mechanical-hydraulic eigen frequency at $x_C = 0.25m$. The plot shows the frequency between each downwards zero crossing of a curve of the normalised values of oscillations at $x_C = 0.25m$.

The lower limit for the mechanical-hydraulic eigen frequency can be found by removing the cylinder friction in the simulation. In Figure 16 this f_{mh}^{NF} is shown as a function of the piston position.

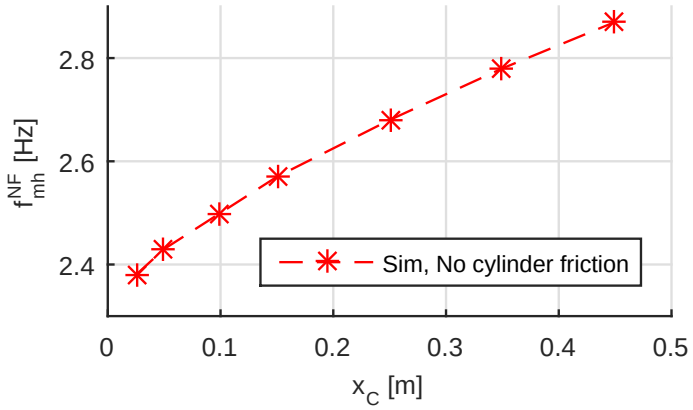

Figure 16: Mechanical-hydraulic eigen frequency without cylinder friction, f_{mh}^{NF} as a function of piston position x_C.

5.3 Secondary circuit

In order to be able to verify the performance of the novel concept the secondary circuit is analysed first. To check the model of the PV in equation (23), it is compared to experimental values when p_C is plotted as a function of u_{PV}, see Figure 17.

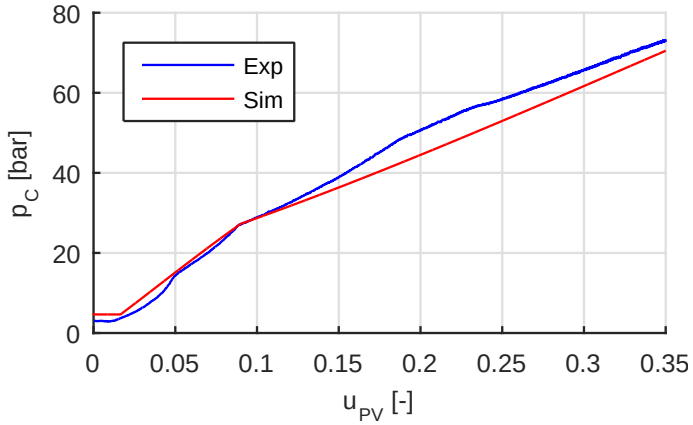

Figure 17: Verification of the PV: Pressure p_C as a function of u_{PV}.

The experiment shows that an input u_{PV} to the model gives the expected pressure p_C. The performance is evaluated by applying a reference step input, p_C^{ref}, of $40bar$ to the secondary circuit. With $p^{min} = 5bar$, the gains were adjusted to: $K_P = 0.01\frac{V}{bar}$ and $K_I = 0.04\frac{V}{bar \cdot s}$. The results are shown in Figure 18.

The experiment has two parts. The blue curve shows the reference step input. The ability of the closed-loop control system to follow this reference is shown in red and black, for the experiment and simulation. These curves are obtained without any filtration, i.e., $\tau = 0s$. The performance when applying the low-pass filter in the system is the other part. The filtered reference p_C^{ref} with a cut-off frequency set to $\tau = 0.32s$, is shown in cyan. The remaining curves, the green and magenta show the ability of p_C to follow p_C^{ref}. In both cases, the model shows good conformity with the experiments both when stepping up and down.

5.4 Total system

To achieve a uniform evaluation of the total system a standard actuation of the DCV is used in the following, see Figure 19. Only situations where the cylinder is retracting are investigated.

The actuation is defined by the cycle time, T, a delay time to ensure static conditions, t_d, the ramp time, t_r, and the wanted steady state DCV input u_{DCV}^{max}. The time parameters are equal for all tests, see Table 7.

In the reminder of the verification section, the dashed green lines in the figures indicate when $u_{DCV}^{ref} \neq 0$.

Table 7: Common parameters for all actuation.

Cycle time, T	Ramp time, t_r	Time delay, t_d
$8s$	$1s$	$1s$

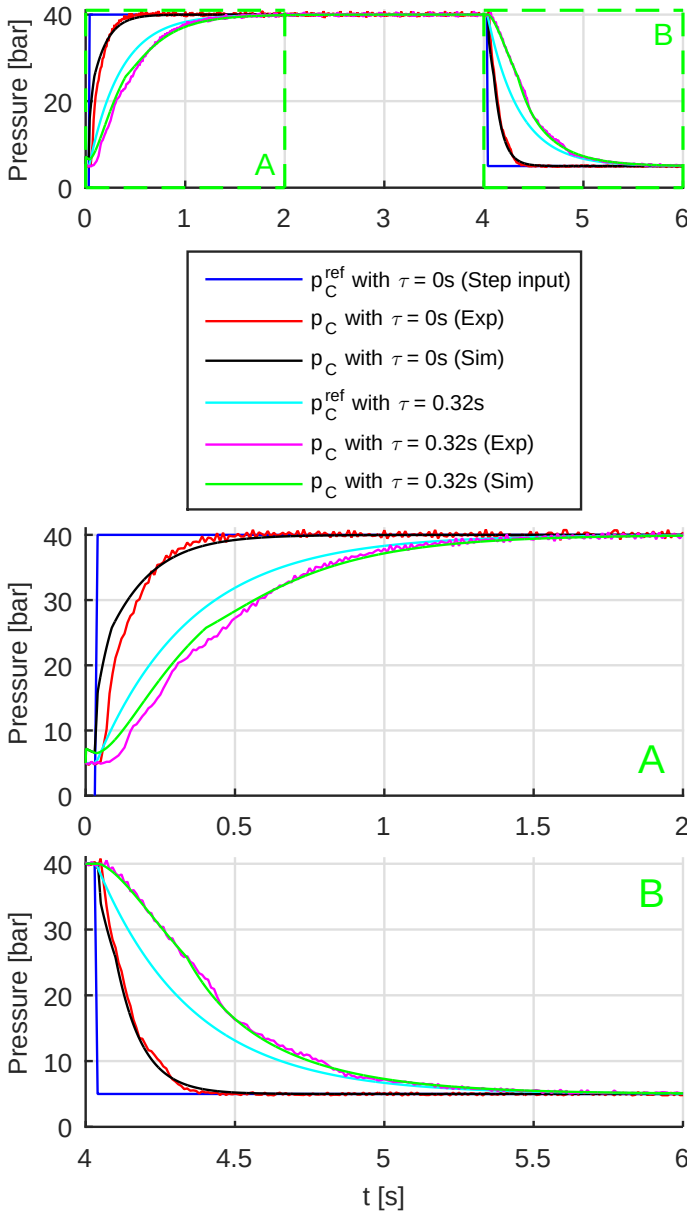

Figure 18: Comparison of the pressure responses of the secondary circuit for a reference step input, p_C^{ref}, of 40*bar*. The figure comprises an overview at the top, legends, and more detailed views of the step up and the step down, respectively.

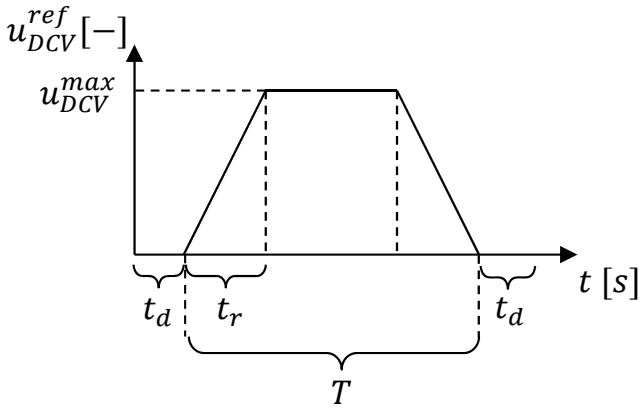

Figure 19: Work cycle - actuation function.

5.4.1 Base circuit

A model of the base circuit is presented to support the later verification of the novel concept. The nonlinear model of the base circuit verifies that the model of the mechanical system together with the hydraulic circuit, is providing realistic results. The system is subjected to an actuation of $u_{DCV}^{max} = 0.15$. In Figure 20 the pressures during the work cycle are shown.

The markedly increased pressure amplitudes and distinct oscillations are characteristic for an unstable system, which corresponds well with the linear stability analysis in Sørensen et al. (2016). The deviations in amplitude that appear as the boom is lowered are considered acceptable due to the very violent oscillations of the physical setup that may have introduced phenomena not included in the model. A section of Figure 20 showing from $1s$ to $5s$, is presented in Figure 21.

The figures 20 and 21 show a satisfactory resemblance between the simulated and the measured values of the pressures. The levels of p_A, p_{A1} and p_B indicate that the mechanical model and the model of the CBV resemble the real system well. The frequencies and amplitudes of the oscillations are satisfactory, although a certain drift is observed after 3-4 periods. The good correspondence of the piston velocity shown in Figure 22 indicates that the characteristics of the DCV is modelled correctly.

To summarise, the model of the base circuit captures the physical tendencies

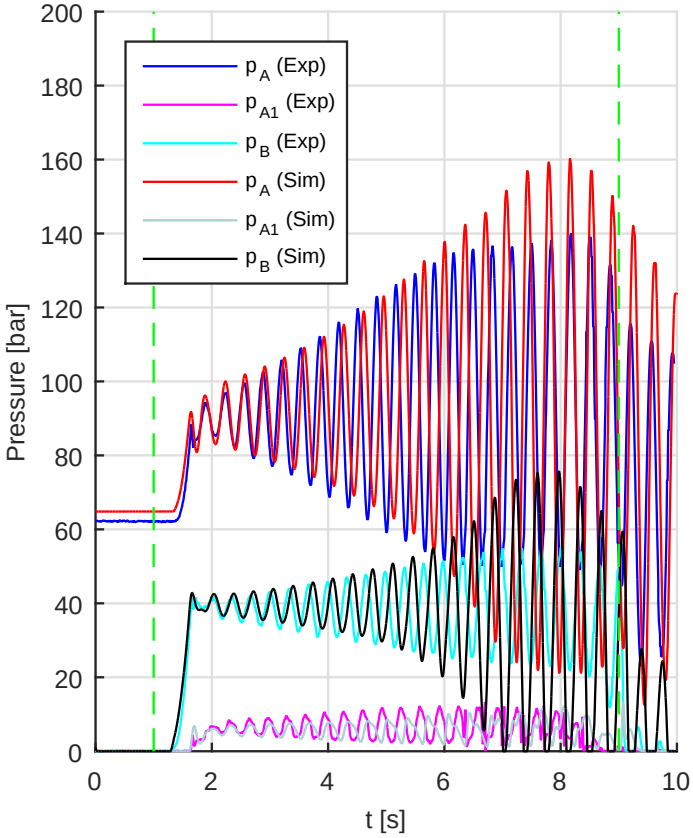

Figure 20: Comparison of pressures of the base circuit ($u_{DCV}^{max} = 0.15$).

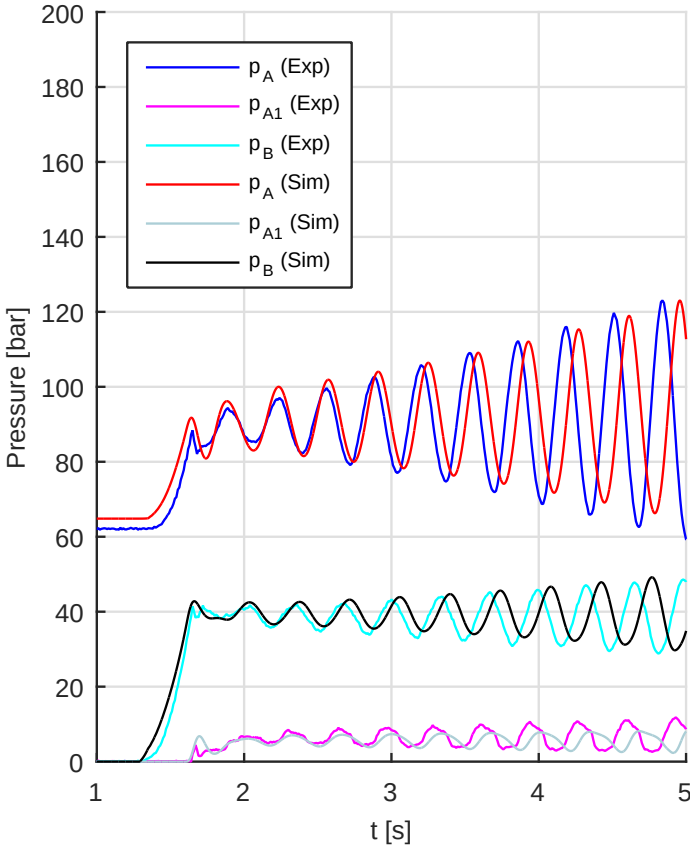

Figure 21: Zoom of pressure comparison of the base circuit ($u_{DCV}^{max} = 0.15$) shown in Figure 20.

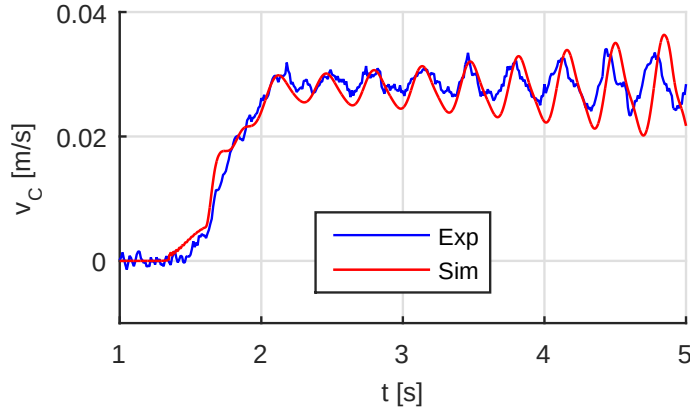

Figure 22: Comparison of piston velocity of the base circuit ($u_{DCV}^{max} = 0.15$).

of the real system well. It shows good resemblance for pressure levels together with the frequencies and amplitude of the oscillations. It is concluded that the behaviour of the following parts of the nonlinear model have been verified:

- Model of mechanical system including stiffness and damping.
- Model of friction in the hydraulic cylinder.
- Model of counterbalance valve.
- Model of directional control valve.
- Model of hydraulic system including stiffness and damping.

5.4.2 Novel concept

The last step in the verification is to attach the secondary circuit to the base circuit and look at the novel concept. The novel concept is first subjected to an actuation of $u_{DCV}^{max} = 0.15$. The controller was implemented with $p^{min} = 35bar$, and the same gains as in section 5.3. Figure 23 shows the pressures during the work cycle.
The simulated values correspond well with the measured ones. The oscillations in pressure p_A at the start show good resemblance with respect to both frequency and amplitude. There are minor differences between model and simulation in both pressure p_A and p_B when the deceleration begins after $8s$, but the general trend is followed and the pressures are deemed satisfying. The pressures of the secondary circuit are shown in Figure 24.
The pressure peaks at the beginning and end of the cycle which only occur in the experiments, indicate that modelling the leakage as a fixed orifice might be an oversimplification of the LS system. A detailed analysis of this would lie outside the scope of this paper and is also considered peripheral to the more generic investigation of the novel concept. The measured pressure p_B in the diagram is added to illustrate how the secondary circuit reacts to inputs from the primary circuit. Comparing the piston position and velocity in

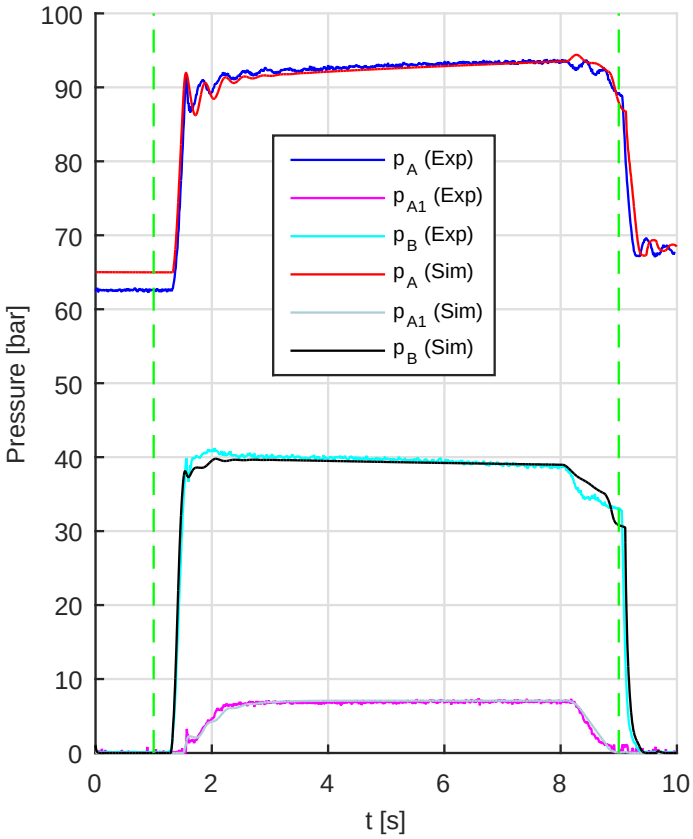

Figure 23: Comparison of pressures of the system with the novel concept implemented ($u_{DCV}^{max} = 0.15$).

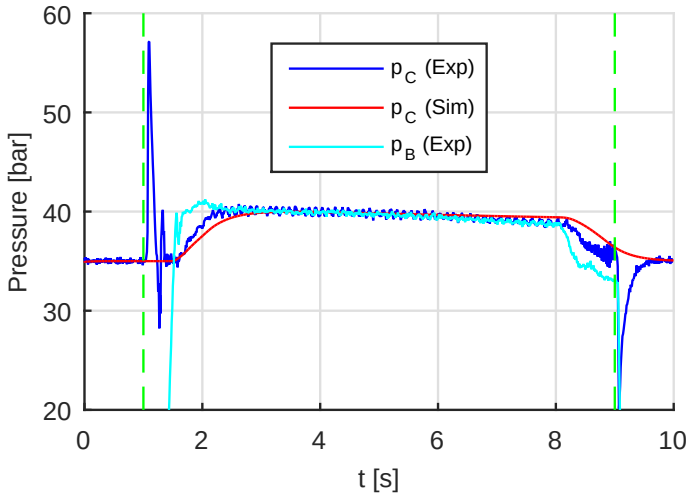

Figure 24: Pressure response of the novel concept's secondary circuit during work cycle ($u_{DCV}^{max} = 0.15$).

Figure 25 and Figure 26, a good resemblance is observed in both figures; for example is the small peak with negative velocity measured in the experiments at approximately $9s$ replicated in the simulation.

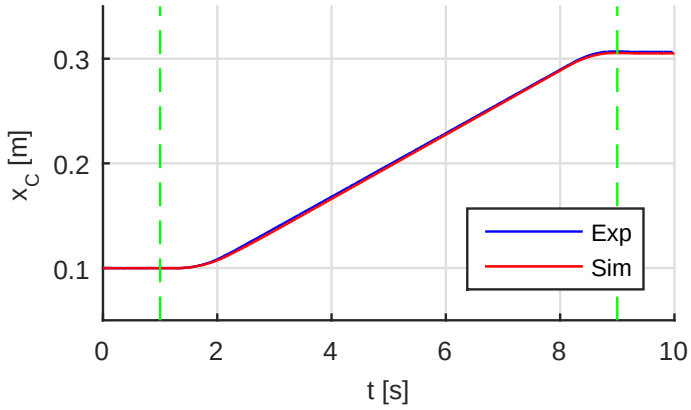

Figure 25: Comparison of piston position of the system with the novel concept implemented ($u_{DCV}^{max} = 0.15$).

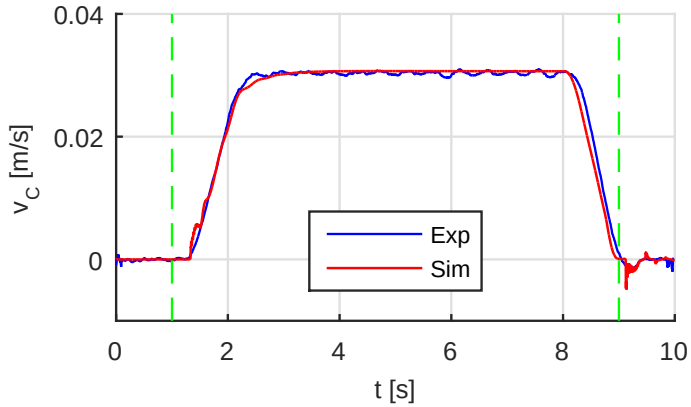

Figure 26: Comparison of piston velocity of the system with the novel concept implemented ($u_{DCV}^{max} = 0.15$).

To add further depth to the verification of the model, an actuation of $u_{DCV}^{max} = 0.05$ is also analysed. Figure 27 shows the pressures during this work cycle. Also in this case the simulated values correspond well with the measured ones. However, the amplitudes are smaller in the simulation for both pressure p_A and p_B, and this is most pronounced at the rod side of the cylinder. Figure 28 highlights this part of the pressure curve.

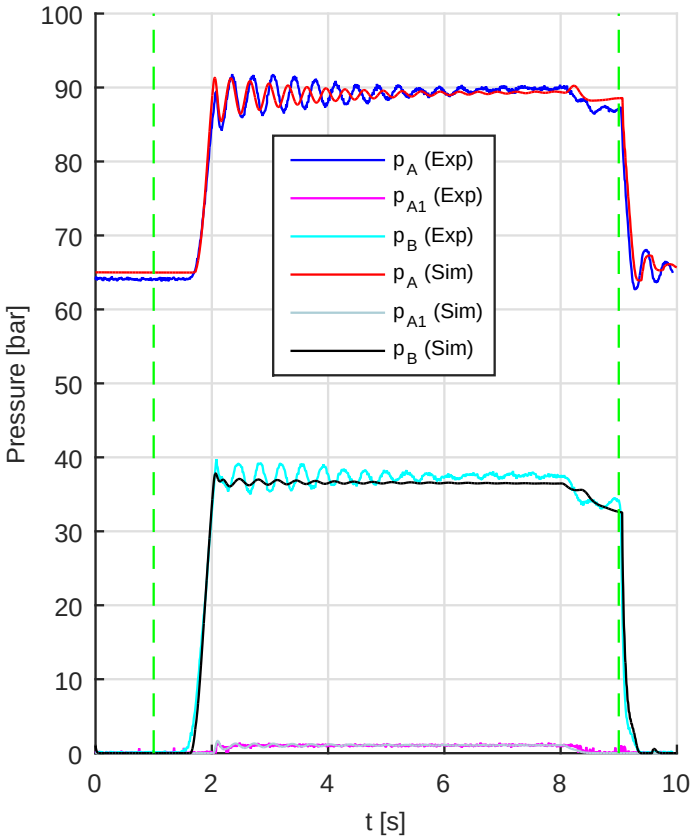

Figure 27: Comparison of pressures of the system with the novel concept implemented ($u_{DCV}^{max} = 0.05$).

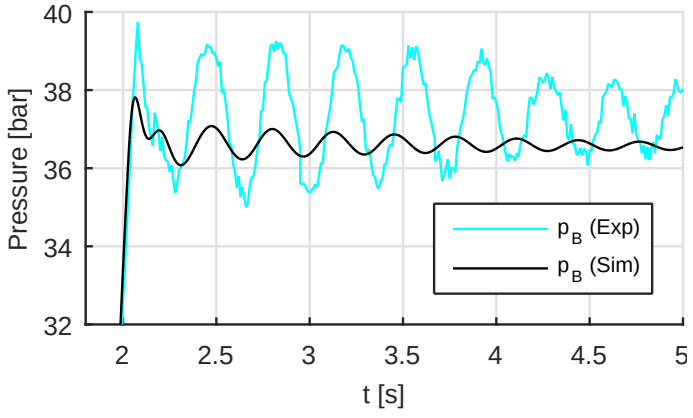

Figure 28: Zoom of part of pressure p_B from the system with the novel concept implemented ($u_{DCV}^{max} = 0.05$) shown in Figure 27.

There is a certain discrepancy which was not seen for the base circuit, hence, the source for this deviation probably lies in the modelling of the modified DCV. As seen in Figure 24 the modifications have led to pressure fluctuations in the secondary circuit not easily accounted for and it may be the same phenomena that give more oscillations in the rod side volume of the physical system. Finally, the flow capability of the DCV is checked by comparing the steady state velocity of the piston. Experiments using the work cycle function for nine different values of u_{DCV}^{max} were conducted. The result of the tailor-made flow characteristics introduced in equation (13) can be seen in Figure 29, clearly indicating that the deviations are virtually eliminated.

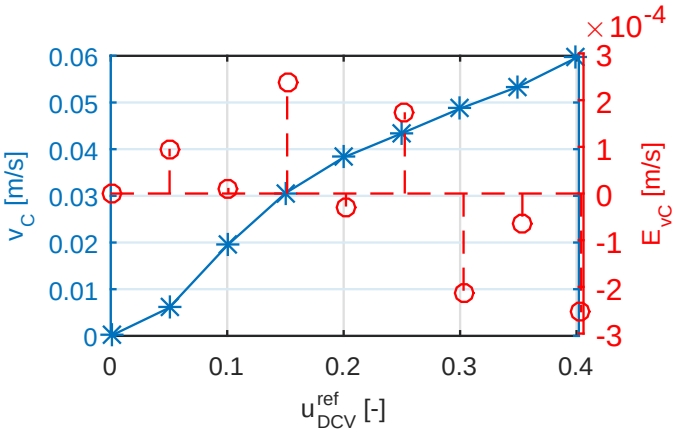

Figure 29: Simulated steady state piston velocities for different valve openings for the system with the novel concept implemented. The velocity error $E_{vC} = v_C(Exp) - v_C(Sim)$.

A nonlinear simulation model has been developed for the novel concept applied as actuation for a specific cylinder-boom mechanism. In general, the model corresponds well both steady state and dynamically with measured data and it is further validated by simulations and experiments conducted using a base circuit as actuation for the same mechanism.

6 Parameter study

The nonlinear model is utilised to investigate which parameters yield the largest influence on the stability of the novel concept. A linear stability analysis has indicated that small openings of the directional control valve result in stability issues (Sørensen et al., 2016). In this section, the evaluation of stability of the system in the nonlinear model is based on how the pressure amplitudes develop after the ramp up is conducted, i.e. $u_{DCV}^{ref} = u_{DCV}^{max}$. Increasing amplitudes are simply considered as representative for an unstable system. The way the novel concept is working with the secondary circuit separated from the primary circuit by a low-pass filter lowers the performance requirements to the components in the secondary circuit, hence its influence on the stability of the system is limited. The cylinder friction does not yield much effect on the stability either. Simulations show that the parameters most influential on the systems stability are the stiffness of the mechanical structure and the pilot area ratio of the CBV. In Figure 30 the blue curve shows the minimum u_{DCV}^{ref} yielding a stable system as a function of f_{mh}^{NF} when the starting position of the piston is $x_C = 0.10m$. The system becomes increasingly unstable when the stiffness and hence the eigen frequency increases. Also notice that for $f_{mh}^{NF} < 2.2Hz$ the simulation becomes stable for all valve openings.

Curves for a varying pilot area ratio of the CBV are shown in Figure 31. Stability is improved by lowering the pilot area ratio. This of course happens at the expense of a more pronounced pressure-load dependency in the cylinder chambers. The blue curve also indicates that for pilot ratios $\alpha_P < 1.9$ stability can be ensured in all cases.

In both Figure 30 and Figure 31 the curves for CV indicate that for the system in the lab ($f_{mh}^{NF} = 2.5Hz$ and $\alpha_P = 3$) instability occurs for u_{DCV}^{ref} below approximately 0.04, for this specific system. In some applications, the possible risk of oscillations for small valve openings might be unacceptable. As mentioned in the presentation of the novel concept the solution also encompasses a version where the secondary circuit besides being connected to the CV also controls the opening of the CBV (CV+CBV). The hydraulic diagram of this

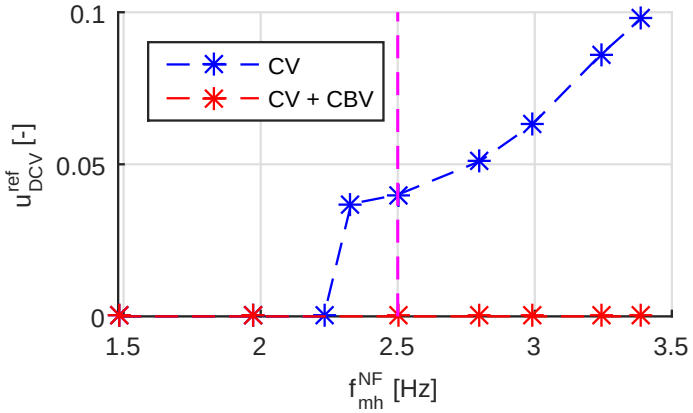

Figure 30: Stability of the nonlinear model of the novel concept; both connected to CV and CV+CBV. The diagram shows the minimum u_{DCV}^{ref} that yields a stable system as a function of f_{mh}^{NF} for $\alpha_P = 3$. The dashed magenta line is the value of the real system.

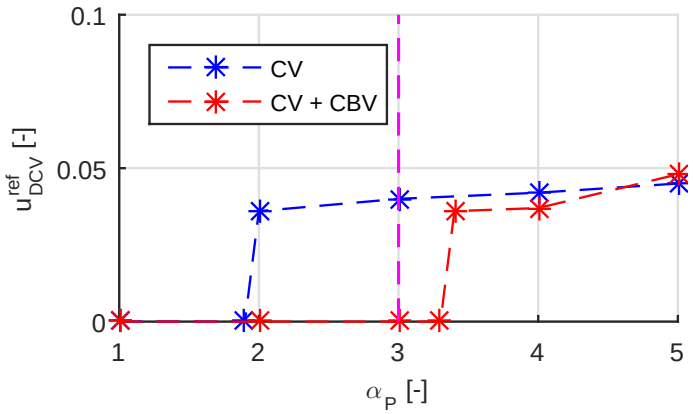

Figure 31: Stability of the nonlinear model of the novel concept; both connected to CV and CV+CBV. The diagram shows the minimum u_{DCV}^{ref} that yields a stable system as a function of α_P for $f_{mh}^{NF} = 2.5Hz$. The dashed magenta line is the value of the real system.

circuit is shown in Figure 32.

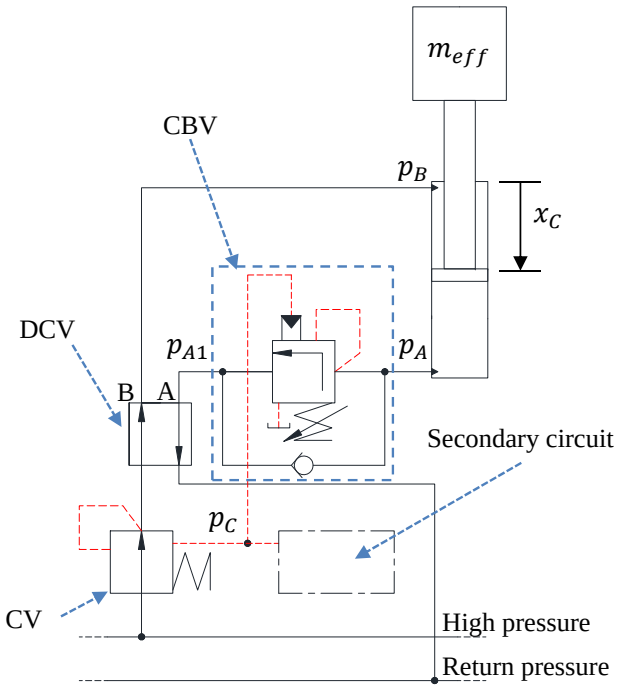

Figure 32: Hydraulic diagram of novel concept. Both the CBV and the CV are connected to the secondary circuit.

The results of this change in the hydraulic circuit are shown in red in Figure 30 and Figure 31. If $\alpha_P = 3$, this solution does not experience instability for any value of f_{mh}^{NF}. When varying the pilot area ratio, a clear improvement can be observed. The stability threshold increases and the system is now stable in the configuration of the real setup ($\alpha_P = 3$). This proves that the novel concept is able to stabilise the experimental setup for all openings of the directional control valve. Controlling the opening area of the CBV via a separate pressure source can be regarded problematic from a reliability point of view in some applications, since the CBV provides different safety functions, among them load holding at hose/pump failure. Therefore, the solution indicated in Figure 32 should only be considered if instability cannot be overcome by lowering the pilot area ratio.

7 Conclusions

The authors have previously presented a novel concept capable of suppressing oscillations in hydraulic systems containing a CBV and a pressure compensated directional control valve (DCV), see Sørensen et al. (2016). The concept utilizes a secondary circuit where a low-pass filtered value of the load pressure is generated and fed back to the compensator of the flow supply valve. This paper has focused on a further investigation of this concept and limitations hereof. A nonlinear dynamic model has been developed and experimentally verified on a cylinder actuated single boom mechanism. The commercial simulation tool SimulationX has been used as platform for the modeling. The mechanical system is modelled as a multi-body system using the finite segment flexibility method. The hydraulic circuit including the main control components have been modelled using a combination of liquid volumes, variable orifices and 1^{st} and 2^{nd} order transfer functions to capture valve dynamics. The eigen frequencies of both the mechanical and the combined mechanical-hydraulic system and the secondary circuit were investigated and validated separately - before being combined to a model of the entire system. In order to strengthen the verification, a model of the same mechanical-hydraulic system actuated by means of a standard base circuit was also investigated both experimentally and numerically. This ensured that the developed models of the mechanical system and the counterbalance valve (CBV) could be verified for two different setups. The full nonlinear model of the mechanical-hydraulic system actuated by the novel concept was in general, in good accordance with measurements. During the modelling of the mechanical-hydraulic system in this paper the following areas showed themselves to be of high importance:

- Flexibility of the mechanical system.
- Friction in the hydraulic cylinder.
- Continuous opening of the CBV.
- Proper characteristics of the DCV.

Since the main feature of the novel concept is its ability to suppress oscillations, the developed model was used for a parameter study with emphasis on instability. The model confirmed the results from the linear analysis in Sørensen et al. (2016), that there is an elevated risk for instability at small DCV openings. The model shows that an improved system stability can be obtained by either reducing the eigen frequency of the mechanical-hydraulic system or lowering the pilot area ratio of the CBV. Finally, the model showed the improved stability characteristics of another version of the novel concept where also the CBV pilot port is connected to the low pass filtered load pressure. This version would normally be considered less desirable from a reliability point of view because the basic safety features of the CBV are controlled electronically, however, the simulations indicate that it could be an alternative for systems that cannot be stabilised otherwise.

Acknowledgments

The work is funded by the Norwegian Ministry of Education & Research and National Oilwell Varco.

References

Bak, M. K. and Hansen, M. R. Analysis of offshore knuckle boom crane - part one: Modeling and parameter identification. *Modeling, Identification and Control*, 2013. 34(4):157–174. doi:10.4173/mic.2013.4.1.

Cristofori, D., Vacca, A., and Ariyur, K. A novel pressure-feedback based adaptive control method to damp instabilities in hydraulic machines. *SAE Int. J. Commer. Veh*, 2012. 5(2):586–596. doi:10.4271/2012-01-2035.

Handroos, H., Halme, J., and Vilenius, M. Steady-state and dynamic properties of counter balance valves. In *Proc. 3rd Scandinavian International Conference on Fluid Power*. Linköping, Sweden, 1993.

Hansen, M. R. and Andersen, T. O. A design procedure for actuator control systems using optimization methods. In *Proc. 7th Scandinavian International Conference on Fluid Power*. Linköping, Sweden, 2001.

Hansen, M. R. and Andersen, T. O. Controlling a negative loaded hydraulic cylinder using pressure feedback. In *Proc. 29th IASTED International Conference on Modelling, Identification and Control*. Innsbruck, Austria, 2010. doi:10.2316/P.2010.675-116.

Hansen, M. R. and Sørensen, J. K. Improvements in the control of hydraulic actuators (pending). 2015.

Huston, R. and Wang, Y. Flexibility effects in multibody systems. In M. Pereira and J. Ambrsio, editors, *Computer-Aided Analysis of Rigid and Flexible Mechanical Systems*, pages 351–376. Kluwer Academic Publishers, Dordrecht, NL, 1994.

Miyakawa, S. Stability of a hydraulic circuit with a counter-balance valve. *Bulletin of the JSME*, 1978. 21(162):1750–1756.

Nordhammer, P., Bak, M. K., and Hansen, M. R. A method for reliable motion control of pressure compensated hydraulic actuation with counterbalance valves. In *Proc. 12th International Conference on Control, automation and systems*. Jeju Island, Korea, 2012.

Persson, T., Krus, P., and Palmberg, J.-O. The dynamic properties of overcenter valves in mobile systems. In *Proc. 2nd International Conference on Fluid Power Transmission and Control*. Hangzhou, China, 1989.

Ritelli, G. and Vacca, A. A general auto-tuning method for active vibration damping of mobile hydraulic machines. In *Proc. 8th FPNI Ph.D. Symposium on Fluid Power*. Lappeenranta, Finland, 2014.

Sørensen, J. K., Hansen, M. R., and Ebbesen, M. K. Boom motion control using pressure control valve. In *Proc. 8th FPNI Ph.D. Symposium on Fluid Power*. Lappeenranta, Finland, 2014.

Sørensen, J. K., Hansen, M. R., and Ebbesen, M. K. Load independent velocity control on boom motion using pressure control valve. In *Proc. 14th Scandinavian International Conference on Fluid Power*. Tampere, Finland, 2015.

Sørensen, J. K., Hansen, M. R., and Ebbesen, M. K. Novel concept for stabilizing a hydraulic circuit containing counterbalance valve and pressure compensated flow supply. *International Journal of Fluid Power*, 2016. 17(3):153–162. doi:10.1080/14399776.2016.1172446.

Zähe, B. Stability of load holding circuits with counterbalance valve. In *Proc. 8th International Bath Fluid Power Workshop*. Bath, UK, 1995.